

Supplementary Information (SI)

Design, synthesis, *in vitro* and *in vivo* evaluation of heterobivalent SiFA/*in*-coupled peptidic radioligands targeting both $\alpha_v\beta_3$ -integrin and MC1-receptor – Suitable for the specific visualization of melanomas?

Xia Cheng ¹, Ralph Hübner ², Valeska von Kiedrowski ¹, Gert Fricker ³, Ralf Schirrmacher ⁴, Carmen Wängler ^{2,*} and Björn Wängler ^{1,*}

¹ Molecular Imaging and Radiochemistry, Department of Clinical Radiology and Nuclear Medicine, Medical Faculty Mannheim of Heidelberg University, Theodor-Kutzer-Ufer 1-3, 68167 Mannheim, Germany

² Biomedical Chemistry, Department of Clinical Radiology and Nuclear Medicine, Medical Faculty Mannheim of Heidelberg University, Theodor-Kutzer-Ufer 1-3, 68167 Mannheim, Germany

³ Institute of Pharmacy and Molecular Biotechnology, University of Heidelberg, Im Neuenheimer Feld 329, 69120 Heidelberg, Germany

⁴ Department of Oncology, Division of Oncological Imaging, University of Alberta, 11560 University Avenue, Edmonton, T6G 1Z2, Alberta, Canada

* Correspondence: Carmen.Waengler@medma.uni-heidelberg.de; Bjoern.Waengler@medma.uni-heidelberg.de

Table of Contents

1. HPLC chromatograms and mass spectra of the peptides 7–9 and the linker-modified peptides 10–21	1
2. NMR and mass spectra of SiFA/ <i>in</i> 28 , SiFA/ <i>in</i> -modified framework 29 and their intermediates 22–27	16
3. Mass and ¹⁹ F NMR spectra of HBPLs 1–6 and mass spectra of their intermediates 30–35	47
4. Mass data, HPLC chromatograms and mass spectra of peptidic side products a–z	65
5. Radio-HPLC chromatograms of [¹⁸ F] 1 -[¹⁸ F] 6 from the investigation regarding serum stability.....	93
6. Binding curves of the monomeric peptides c(RGDfK) and GG-Nle-c(DHfRWK).....	93
7. <i>Ex vivo</i> biodistribution data of [¹⁸ F] 2 and [¹⁸ F] 4	94

1. HPLC chromatograms and mass spectra of the peptides 7–9 and the linker-modified peptides 10–21

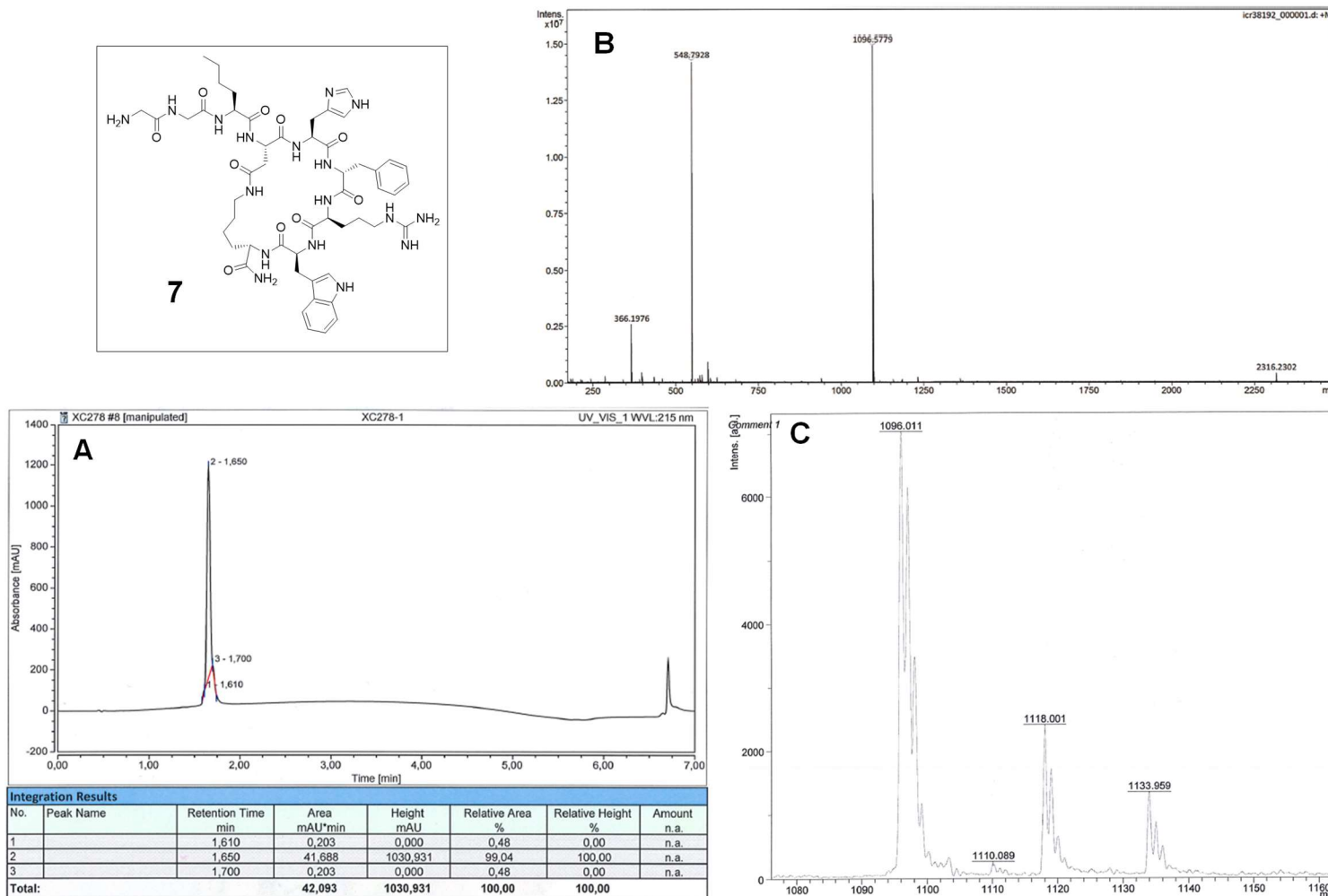
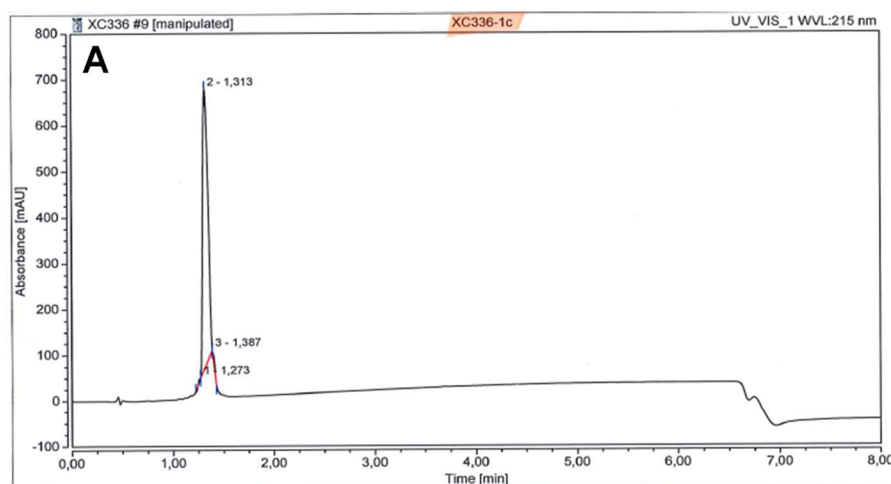
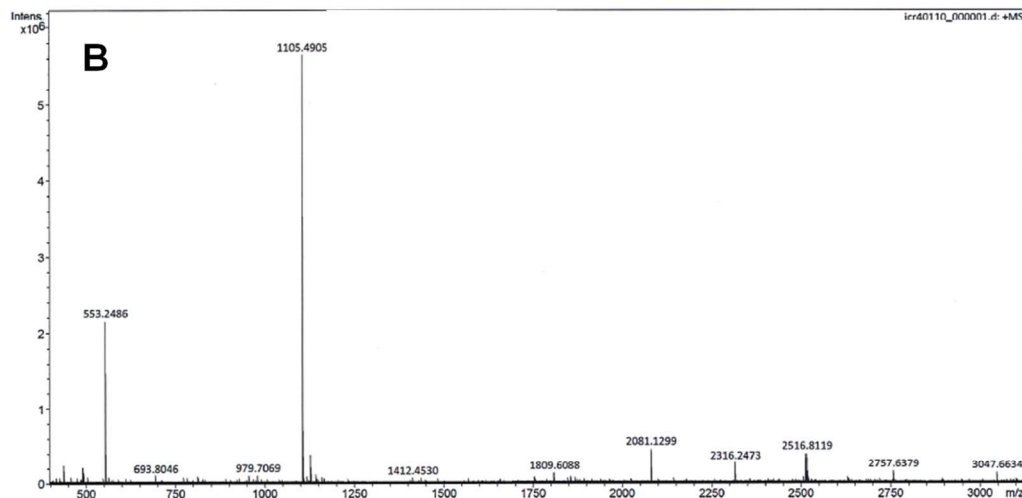
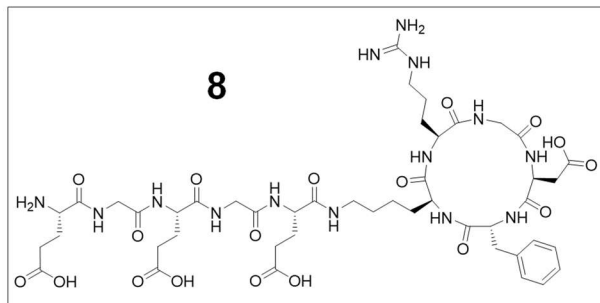


Figure S1. HPLC chromatogram (**A**) and mass spectra (**B**: ESI, **C**: MALDI) of GG-Nle-c(DHfRWK) (**7**).



Integration Results

No.	Peak Name	Retention Time [min]	Area [mAU·min]	Height [mAU]	Relative Area %	Relative Height %	Amount n.a.
1		1.273	0.044	0.000	0,12	0.00	n.a.
2		1,313	35.032	606.374	99,17	100,00	n.a.
3		1,387	0,249	0,000	0,70	0,00	n.a.
Total:			35,325	606,374	100,00	100,00	

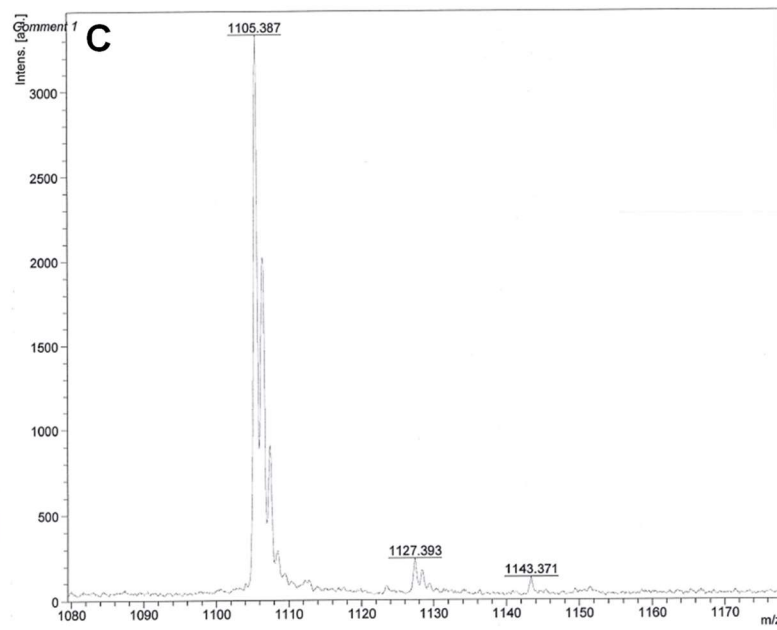


Figure S2. HPLC chromatogram (**A**) and mass spectra (**B**: ESI, **C**: MALDI) of c(RGDfK)-EGEGE (**8**).

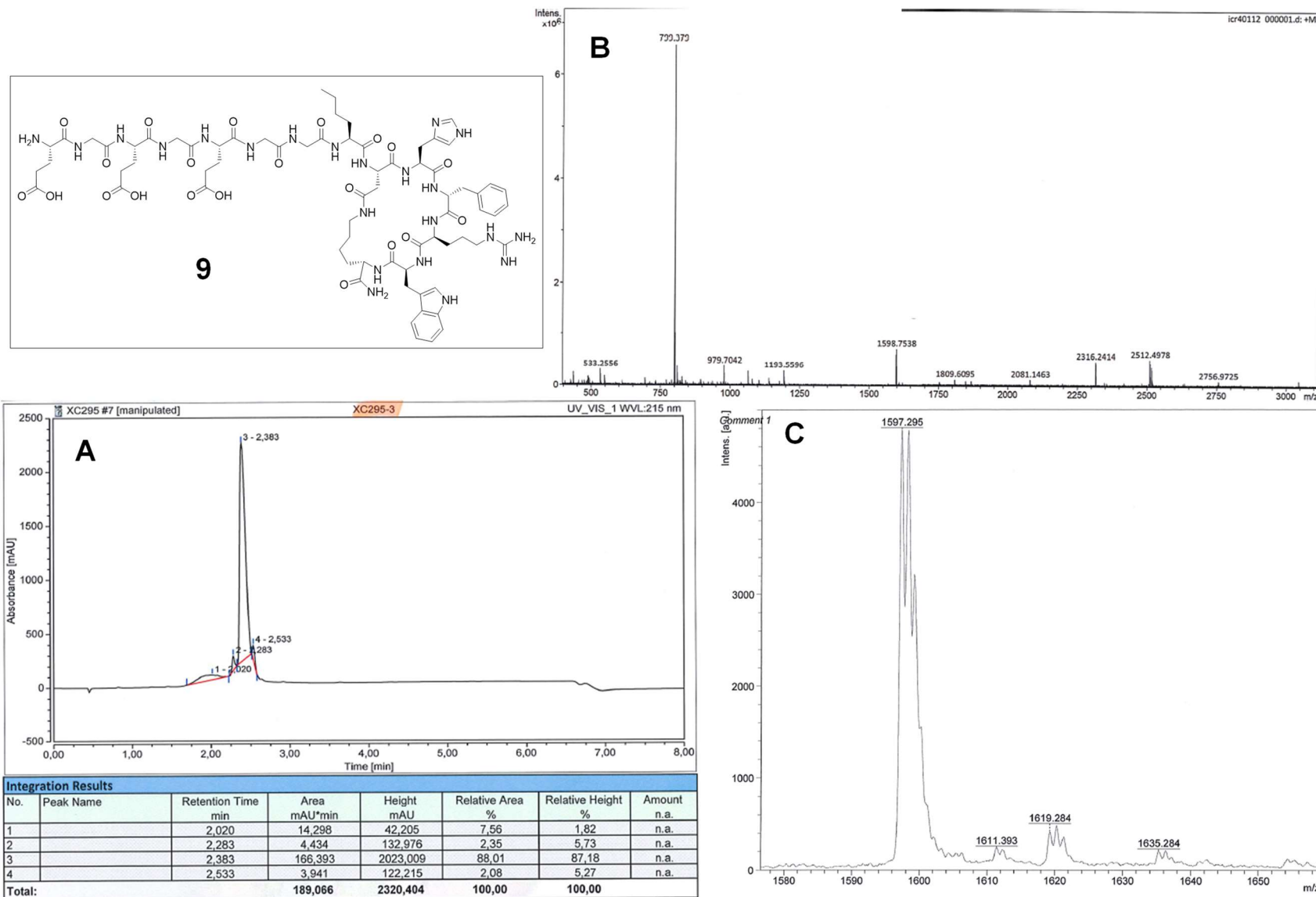


Figure S3. HPLC chromatogram (**A**) and mass spectra (**B**: ESI, **C**: MALDI) of EGEGE-GG-Nle-c(DHfRWK) (**9**).

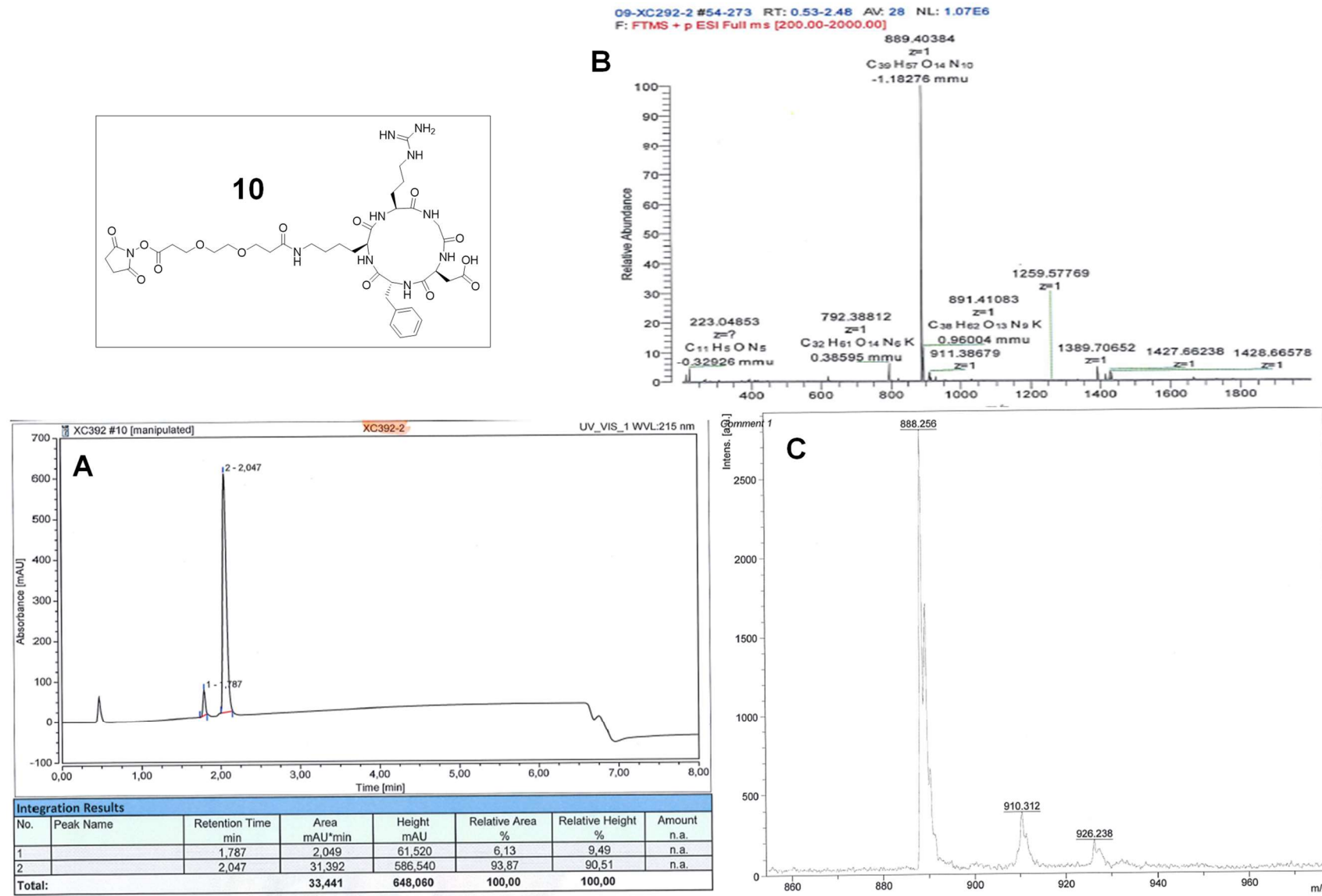


Figure S4. HPLC chromatogram (**A**) and mass spectra (**B**: ESI, **C**: MALDI) of NHS-PEG₁-c(RGDfK) (**10**).

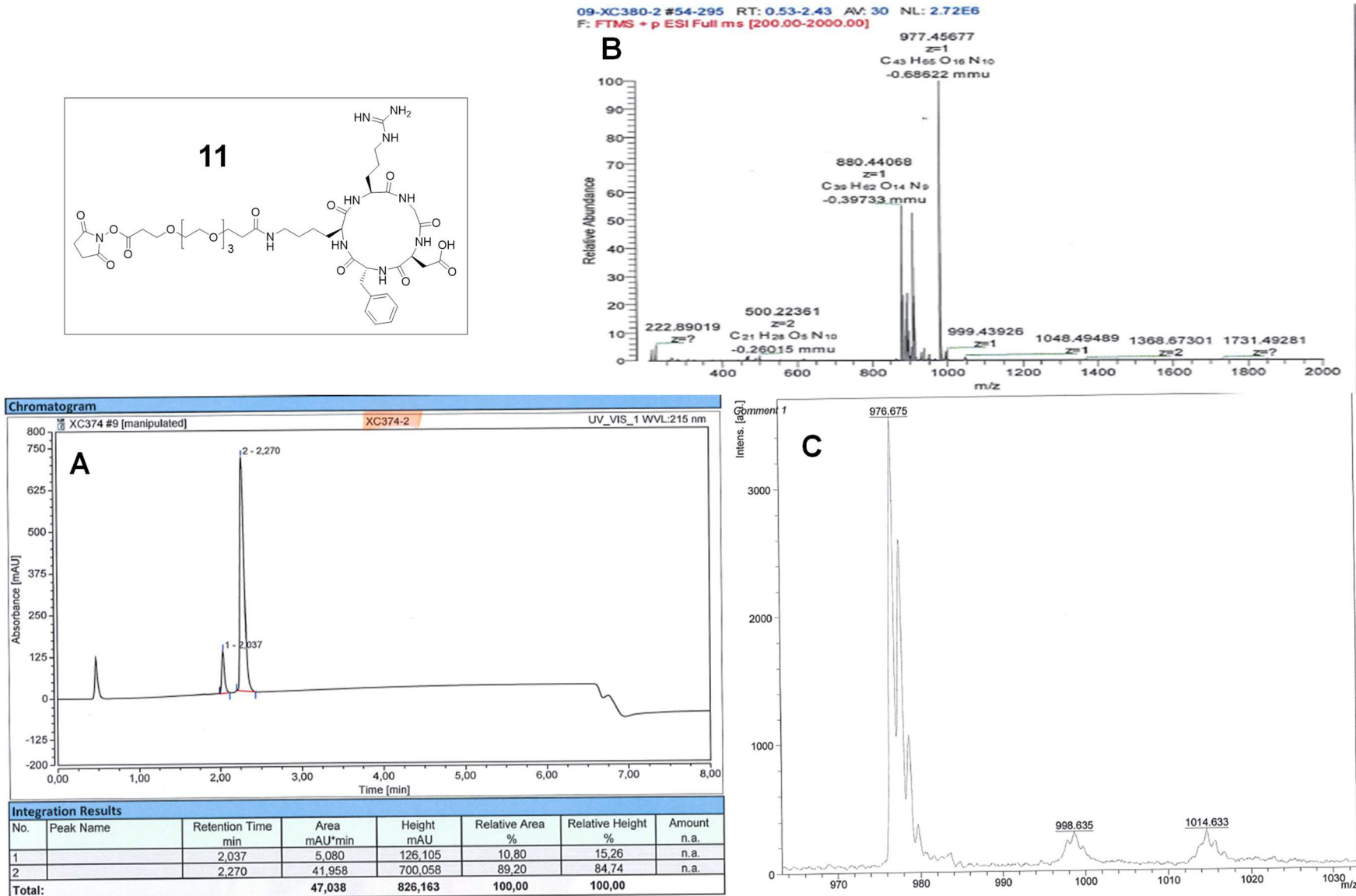


Figure S5. HPLC chromatogram (**A**) and mass spectra (**B**: ESI, **C**: MALDI) of NHS-PEG₃-c(RGDfK) (**11**).

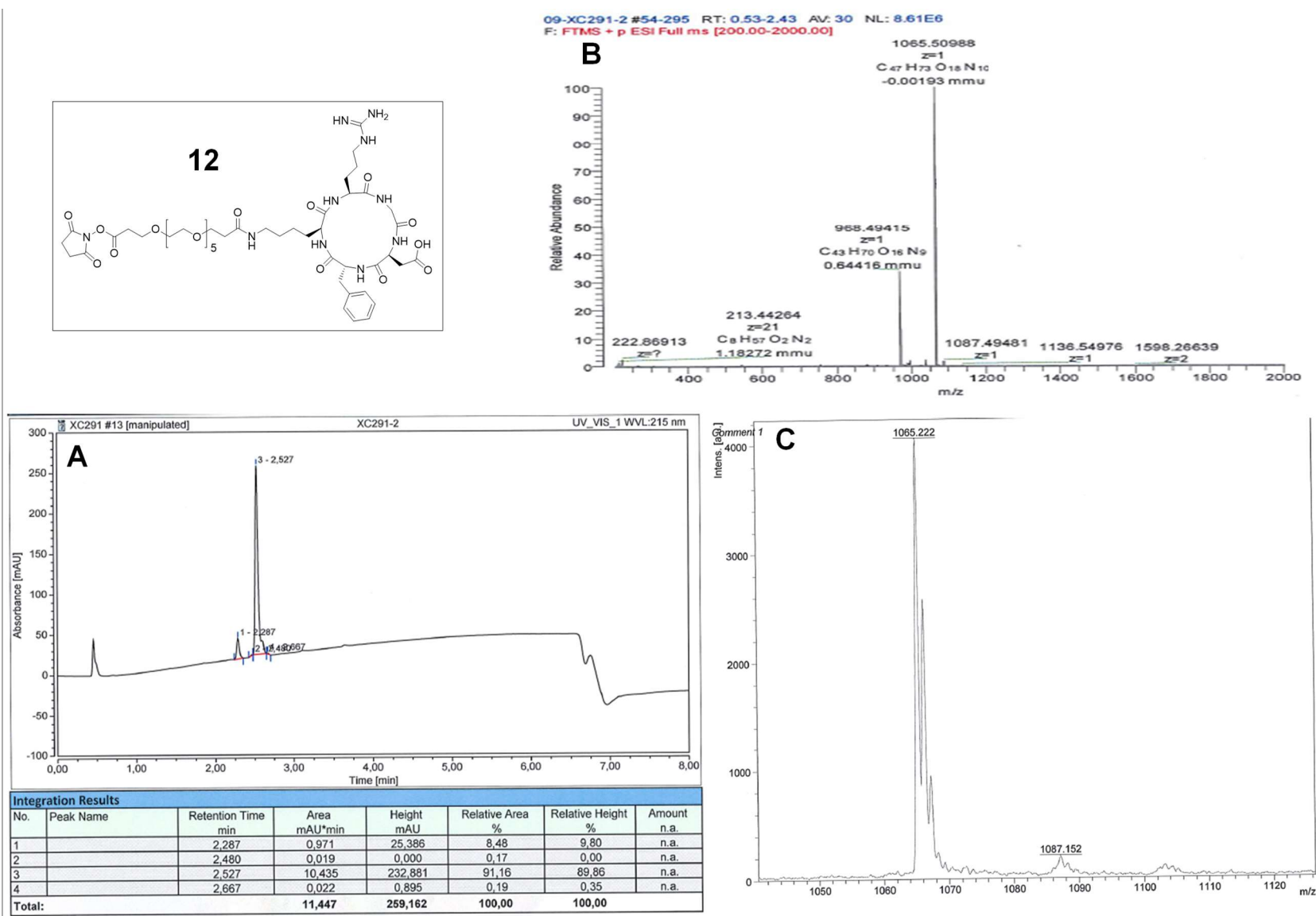


Figure S6. HPLC chromatogram (**A**) and mass spectra (**B**: ESI, **C**: MALDI) of NHS-PEG₅-c(RGDfK) (**12**).

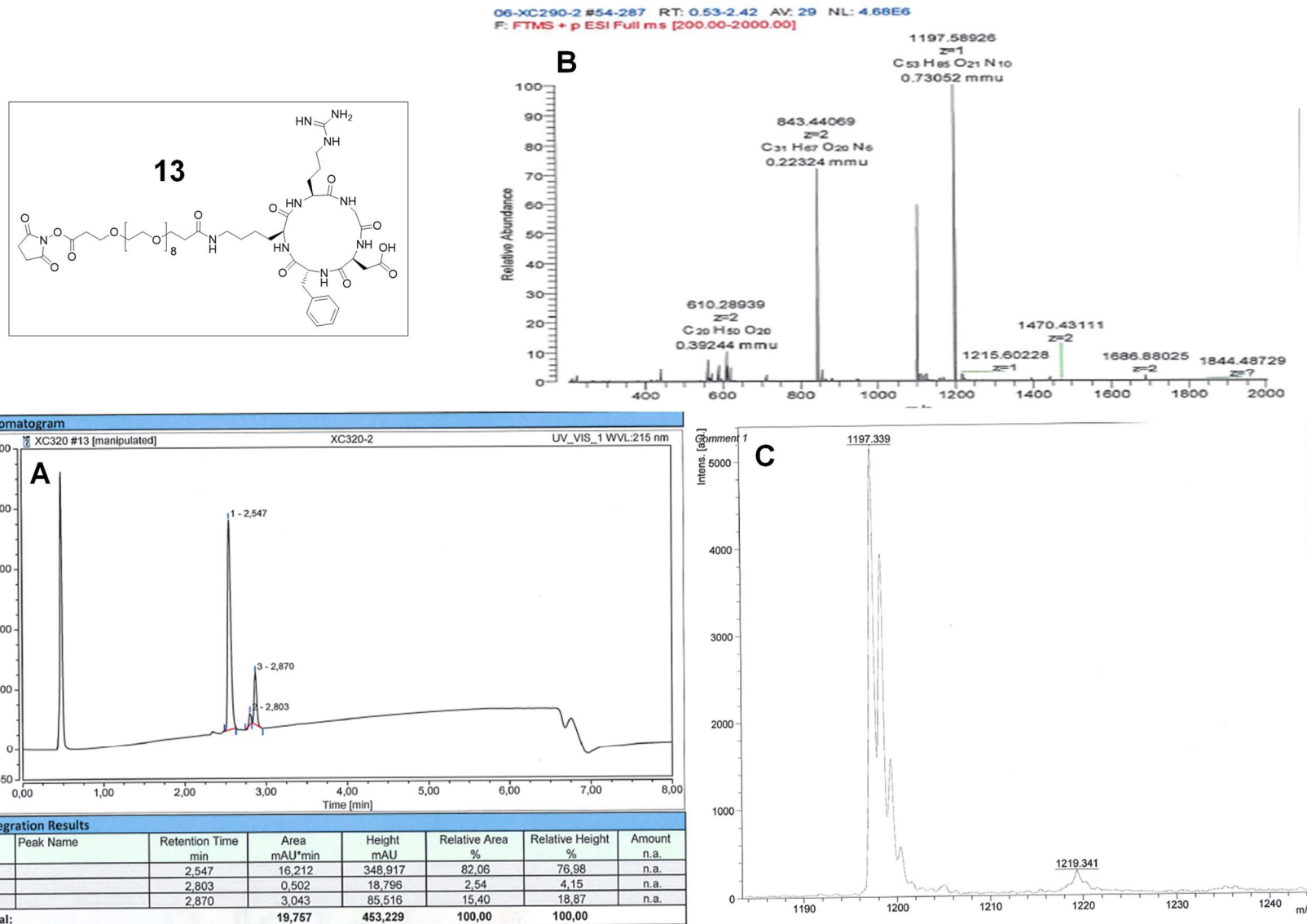


Figure S7. HPLC chromatogram (**A**) and mass spectra (**B**: ESI, **C**: MALDI) of NHS-PEG₈-c(RGDfK) (**13**).

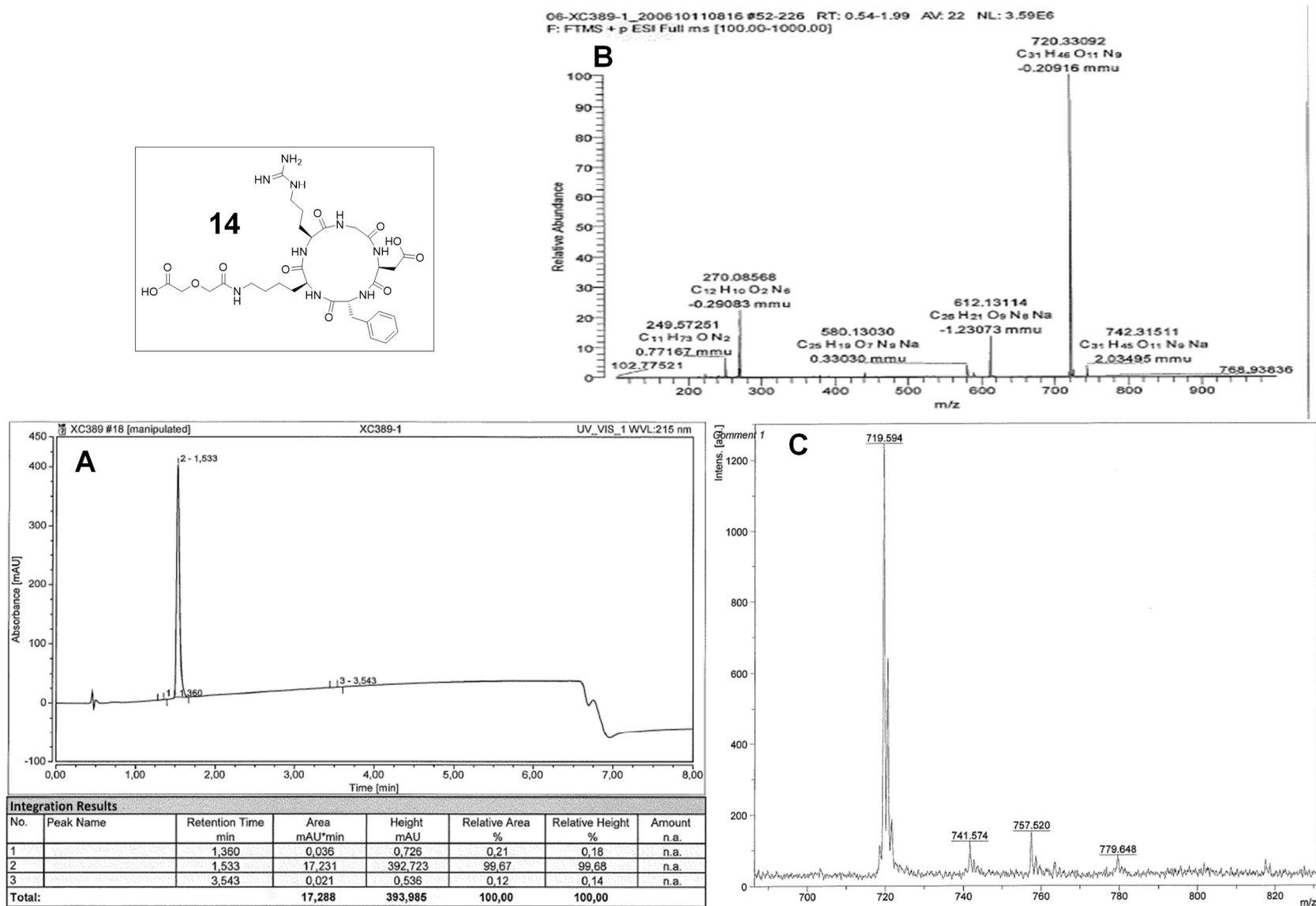


Figure S8. HPLC chromatogram (**A**) and mass spectra (**B**: ESI, **C**: MALDI) of HO-DIG-c(RGDfK) (**14**).

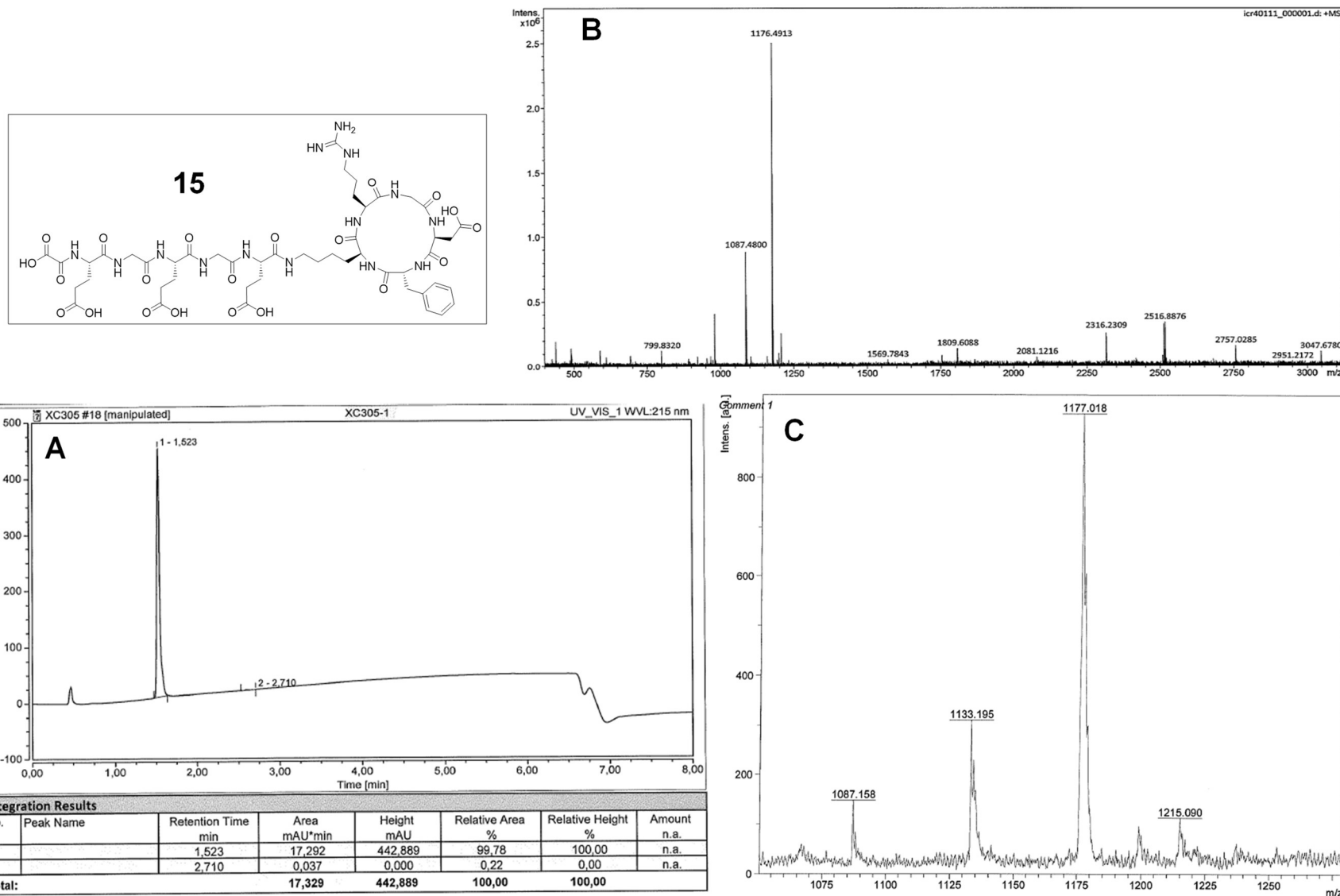


Figure S9. HPLC chromatogram (**A**) and mass spectra (**B**: ESI, **C**: MALDI) of HO-Ox-EGEGE-c(RGDfK) (**15**).

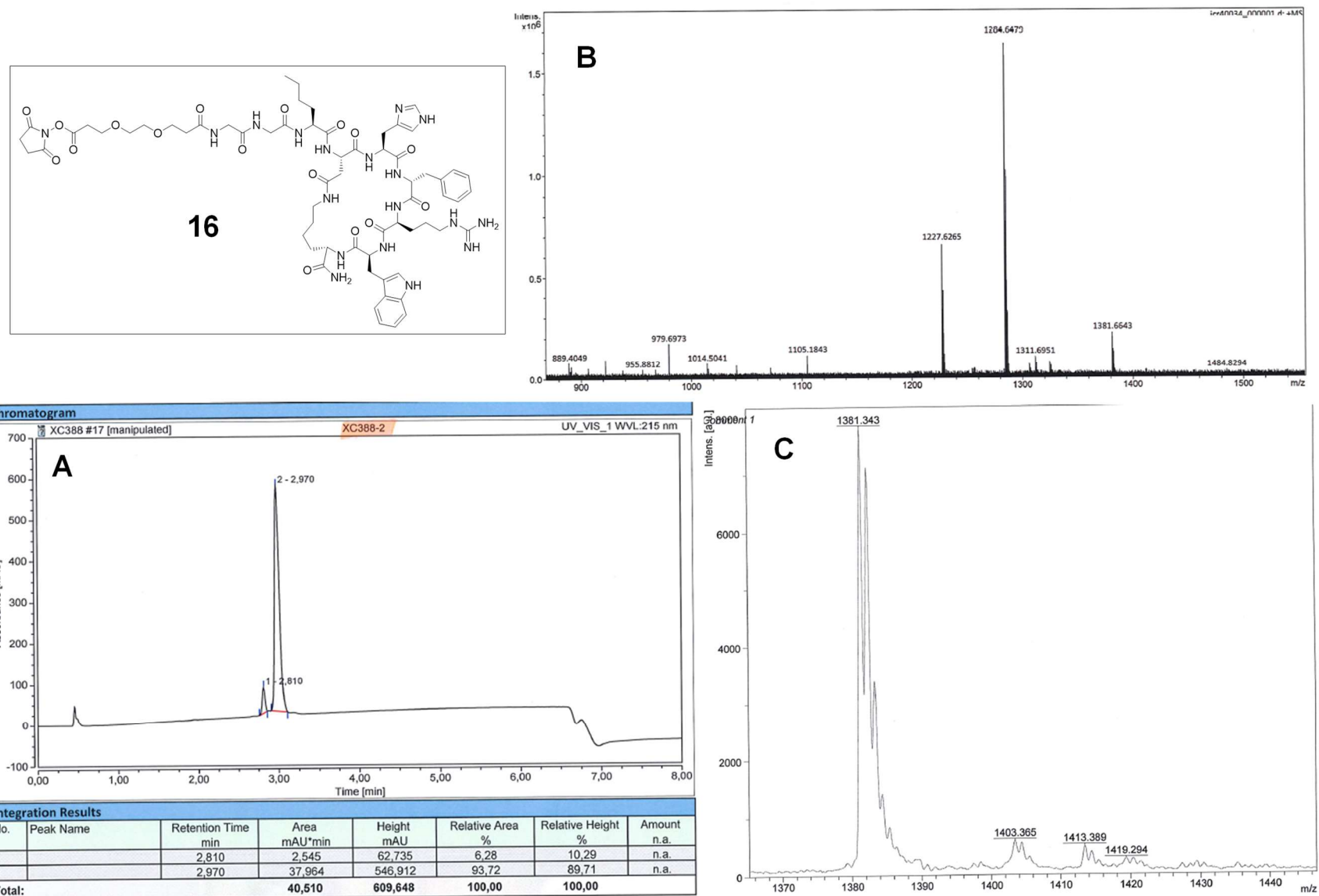


Figure S10. HPLC chromatogram (**A**) and mass spectra (**B**: ESI, **C**: MALDI) of NHS-PEG₁-GG-Nle-c(DHfRWK) (**16**).

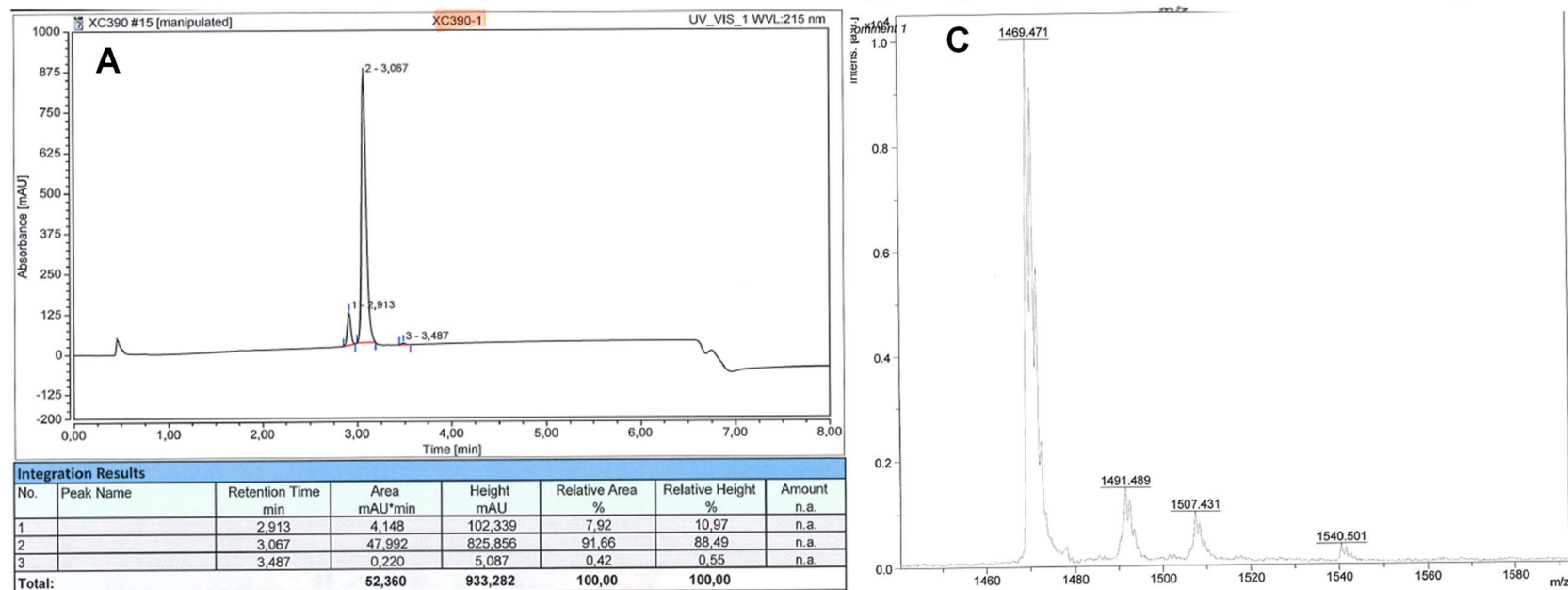
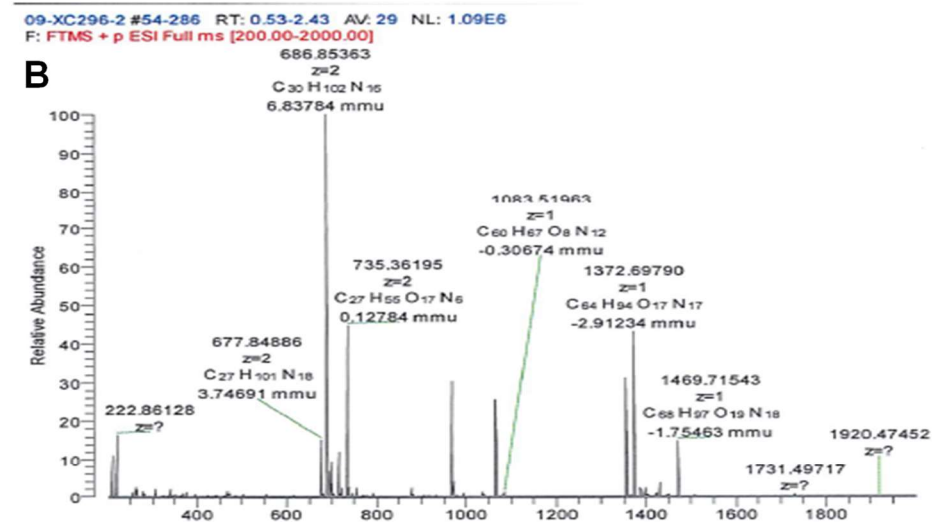
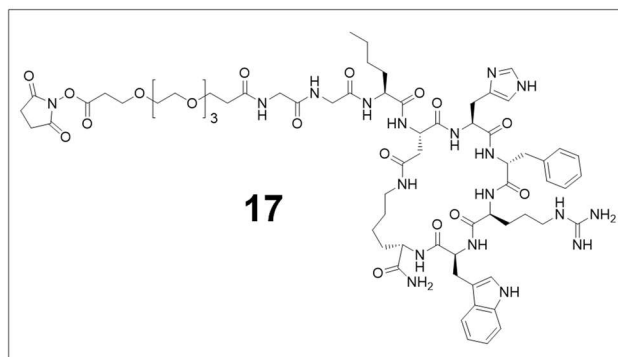


Figure S11. HPLC chromatogram (**A**) and mass spectra (**B**: ESI, **C**: MALDI) of NHS-PEG₃-GG-Nle-c(DHfRWK) (**17**).

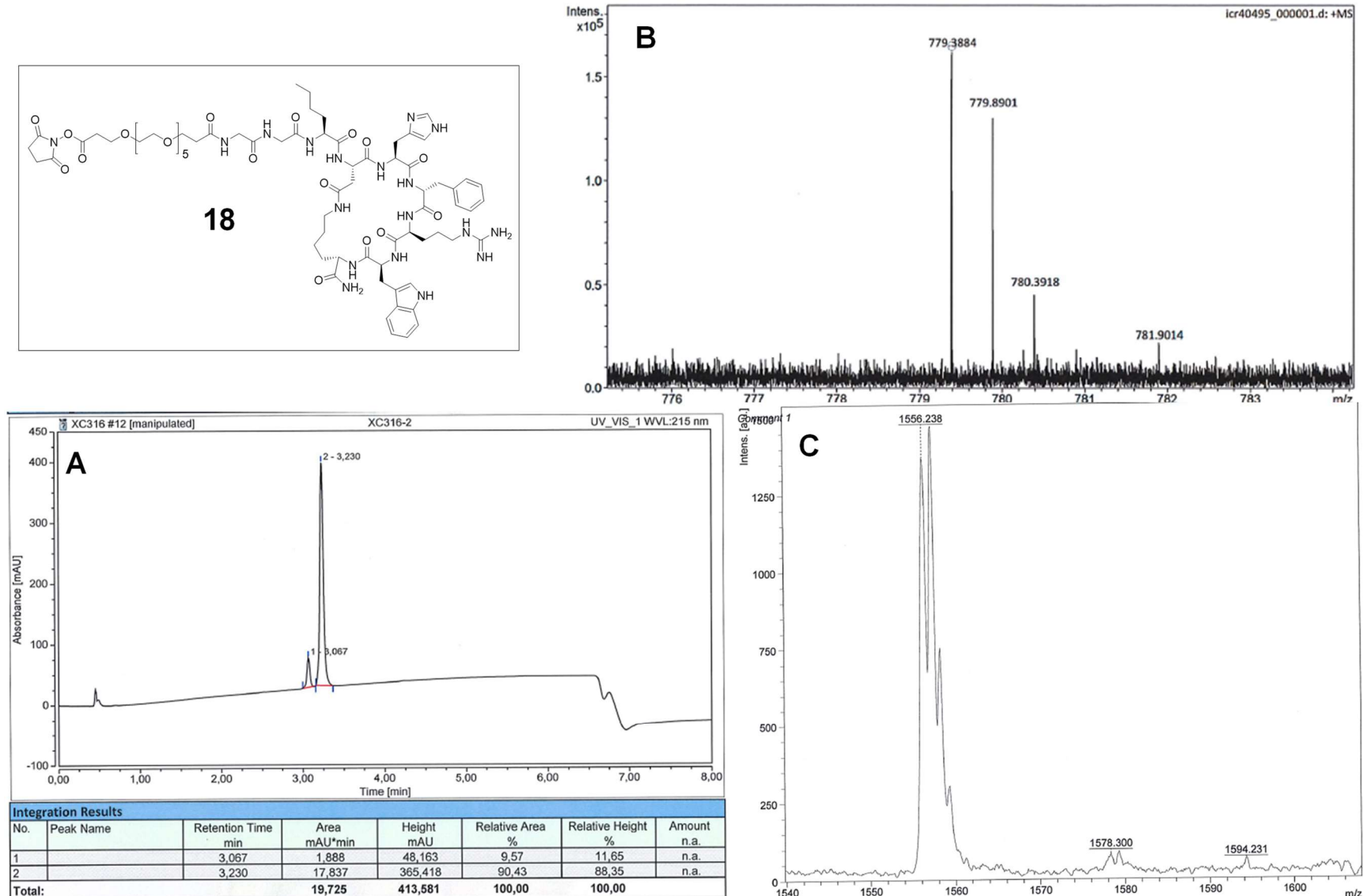
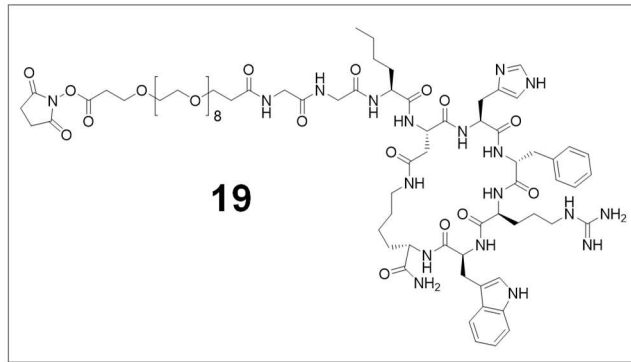


Figure S12. HPLC chromatogram (**A**) and mass spectra (**B**: ESI, **C**: MALDI) of NHS-PEG₅-GG-Nle-c(DHfRWK) (**18**).



06-XC323-2 #54-280 RT: 0.53-2.42 AV: 28 NL: 2.49E6
F: FTMS + p ESI Full ms [200.00-2000.00]

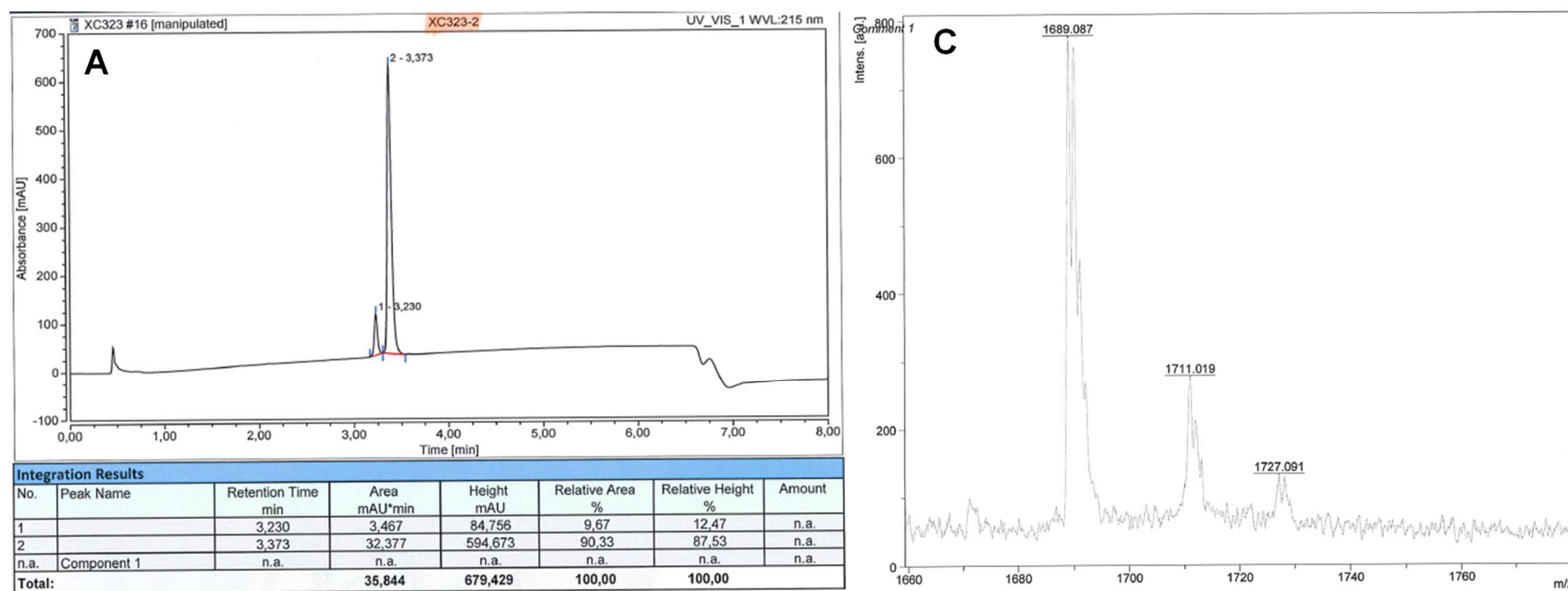
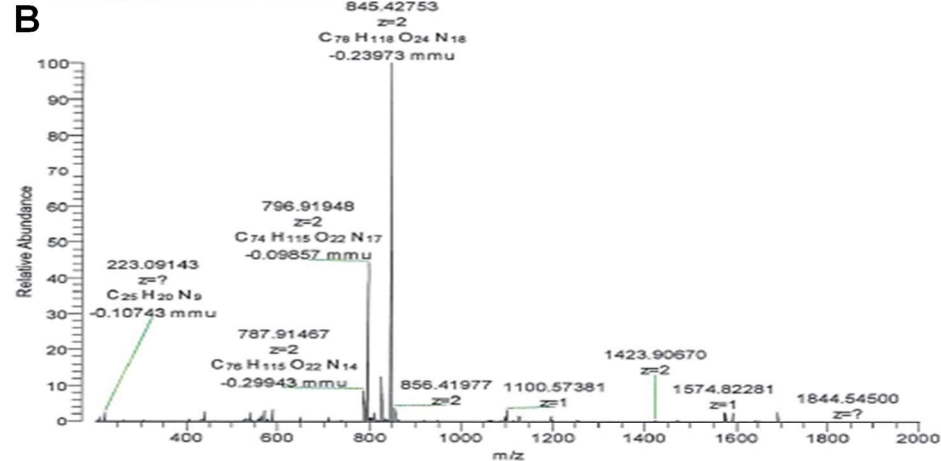
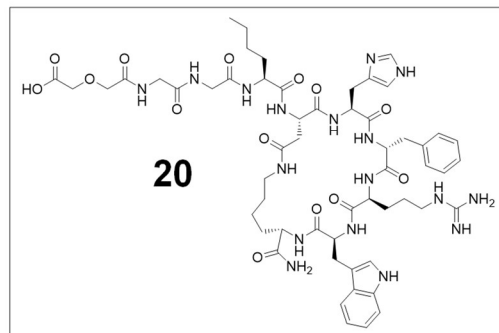
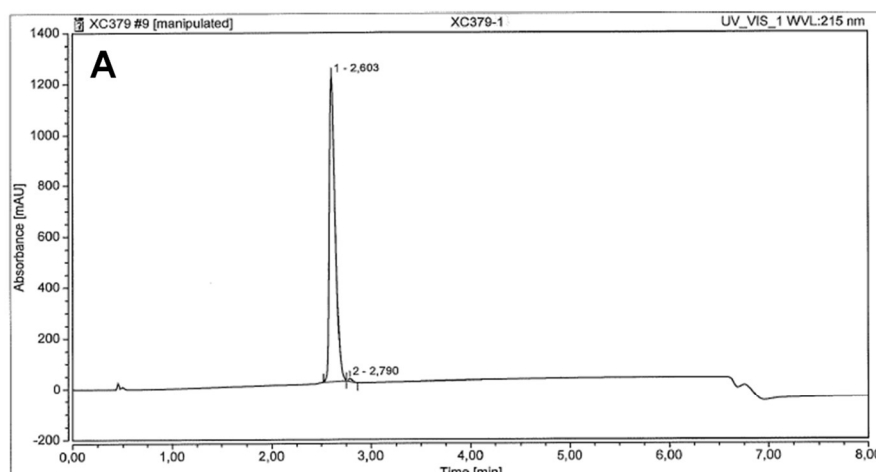
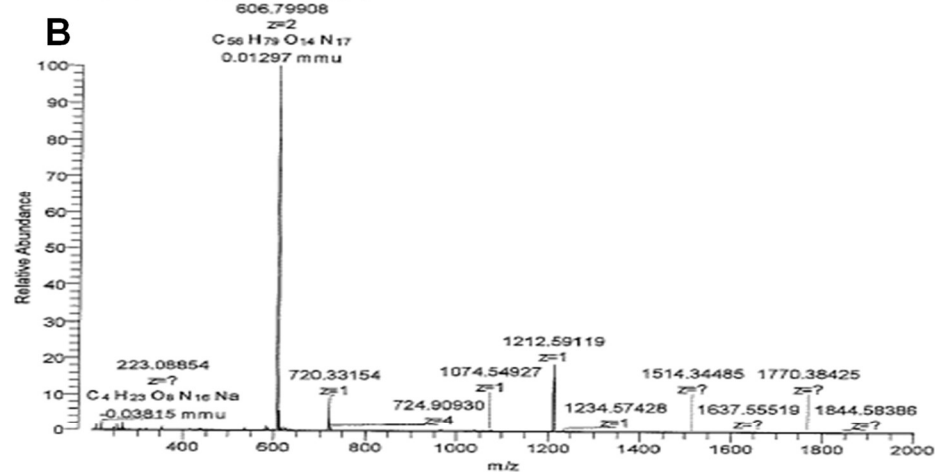


Figure S13. HPLC chromatogram (**A**) and mass spectra (**B**: ESI, **C**: MALDI) of NHS-PEG₈-GG-Nle-c(DHfRWK) (**19**).



06-XC393-1 #55-287 RT: 0.52-2.42 AV: 29 NL: 2.43E6
F: FTMS + p ESI Full ms [200.00-2000.00]



Integration Results							
No.	Peak Name	Retention Time min	Area mAU*min	Height mAU	Relative Area %	Relative Height %	Amount
1		2,603	83,686	1201.263	99.56	99.21	n.a.
2		2,790	0,367	9.554	0.44	0.79	n.a.
Total:			84,053	1210.817	100,00	100,00	

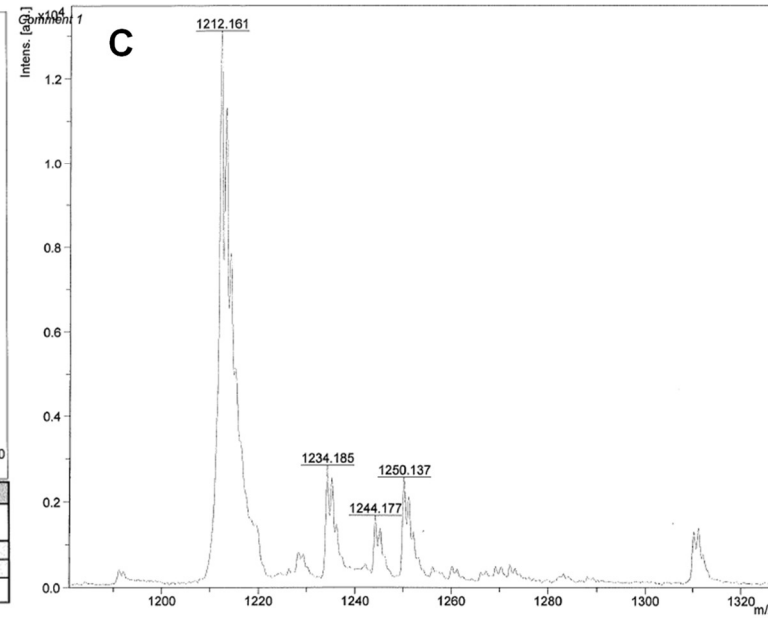


Figure S14. HPLC chromatogram (**A**) and mass spectra (**B**: ESI, **C**: MALDI) of HO-DIG-GG-Nle-c(DHfRWK) (**20**).

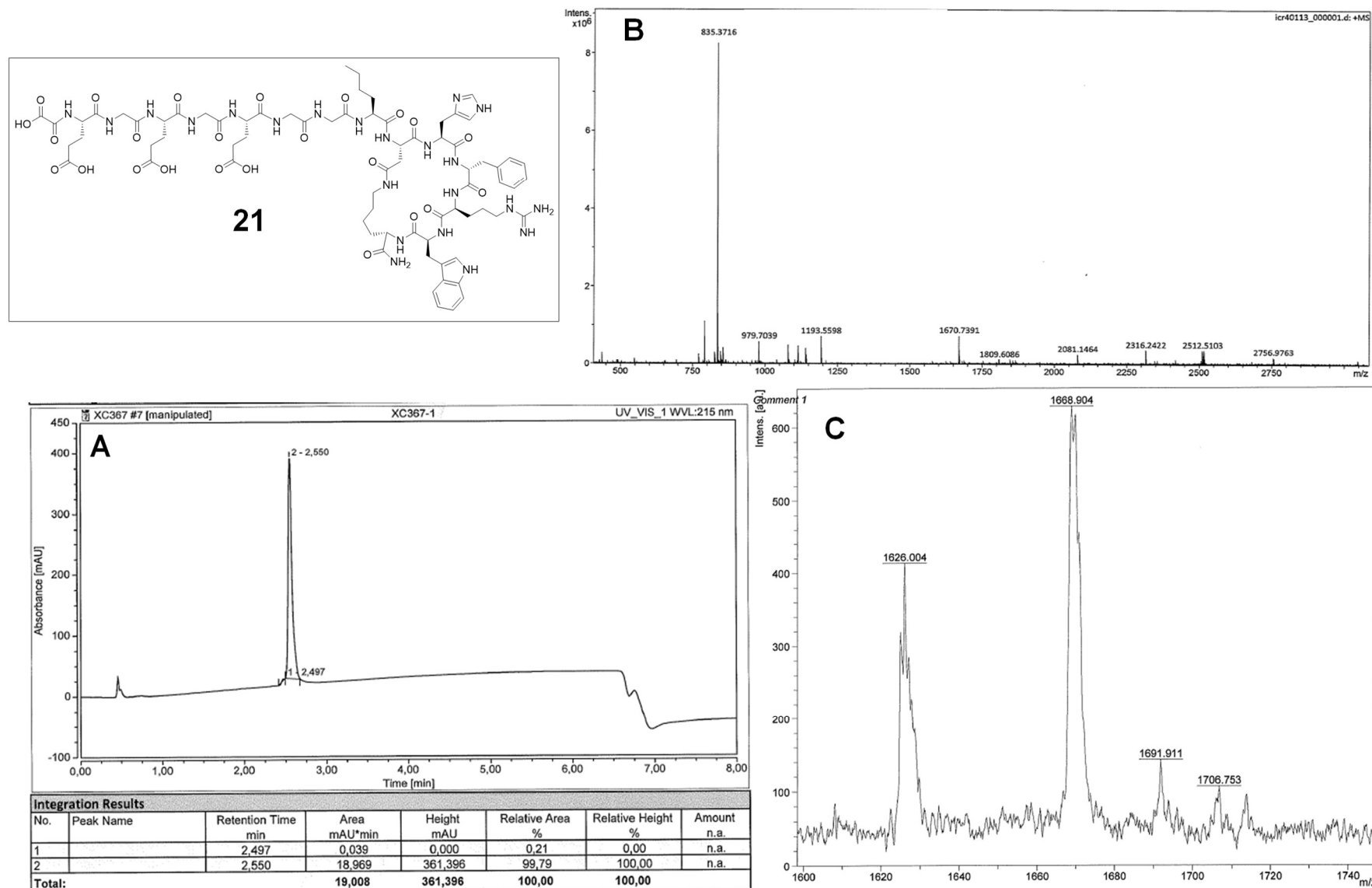


Figure S15. HPLC chromatogram (**A**) and mass spectra (**B**: ESI, **C**: MALDI) of HO-Ox-EGEGE-GG-Nle-c(DHfRWK) (**21**).

2. NMR and mass spectra of SiFAlin 28, SiFAlin-modified framework 29 and their intermediates 22–27

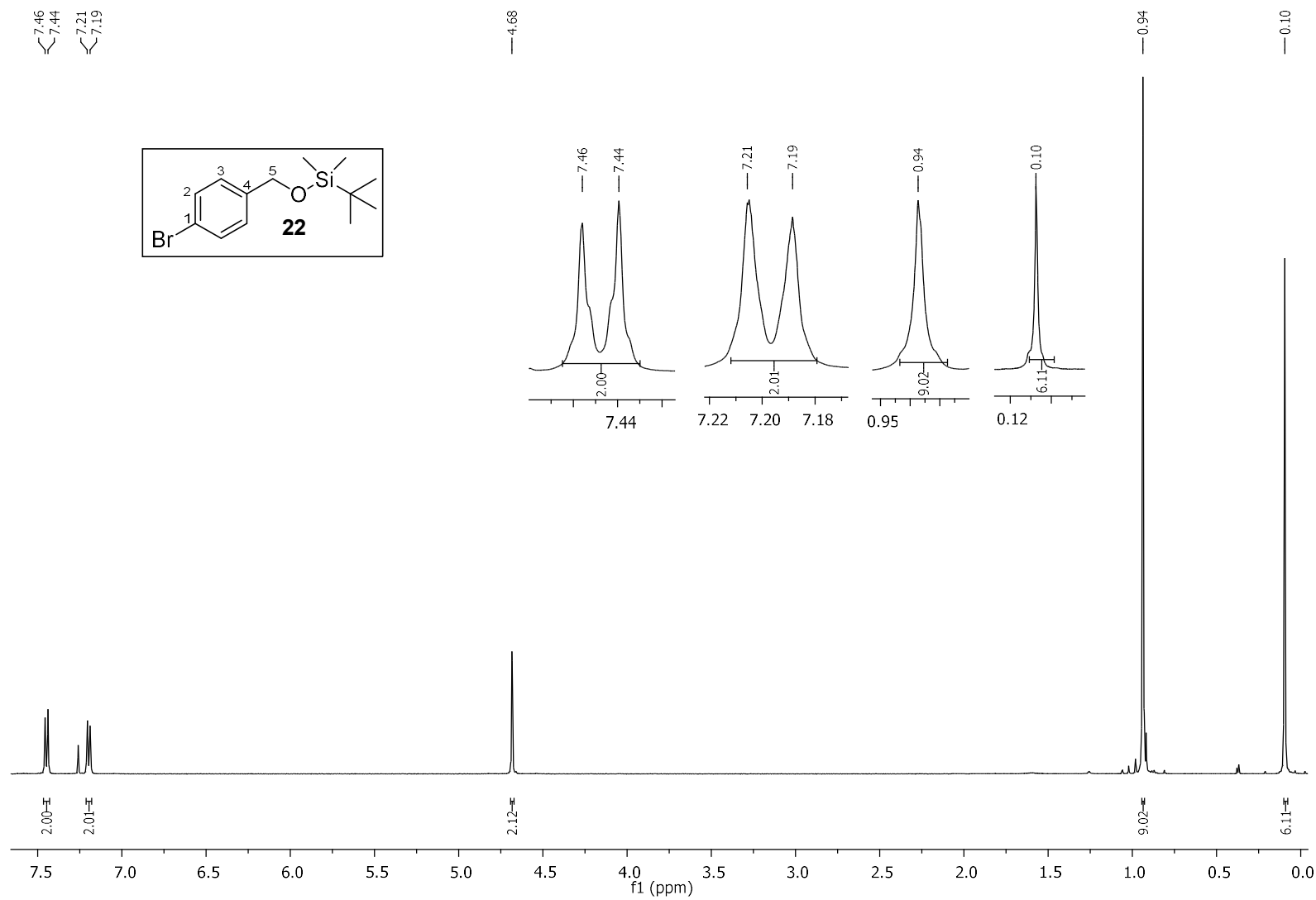


Figure S16: ¹H NMR spectrum of ((4-Bromobenzyl)oxy)(*tert*-butyl)dimethylsilane (**22**).

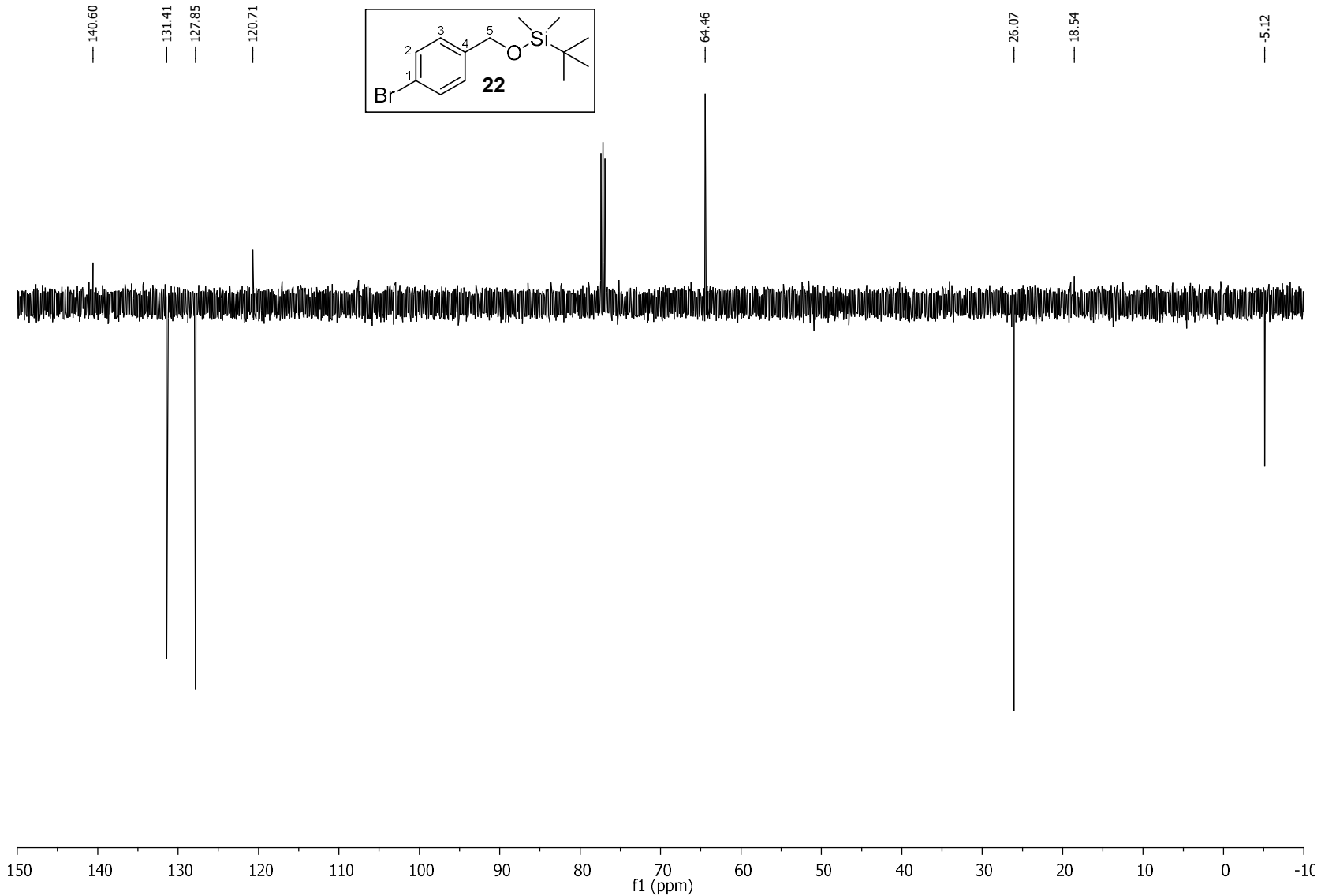


Figure S17. ^{13}C NMR spectrum of ((4-Bromobenzyl)oxy)(*tert*-butyl)dimethylsilane (**22**).

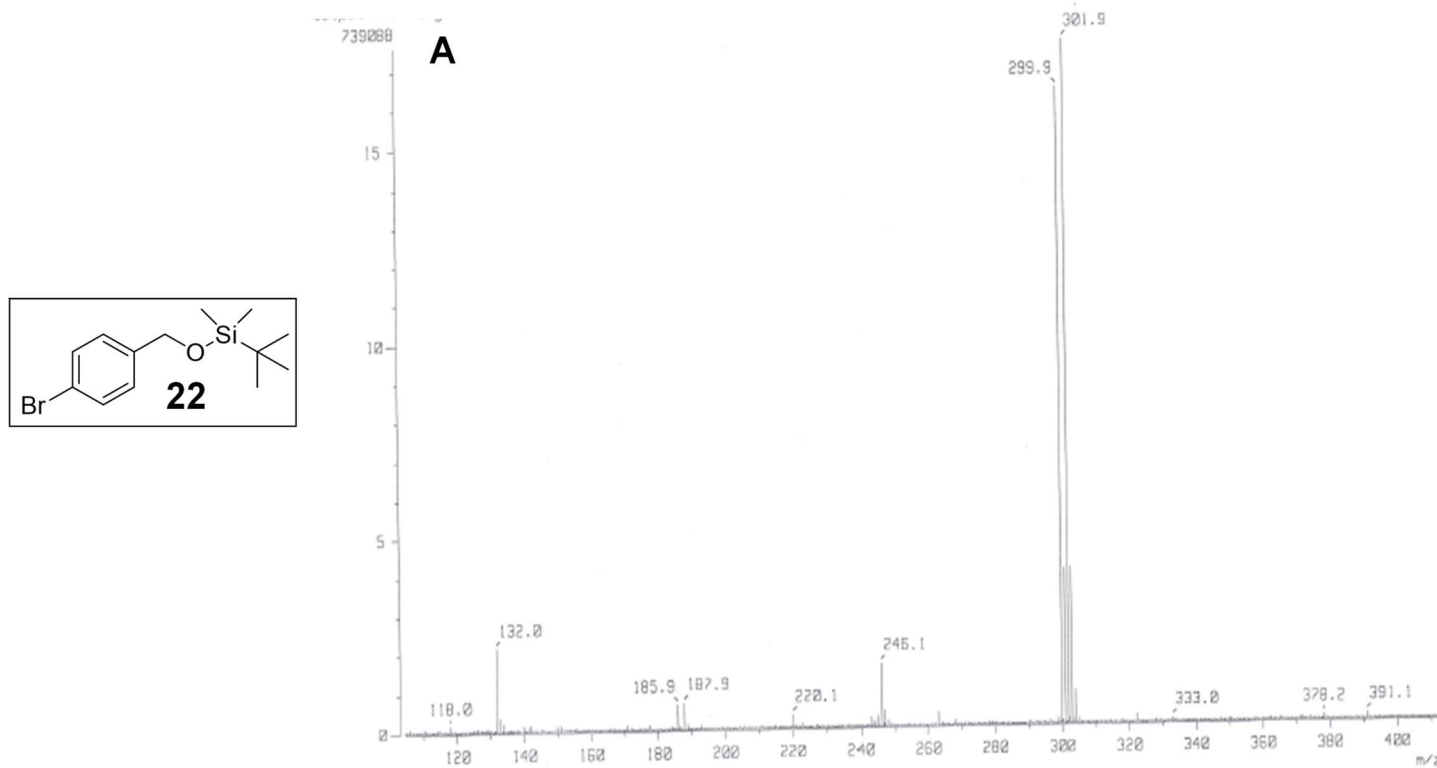
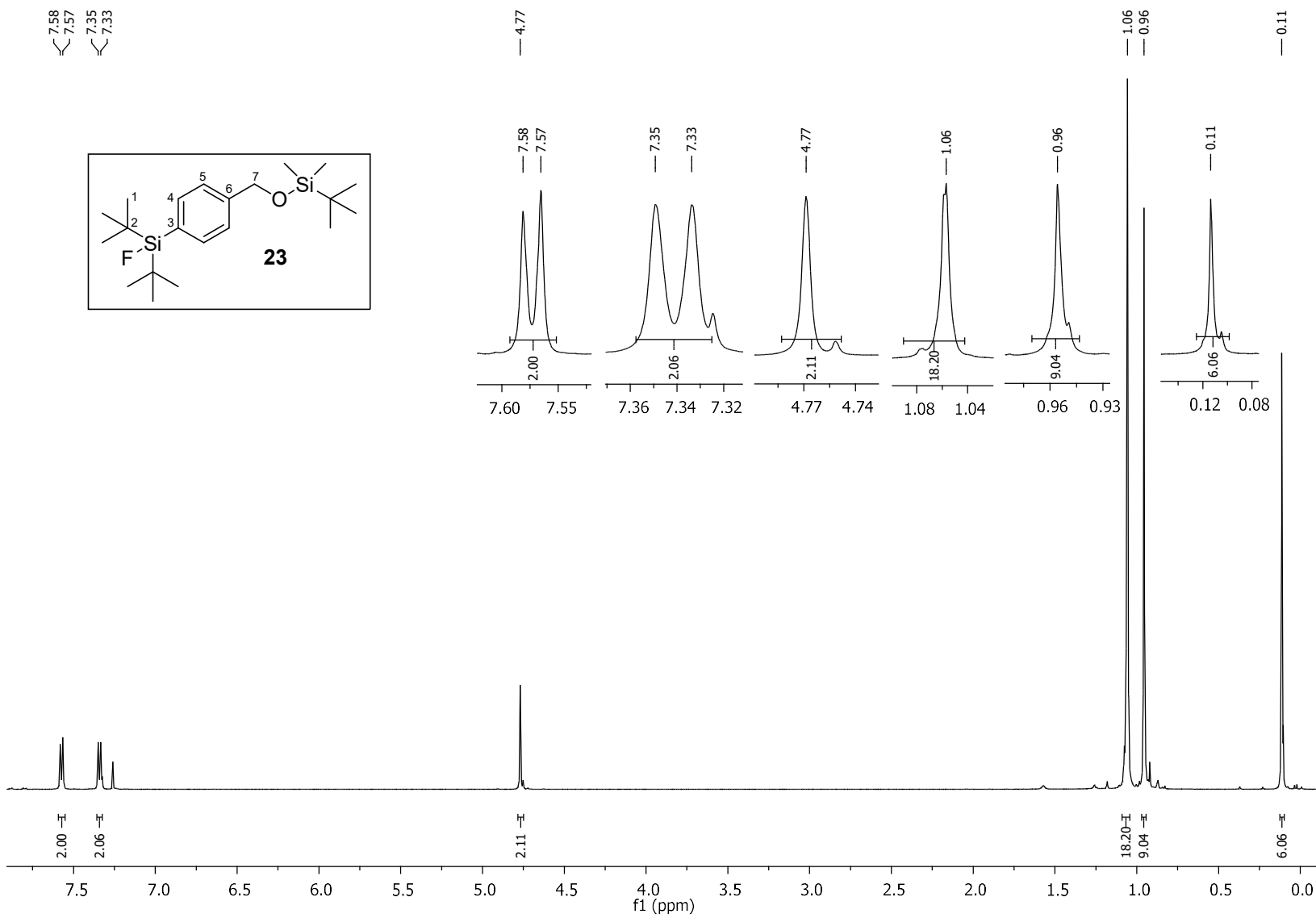


Figure S18. Mass spectrum (A: FI) of ((4-Bromobenzyl)oxy)(*tert*-butyl)dimethylsilane (**22**).



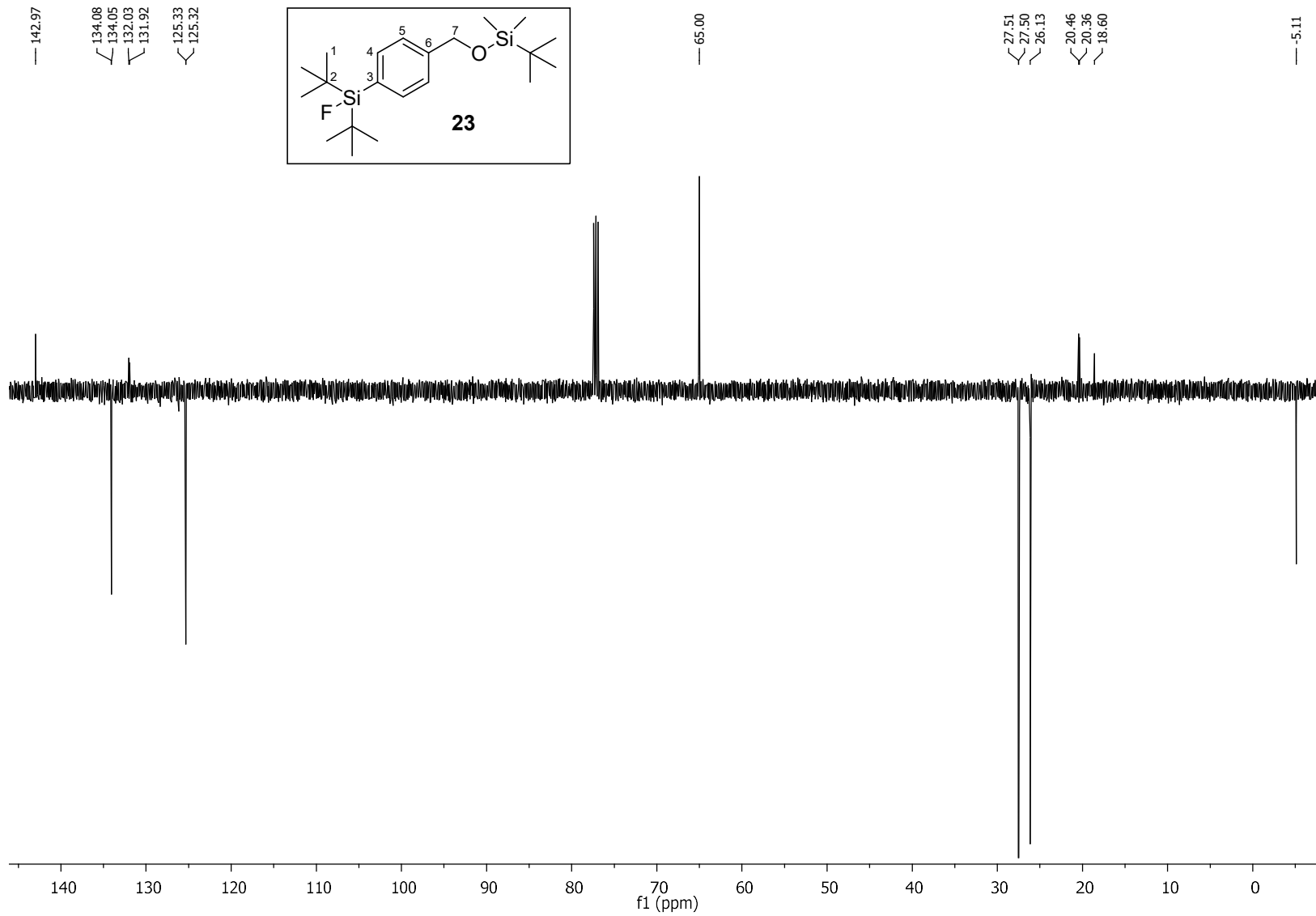


Figure S20. ^{13}C NMR spectrum of Di-*tert*-butyl(4-((*tert*-butyldimethylsilyl)oxy)methyl)phenyl)fluorosilane (**23**).

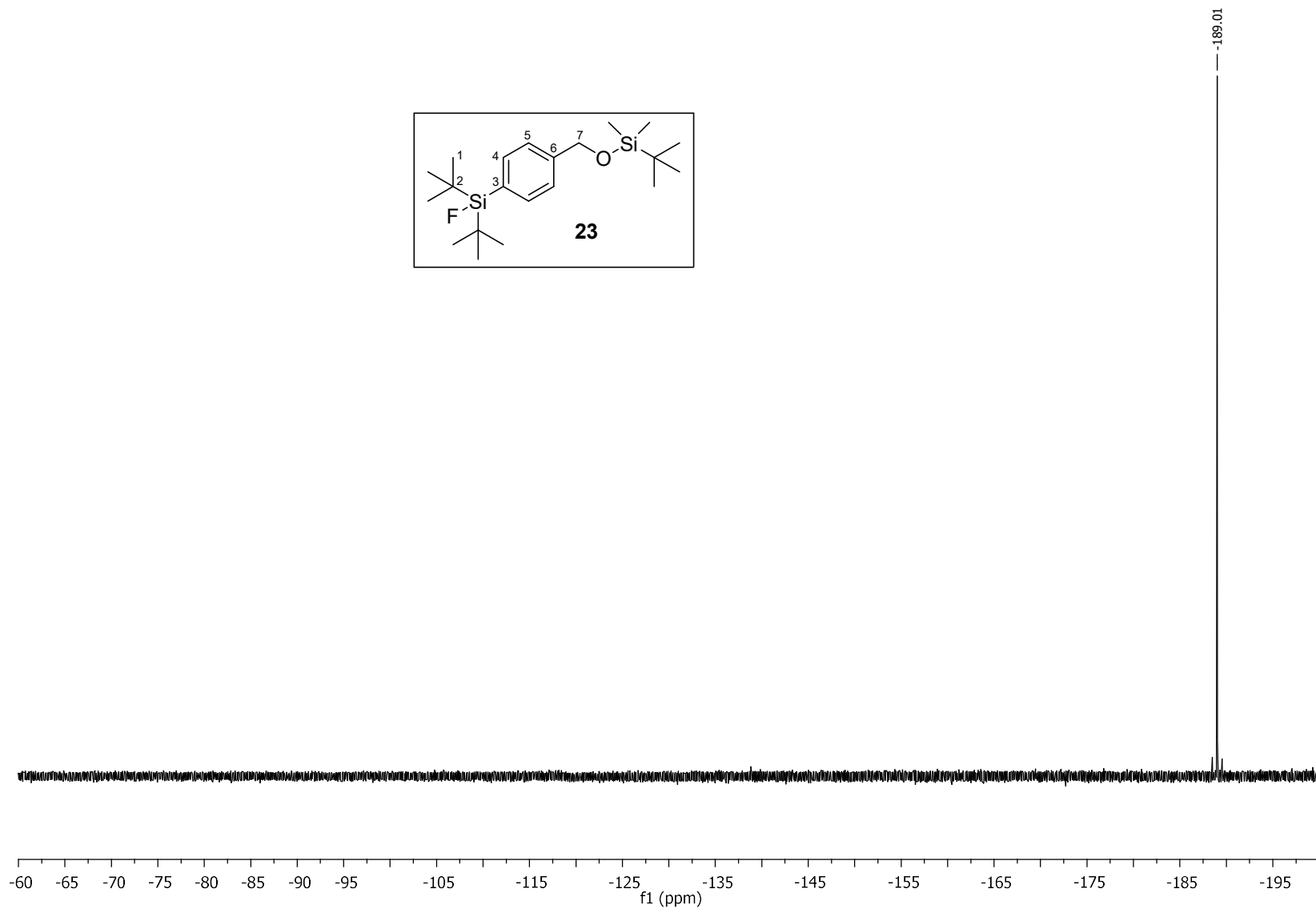


Figure S21. ^{19}F NMR spectrum of Di-*tert*-butyl(4-(((*tert*-butyldimethylsilyl)oxy)methyl)phenyl)fluorosilane (**23**).

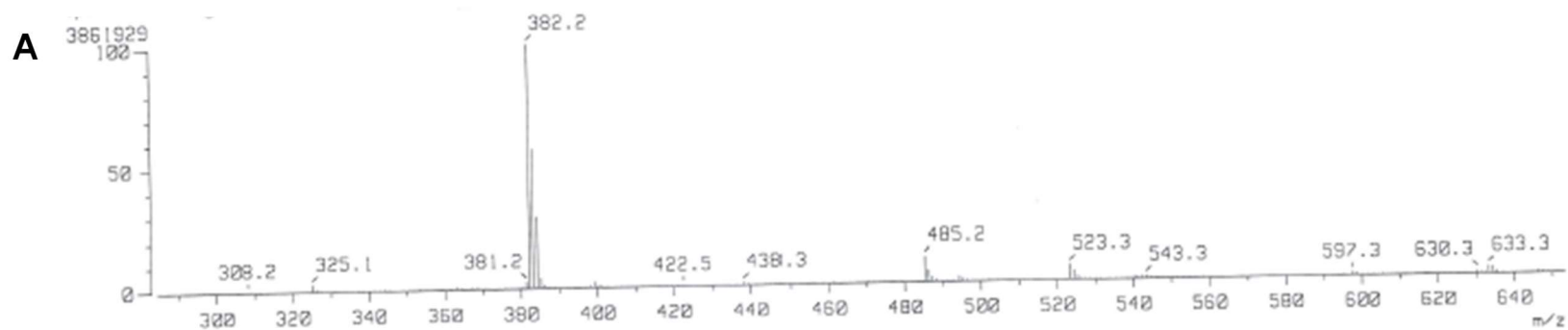
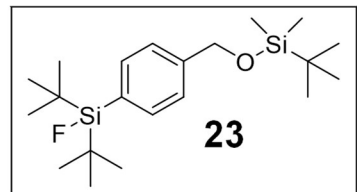
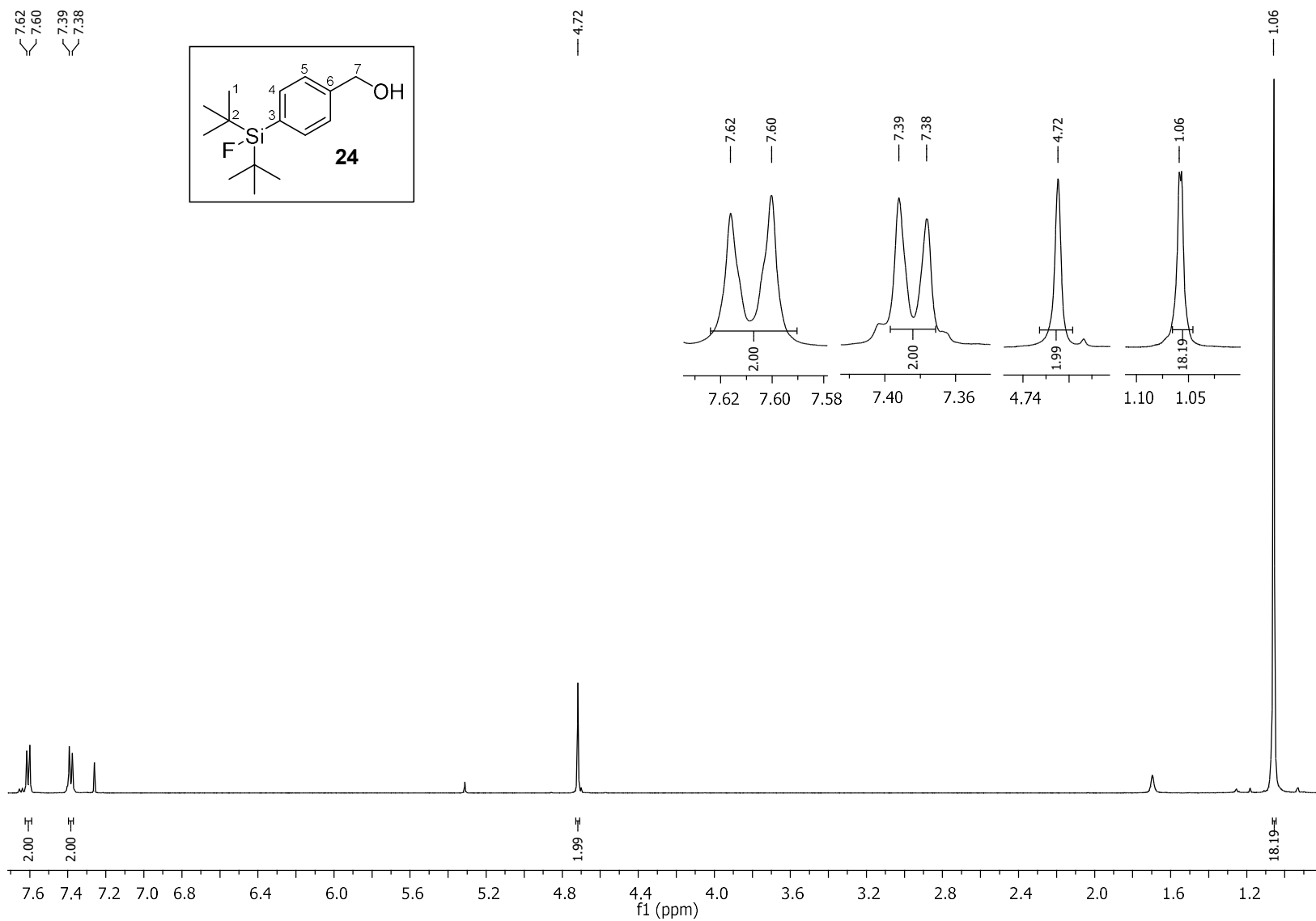


Figure S22. Mass spectrum (A: FD) of Di-*tert*-butyl(4-(((*tert*-butyldimethylsilyl)oxy)methyl)phenyl)fluorosilane (**23**).



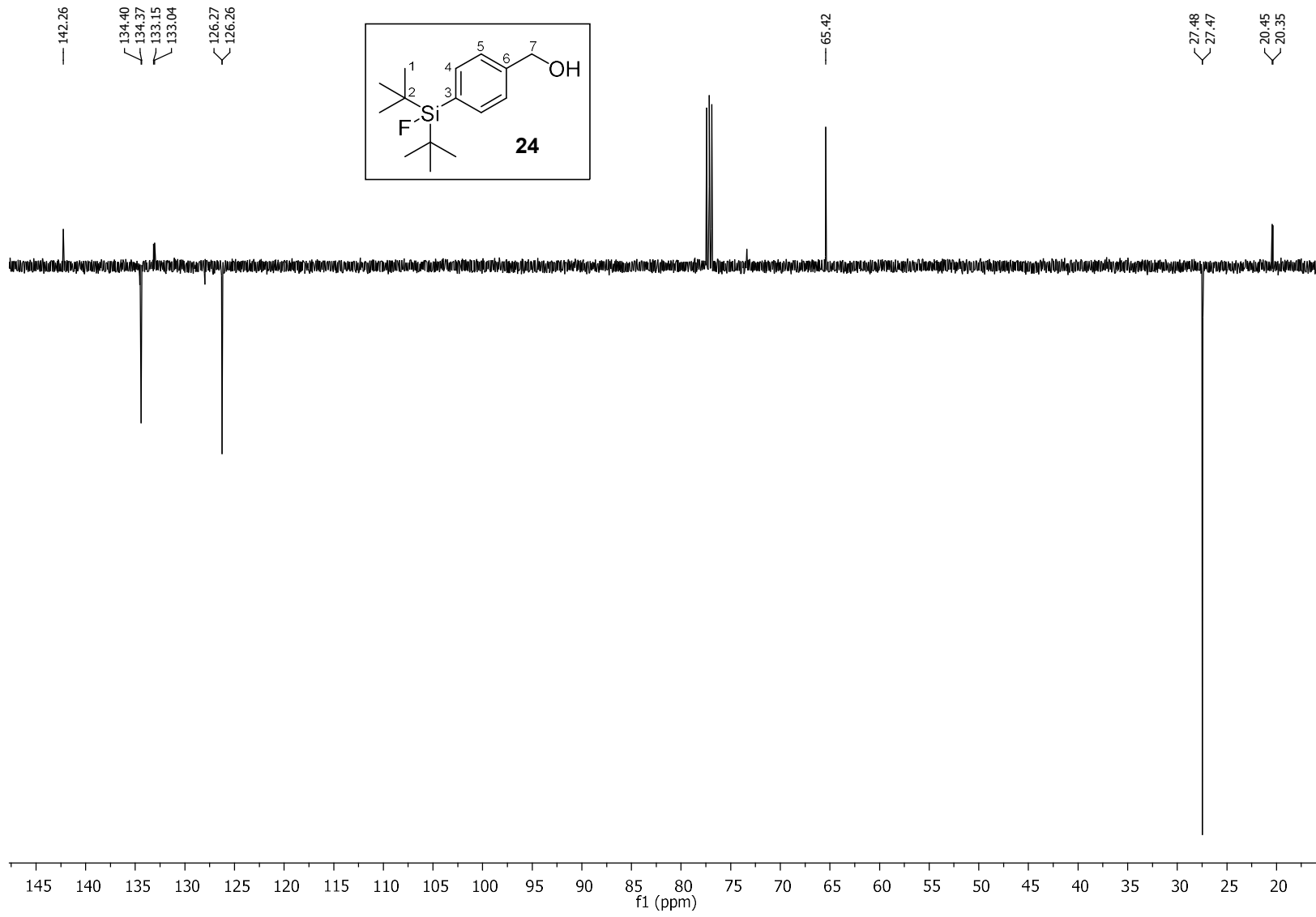


Figure S24. ^{13}C NMR spectrum of (4-(Di-*tert*-butylfluorosilyl)phenyl)methanol (**24**).

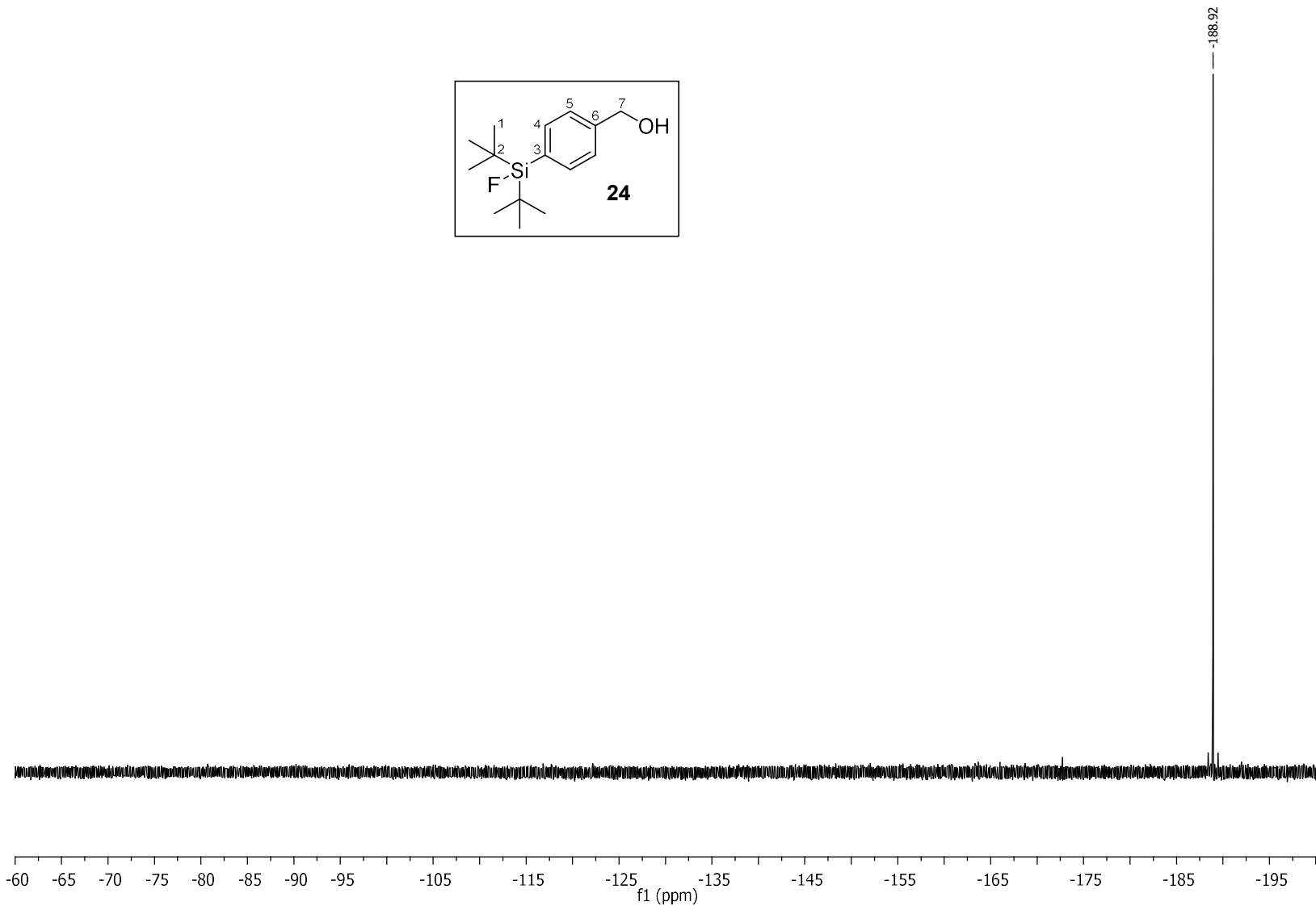


Figure S25. ^{19}F NMR spectrum of (4-(Di-*tert*-butylfluorosilyl)phenyl)methanol (**24**).

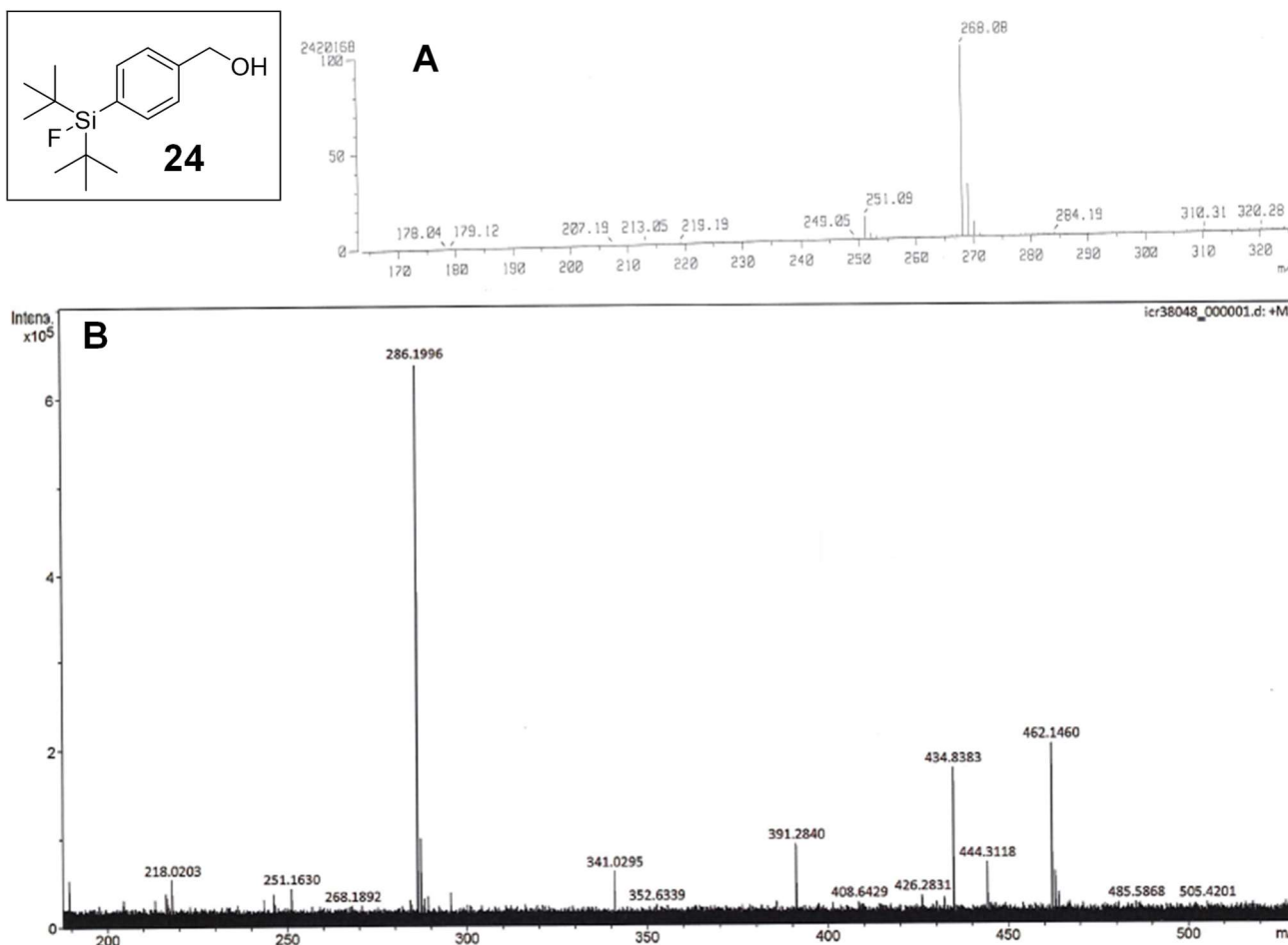


Figure S26. Mass spectra (**A**: FD, **B**: DART) of (4-(Di-*tert*-butylfluorosilyl)phenyl)methanol (**24**).

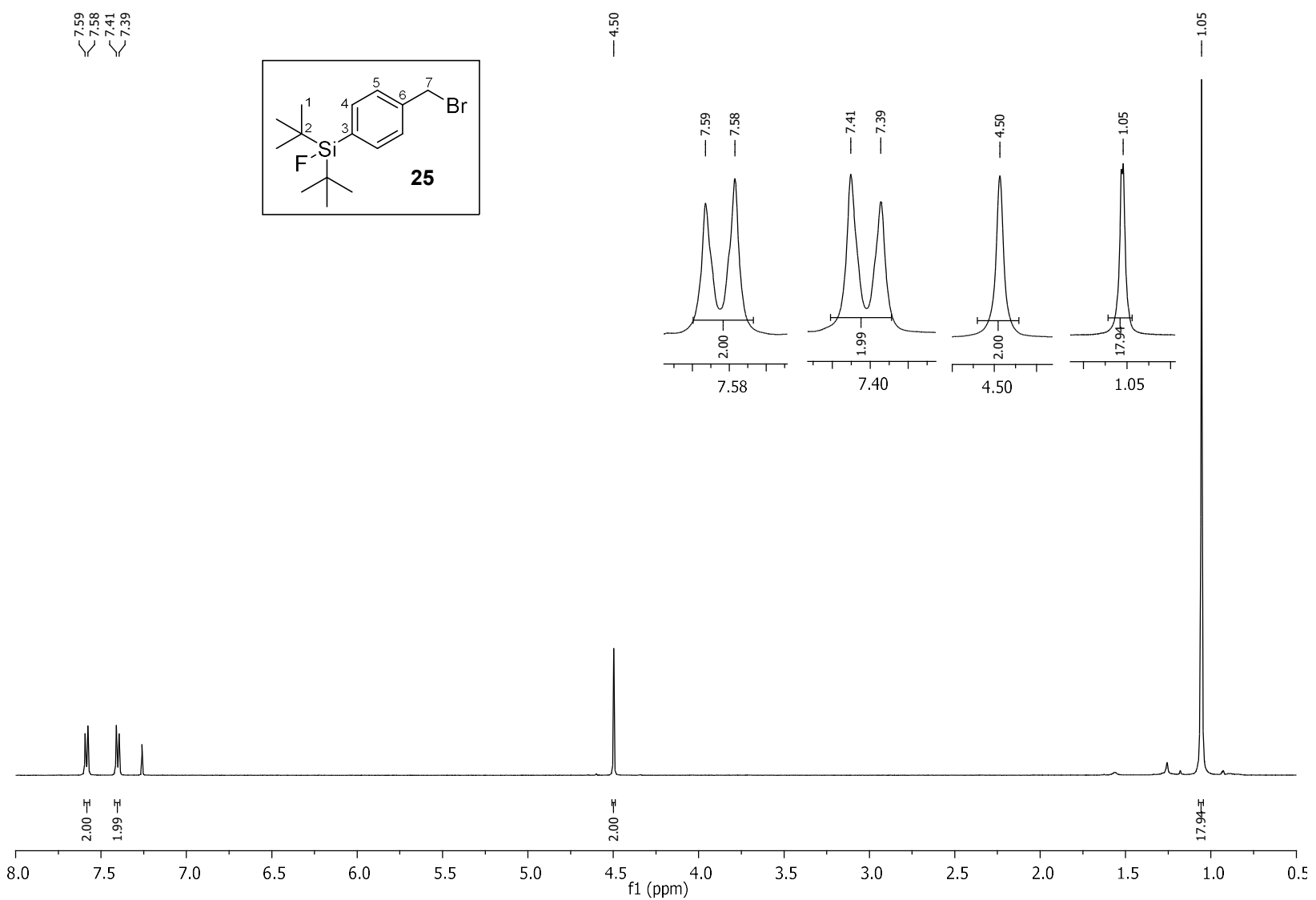


Figure S27. ^1H NMR spectrum of (4-(Bromomethyl)phenyl)di-*tert*-butylfluorosilane (**25**).

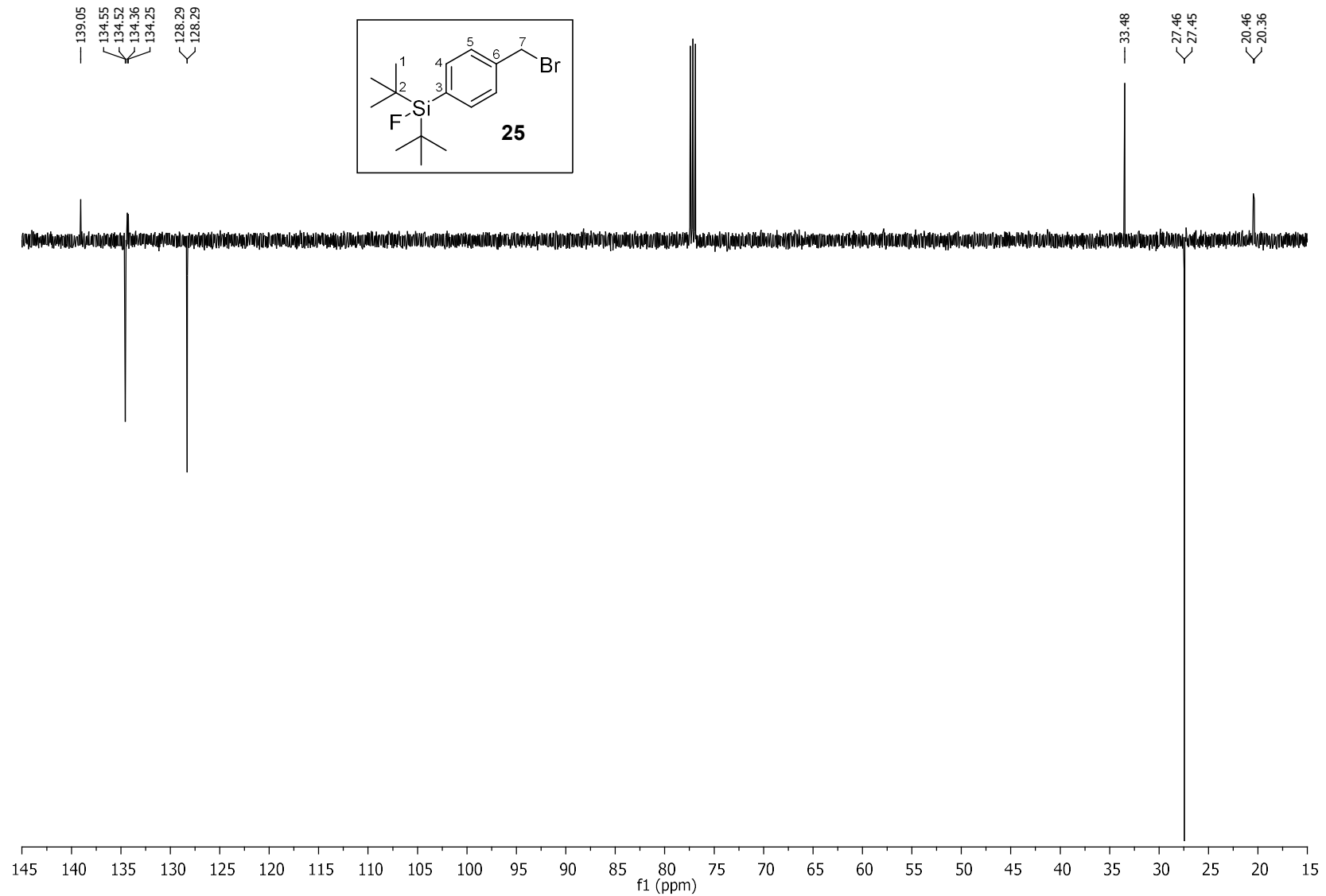


Figure S28. ^{13}C NMR spectrum of (4-(Bromomethyl)phenyl)di-*tert*-butylfluorosilane (**25**).

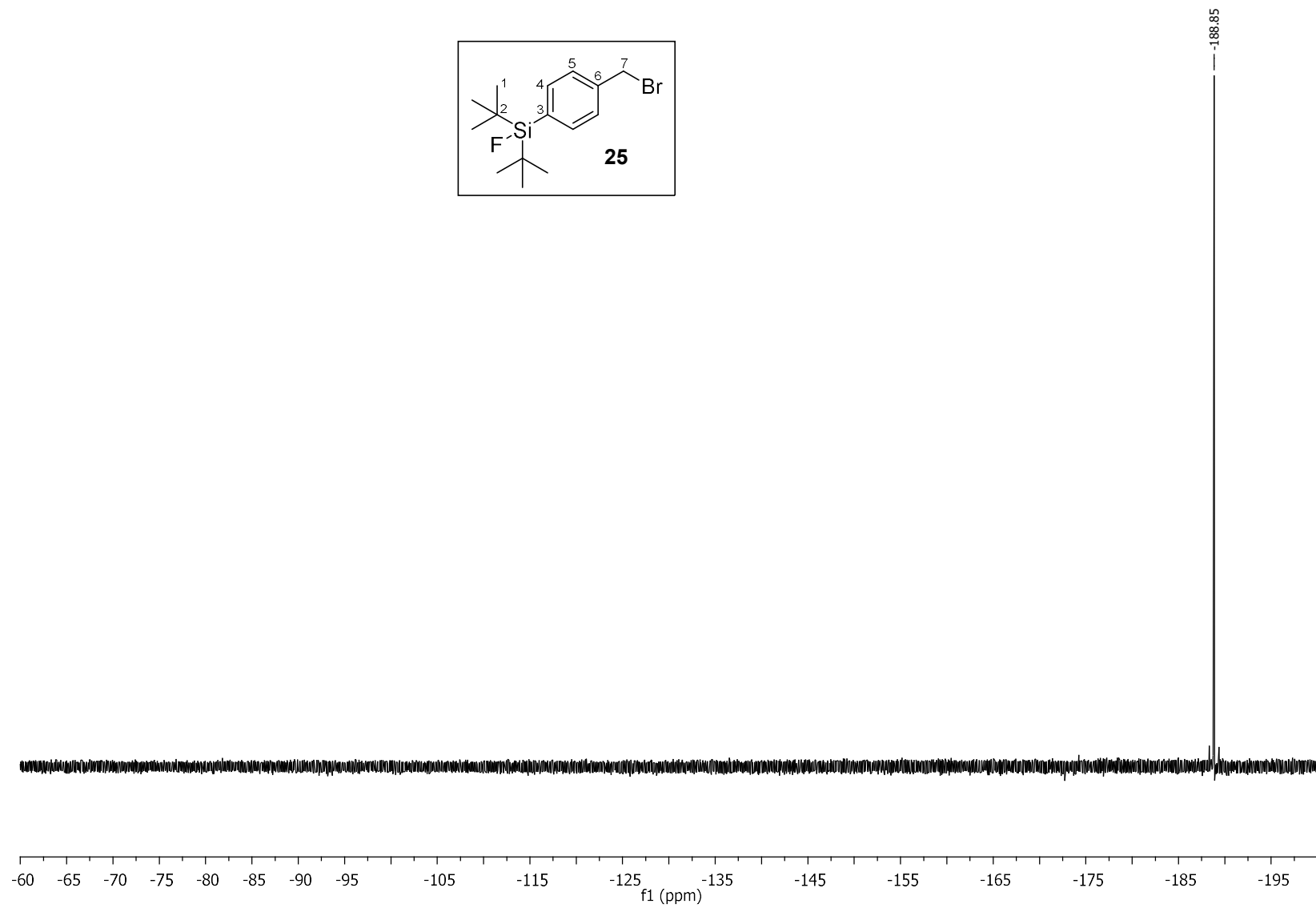


Figure S29. ${}^{19}\text{F}$ NMR spectrum of (4-(Bromomethyl)phenyl)di-*tert*-butylfluorosilane (**25**).

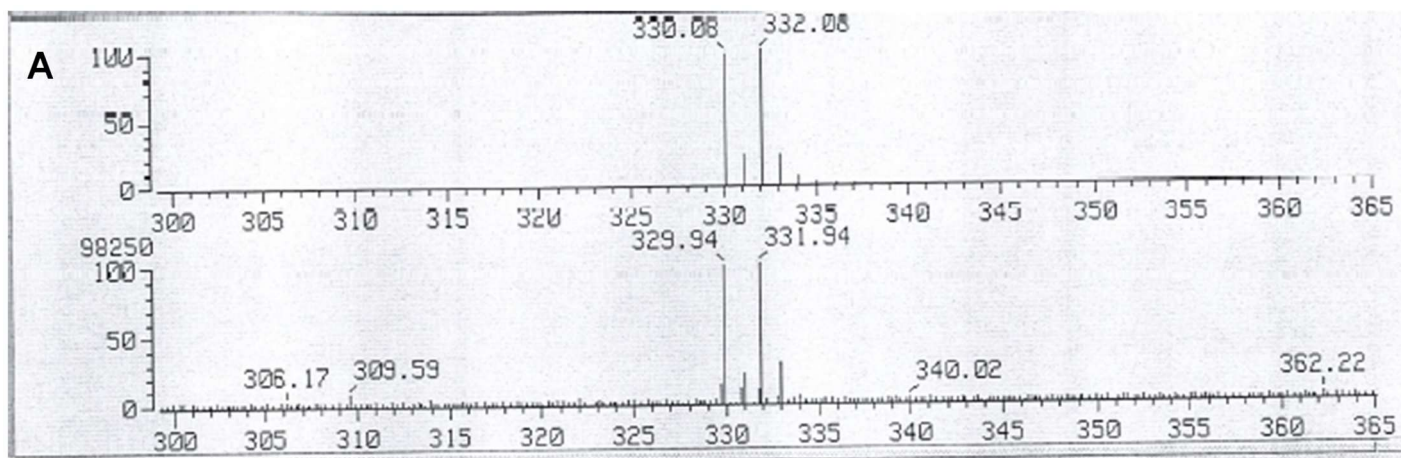
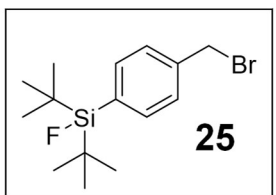


Figure S30. Mass spectrum (A: FD) of (4-(Bromomethyl)phenyl)di-*tert*-butylfluorosilane (**25**).

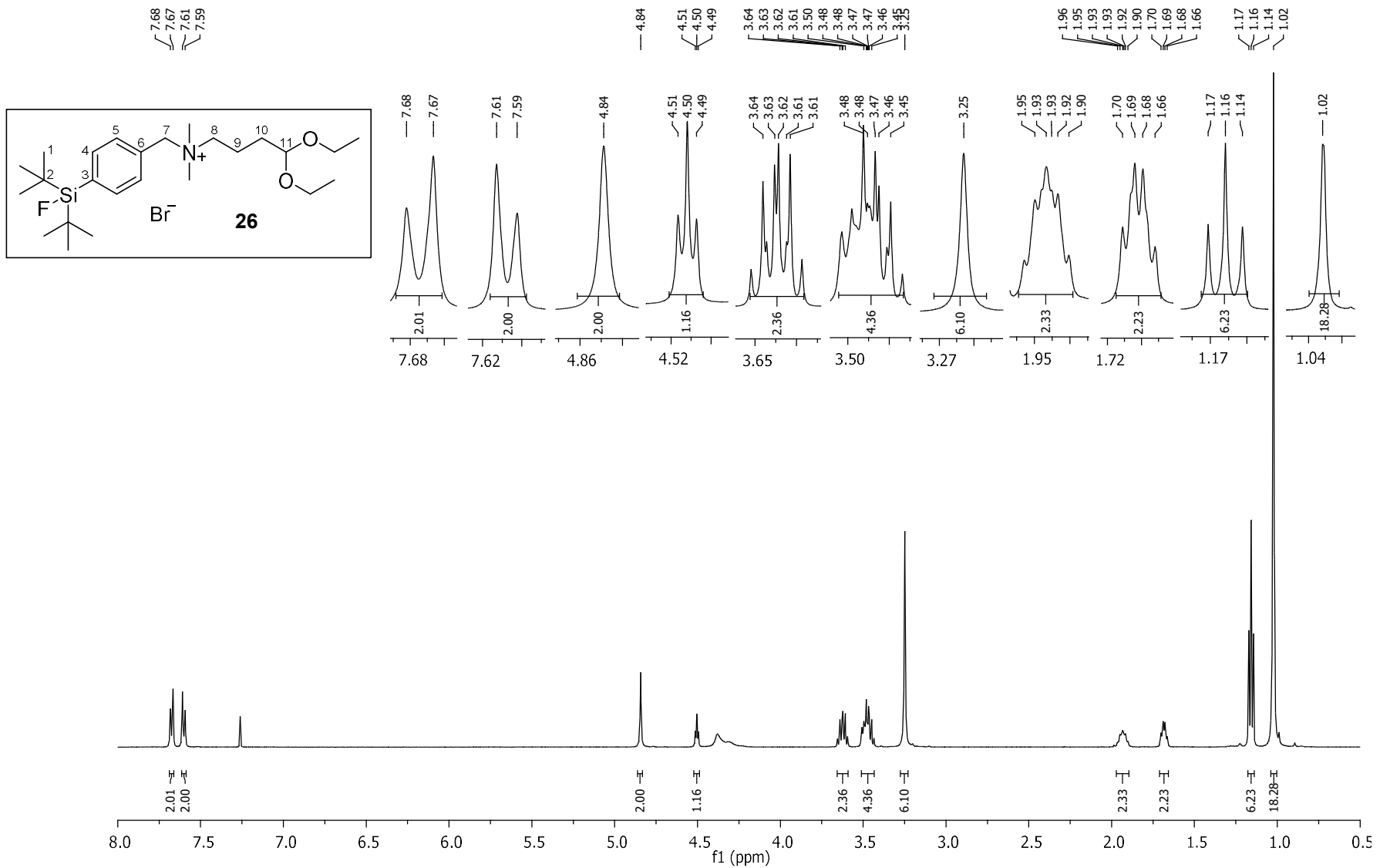


Figure S31. ^1H NMR spectrum of *N*-(4-(*Di-tert*-butylfluorosilyl)benzyl)-4,4-diethoxy-*N,N*-dimethylbutan-1-aminium bromide (**26**).

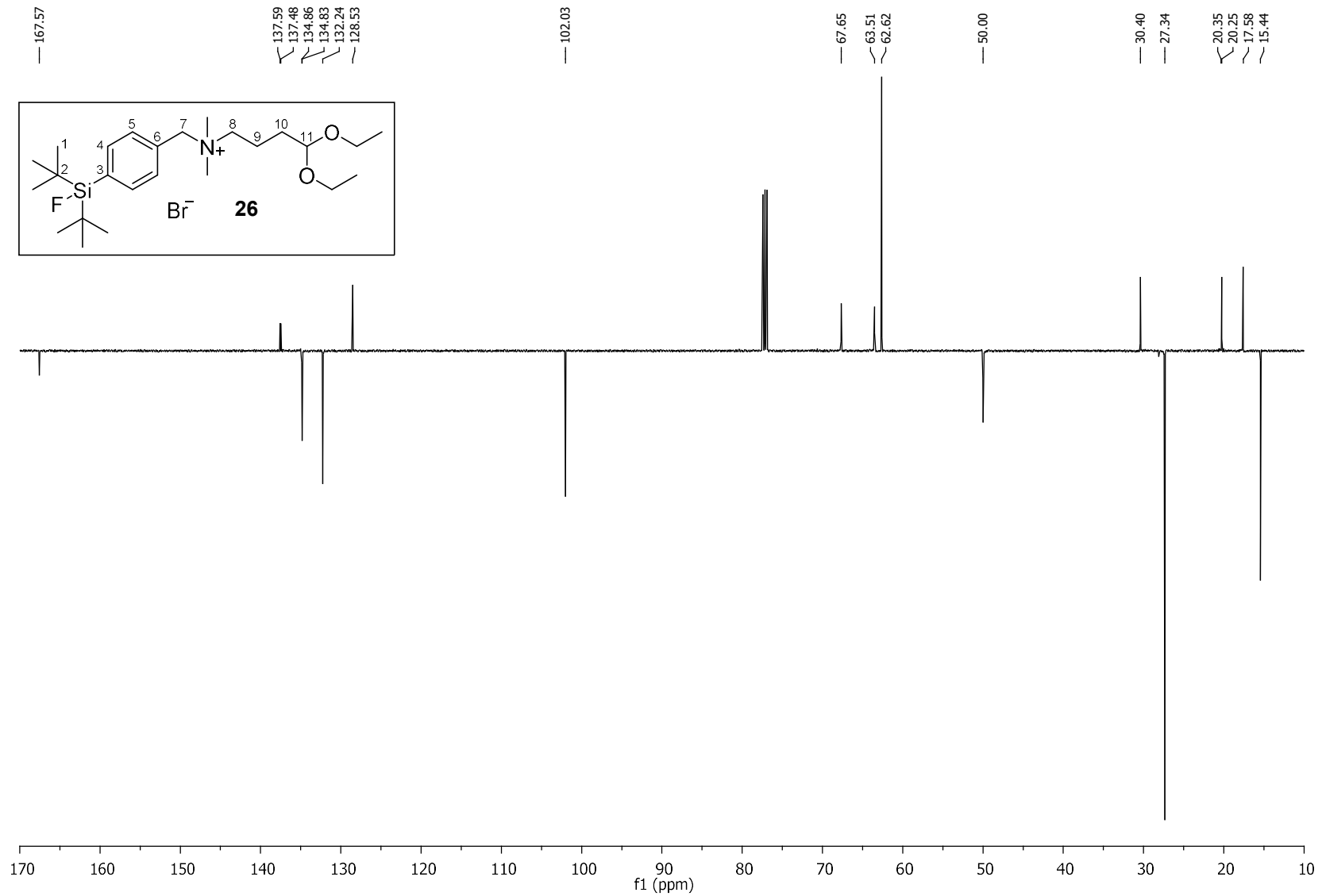


Figure S32. ^{13}C NMR spectrum of *N*-(4-(*Di-tert*-butylfluorosilyl)benzyl)-4,4-diethoxy-*N,N*-dimethylbutan-1-aminium bromide (**26**).

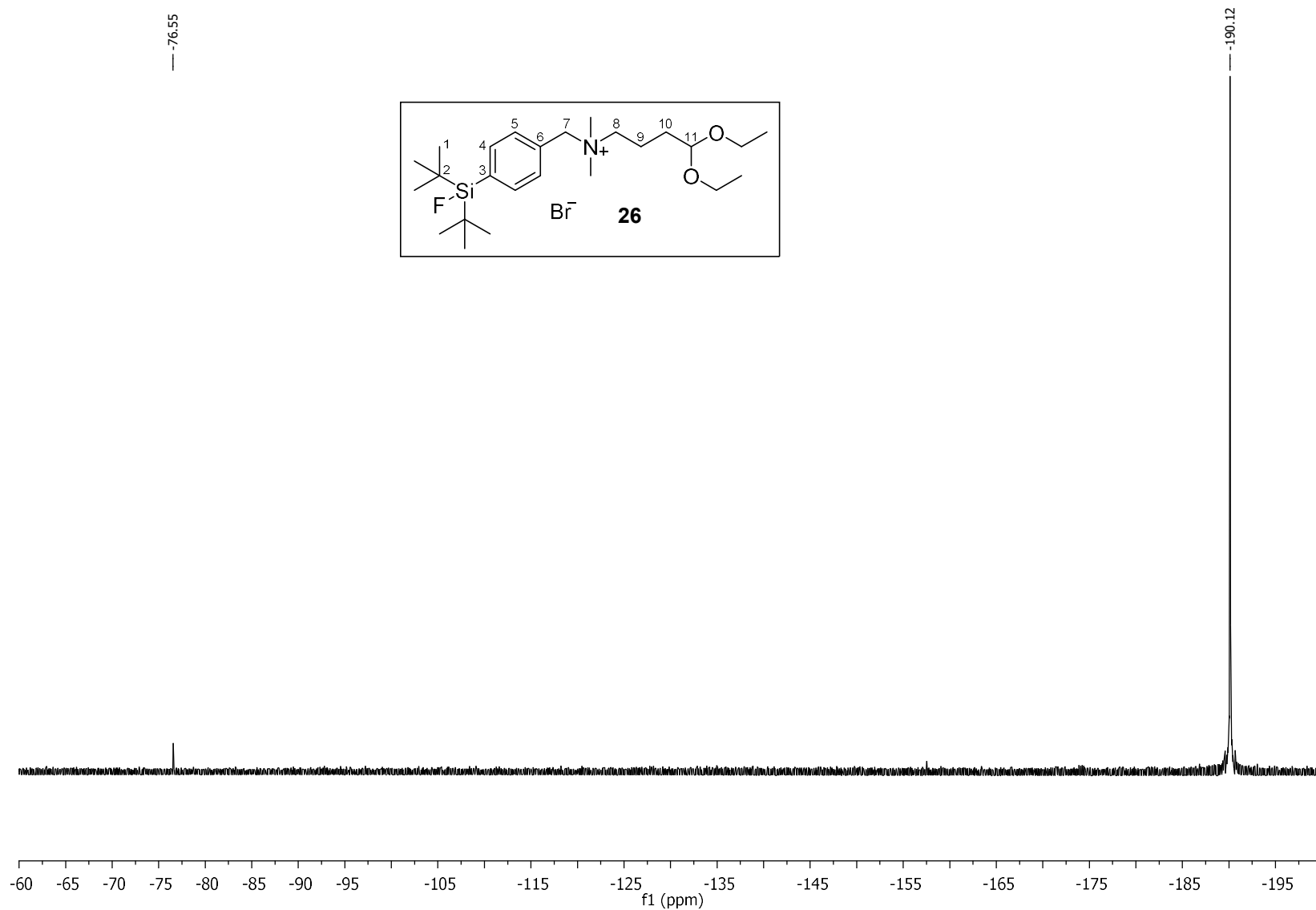


Figure S33. ^{19}F NMR spectrum of *N*-(4-(Di-*tert*-butylfluorosilyl)benzyl)-4,4-diethoxy-*N,N*-dimethylbutan-1-aminium bromide (**26**).

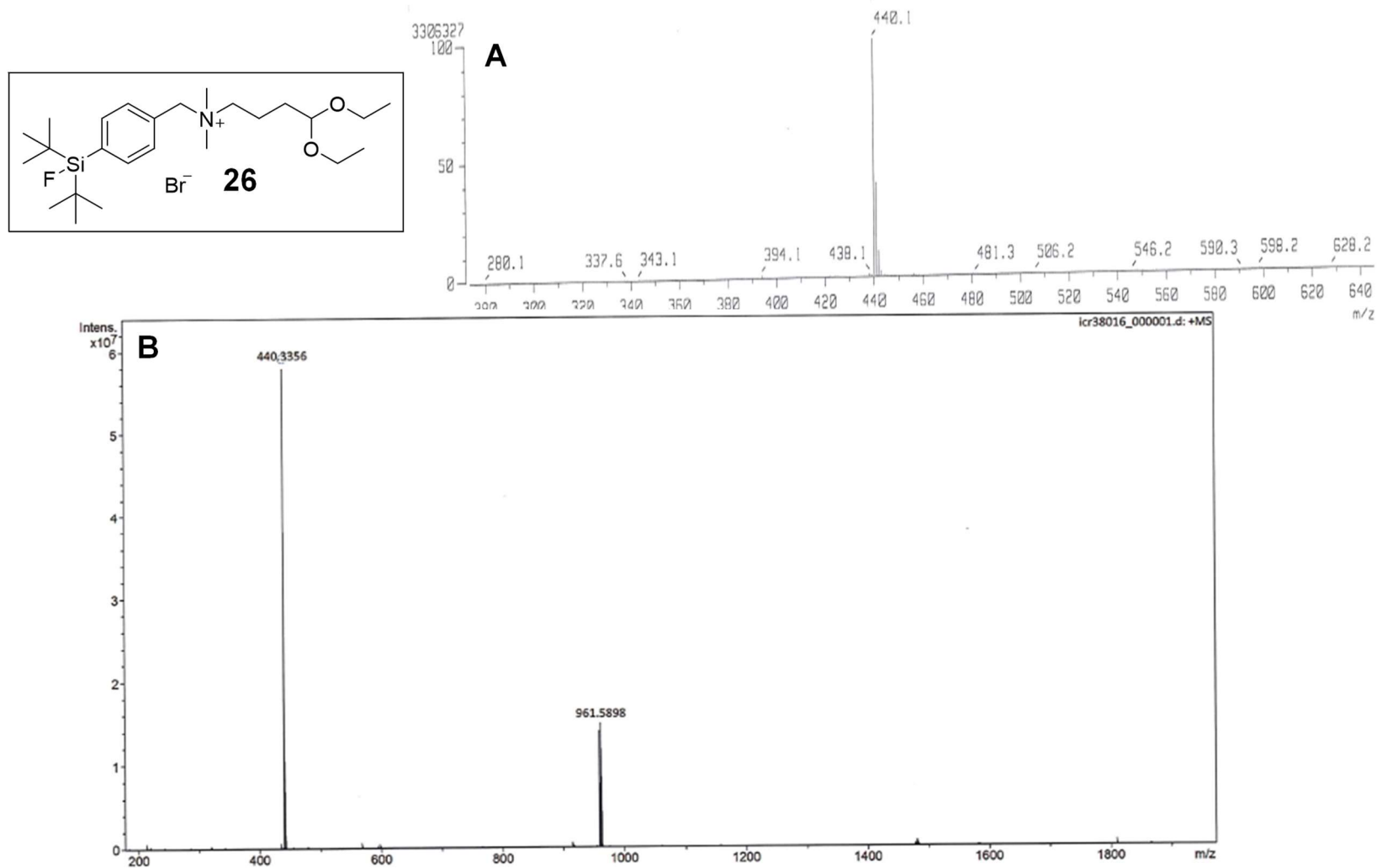


Figure S34. Mass spectra (**A**: FD, **B** ESI) of *N*-(4-(Di-*tert*-butylfluorosilyl)benzyl)-4,4-diethoxy-*N,N*-dimethylbutan-1-aminium bromide (**26**).

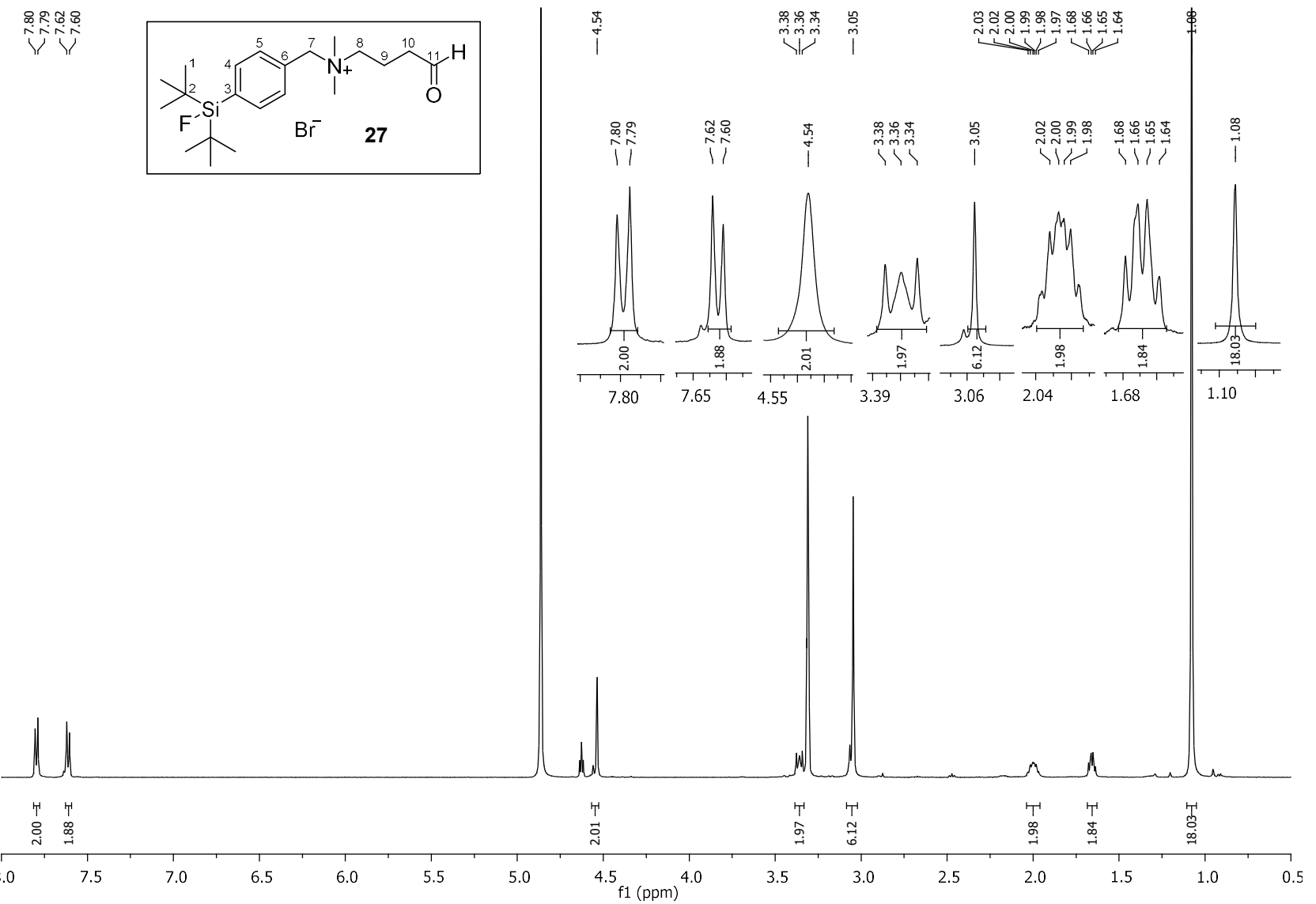


Figure S35. ^1H NMR spectrum of *N*-(4-(Di-*tert*-butylfluorosilyl)benzyl)-*N,N*-dimethyl-4-oxobutan-1-aminium bromide (**27**).

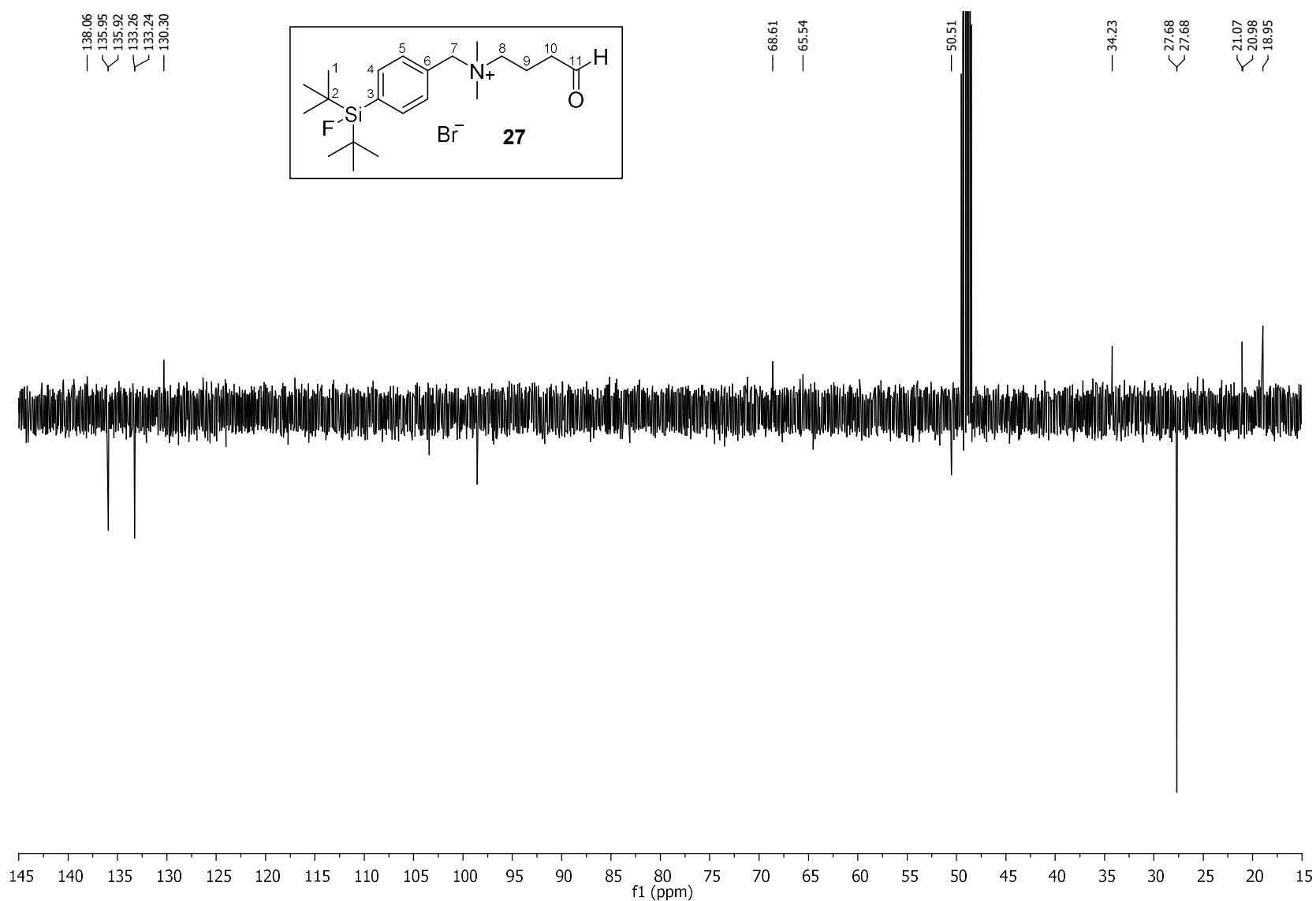


Figure S36. ^{13}C NMR spectrum of *N*-(4-(Di-*tert*-butylfluorosilyl)benzyl)-*N,N*-dimethyl-4-oxobutan-1-aminium bromide (**27**).

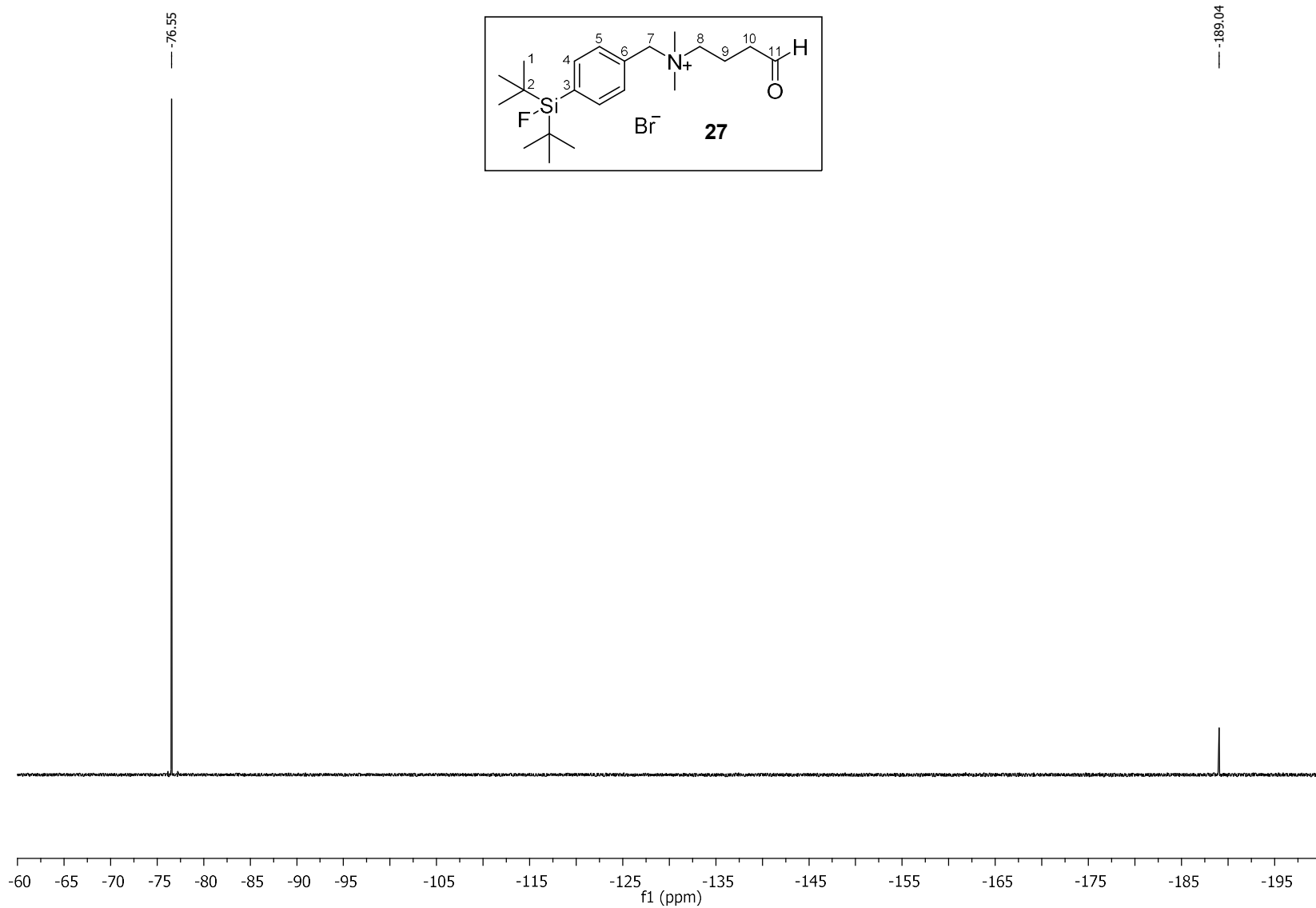


Figure S37. ${}^{19}\text{F}$ NMR spectrum of *N*-(4-(Di-*tert*-butylfluorosilyl)benzyl)-*N,N*-dimethyl-4-oxobutan-1-aminium bromide (**27**).

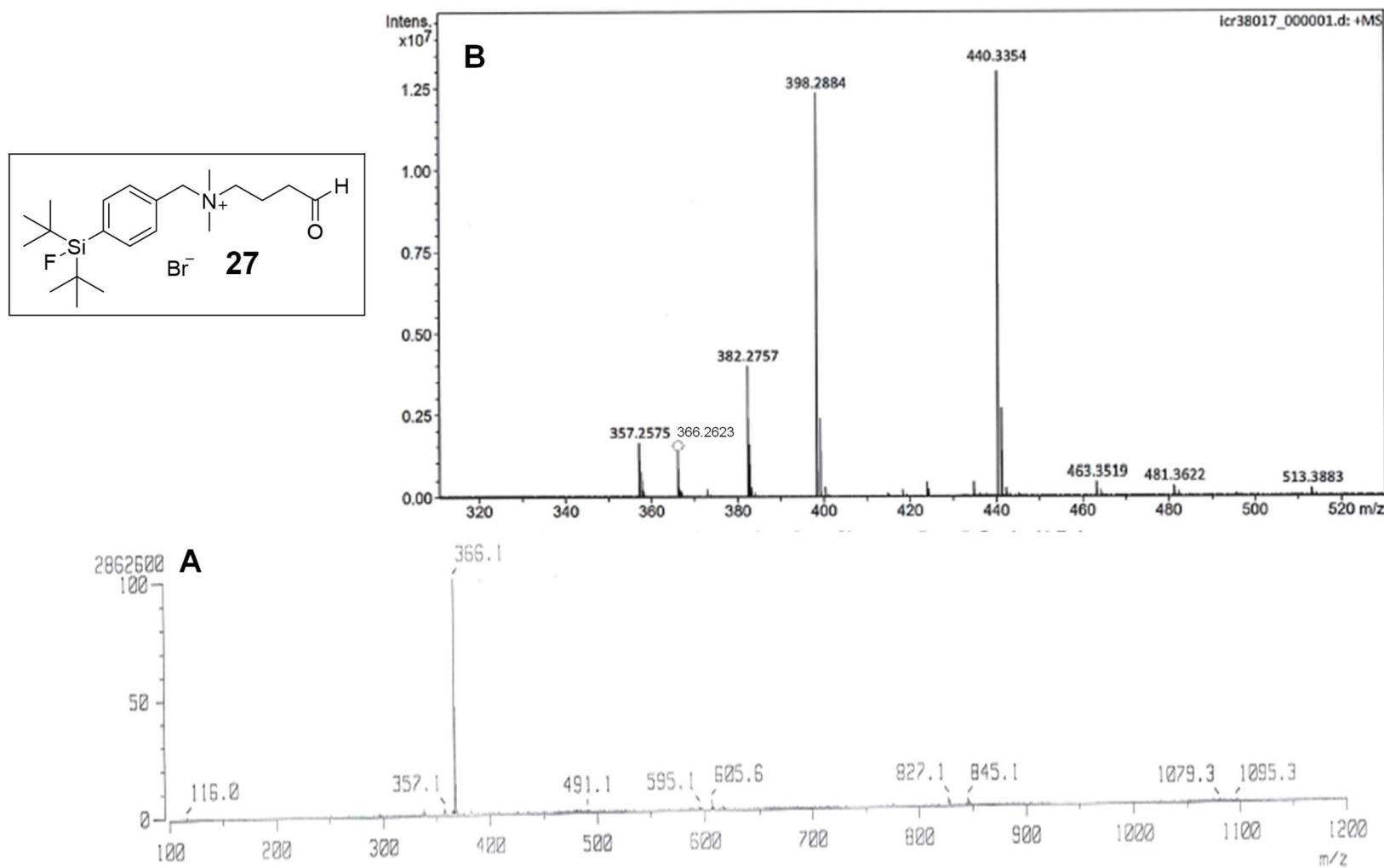


Figure S38. Mass spectra (**A**: FD, **B** ESI) of *N*-(4-(Di-*tert*-butylfluorosilyl)benzyl)-*N,N*-dimethyl-4-oxobutan-1-aminium bromide (**27**).

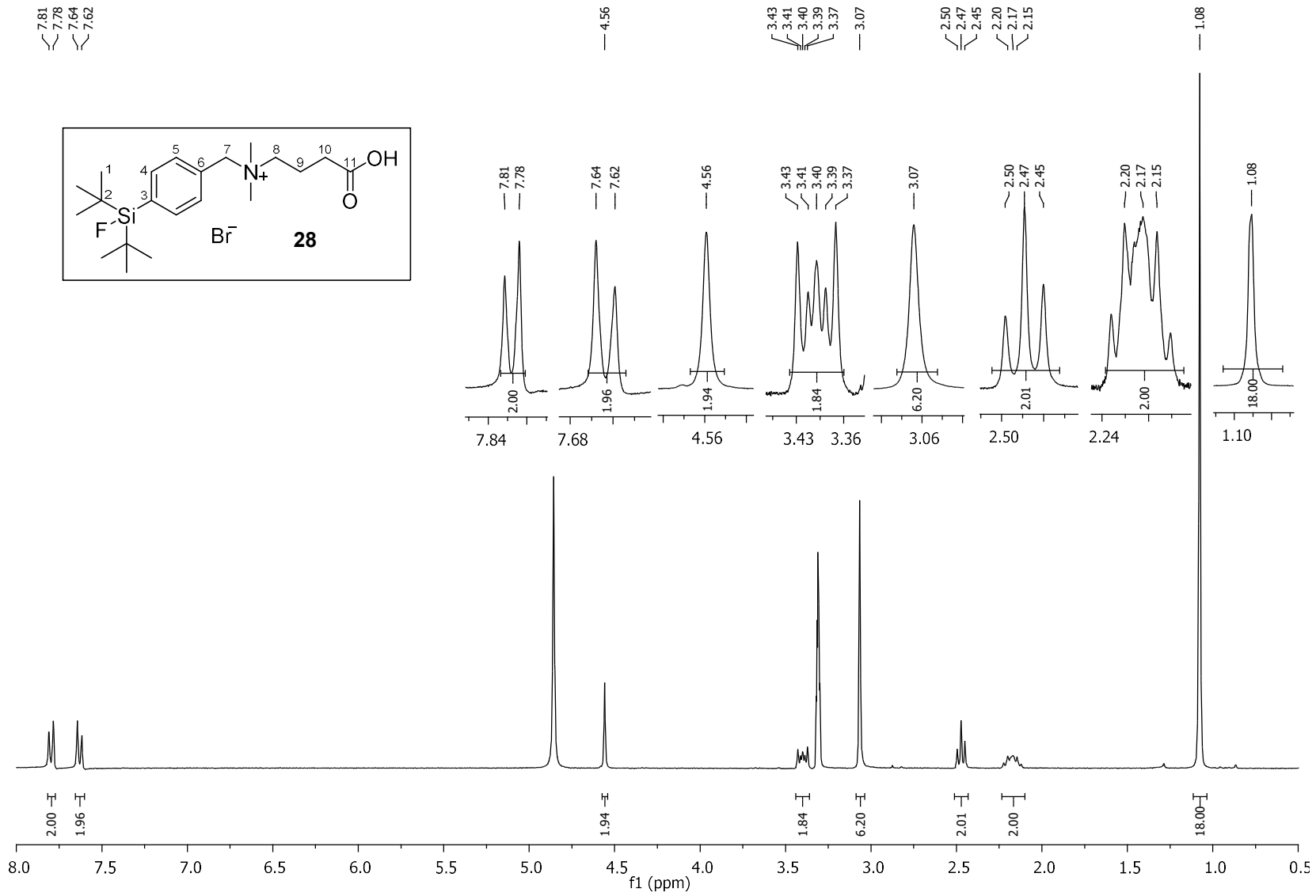


Figure S39. ¹H NMR spectrum of 3-Carboxy-N-(4-(di-tert-butylfluorosilyl)benzyl)-N,N-dimethylpropan-1-aminium bromide (**28**).

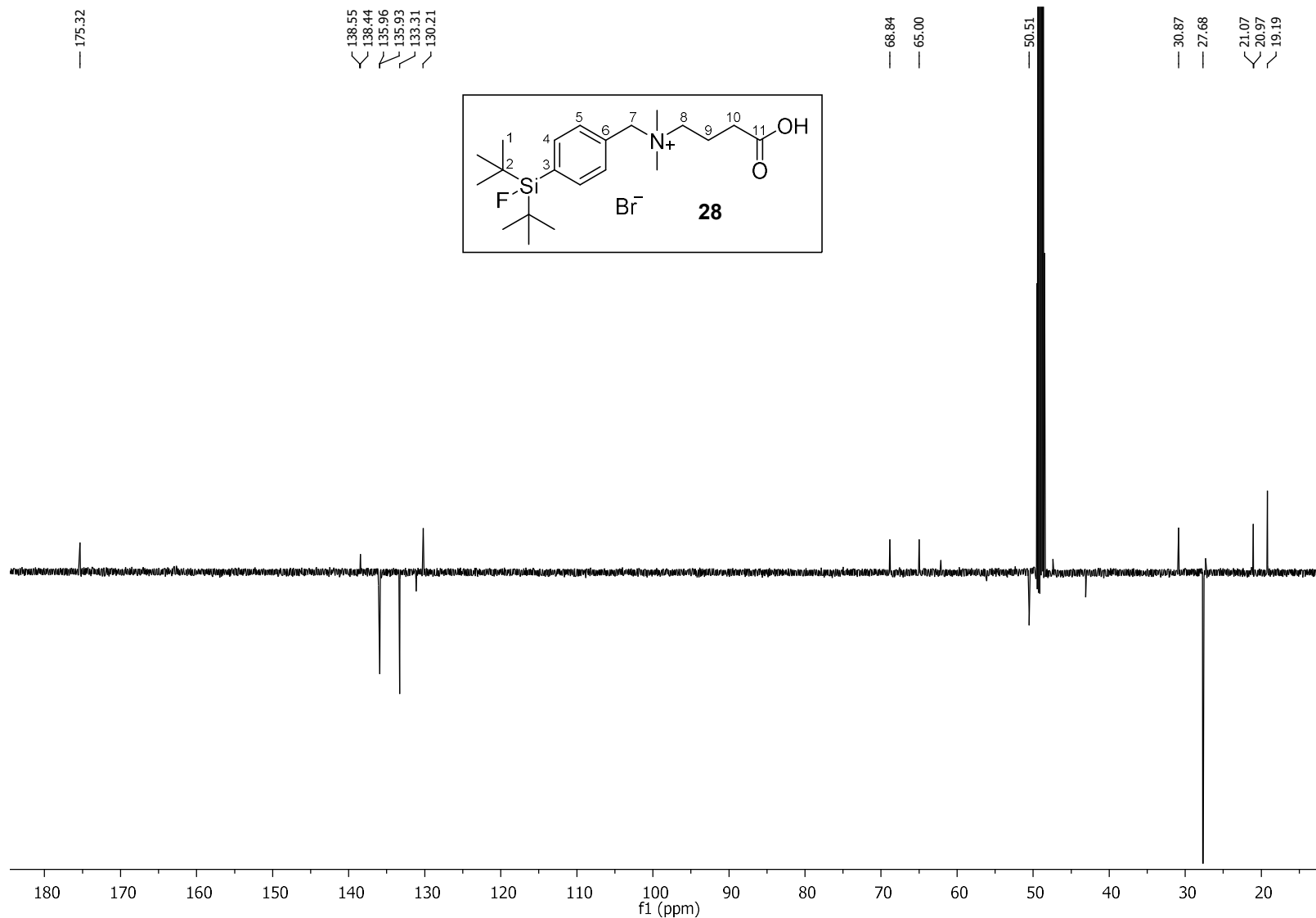


Figure S40. ^{13}C NMR spectrum of 3-Carboxy-*N*-(4-(di-*tert*-butylfluorosilyl)benzyl)-*N,N*-dimethylpropan-1-aminium bromide (**28**).

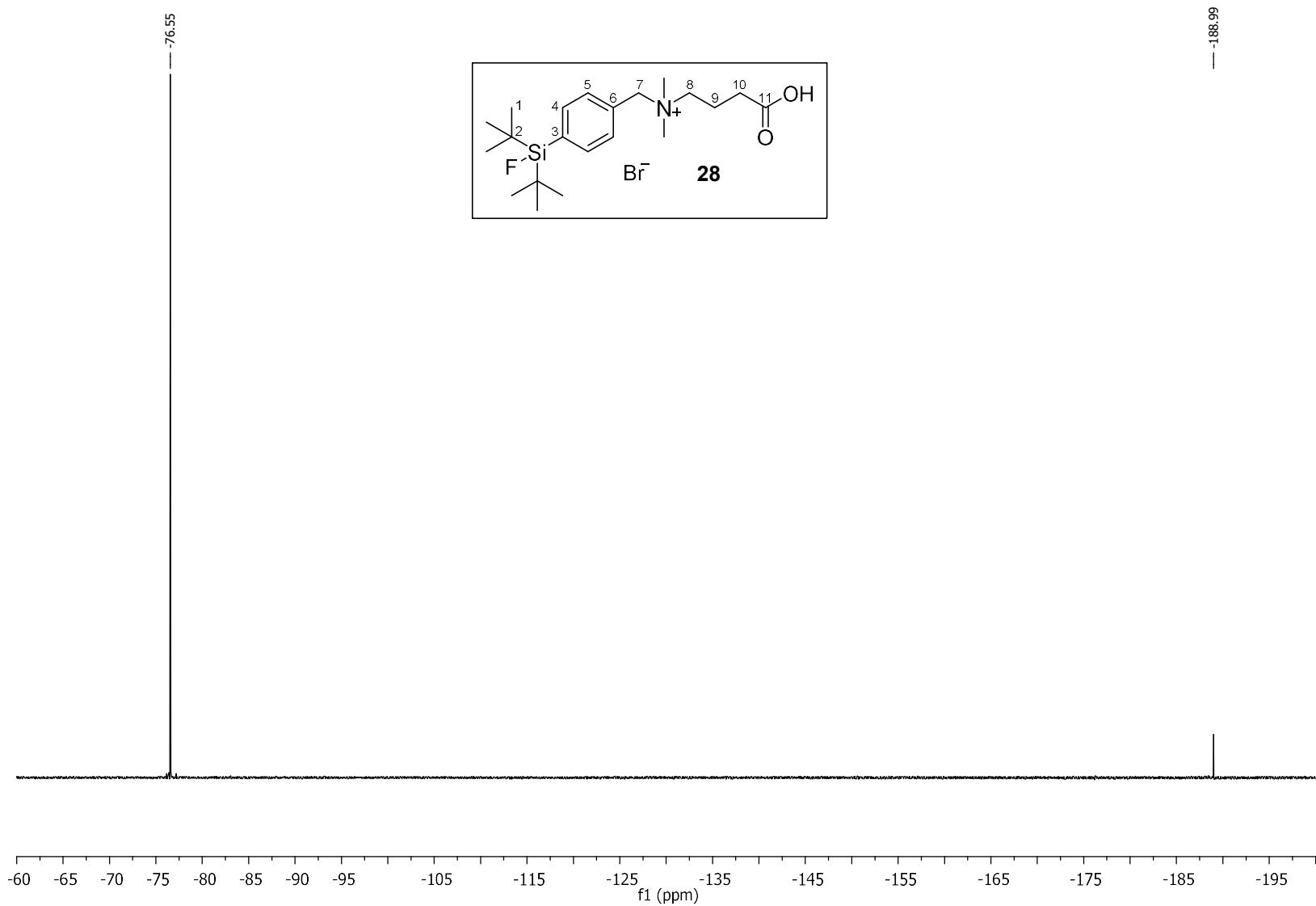


Figure S41. ${}^{19}\text{F}$ NMR spectrum of 3-Carboxy-*N*-(4-(di-*tert*-butylfluorosilyl)benzyl)-*N,N*-dimethylpropan-1-aminium bromide (**28**).

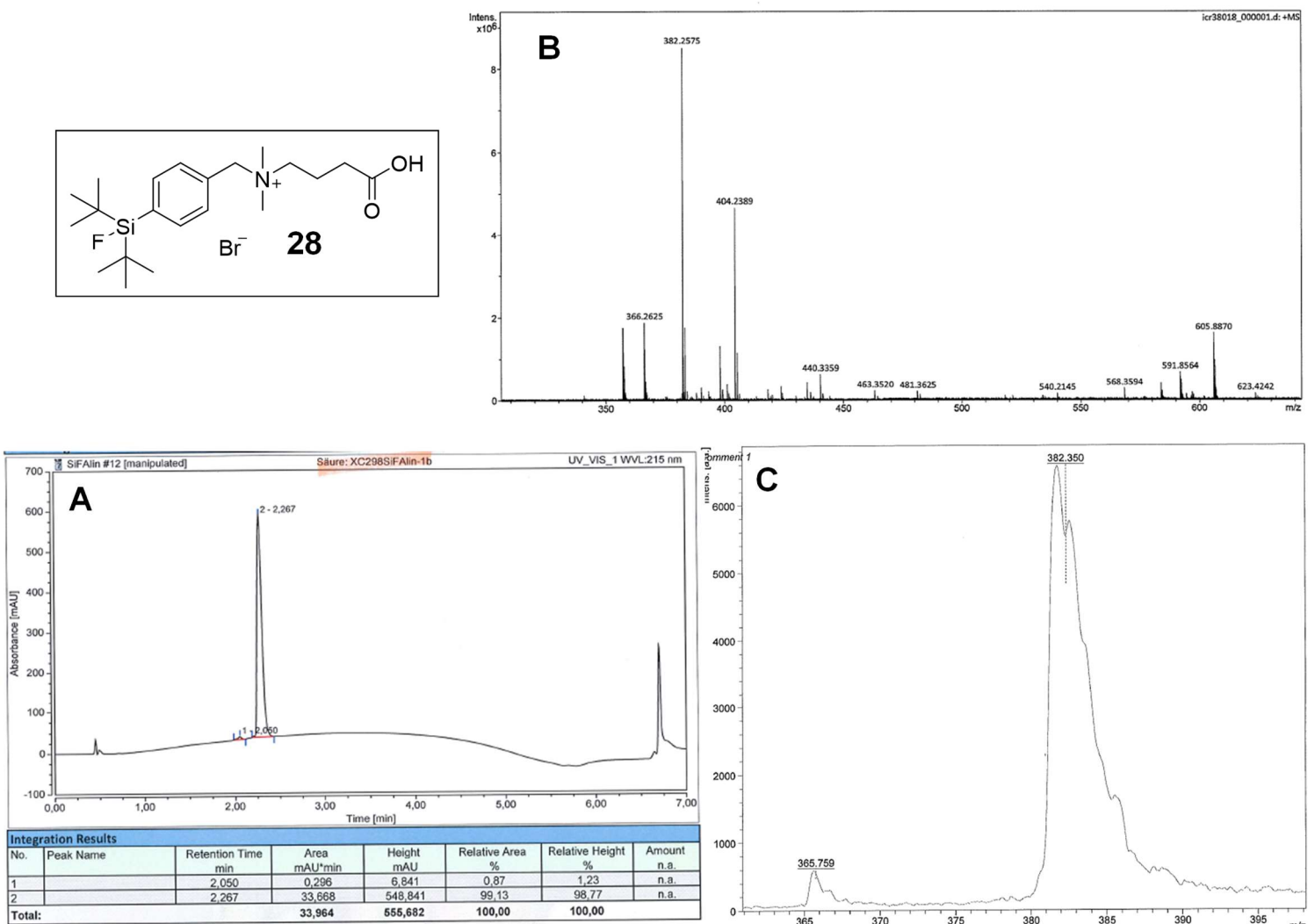


Figure S42. HPLC chromatogram (**A**) and mass spectra (**B**: ESI, **C** MALDI) of 3-Carboxy-N-(4-(di-*tert*-butylfluorosilyl)benzyl)-*N,N*-dimethylpropan-1-aminium bromide (**28**).

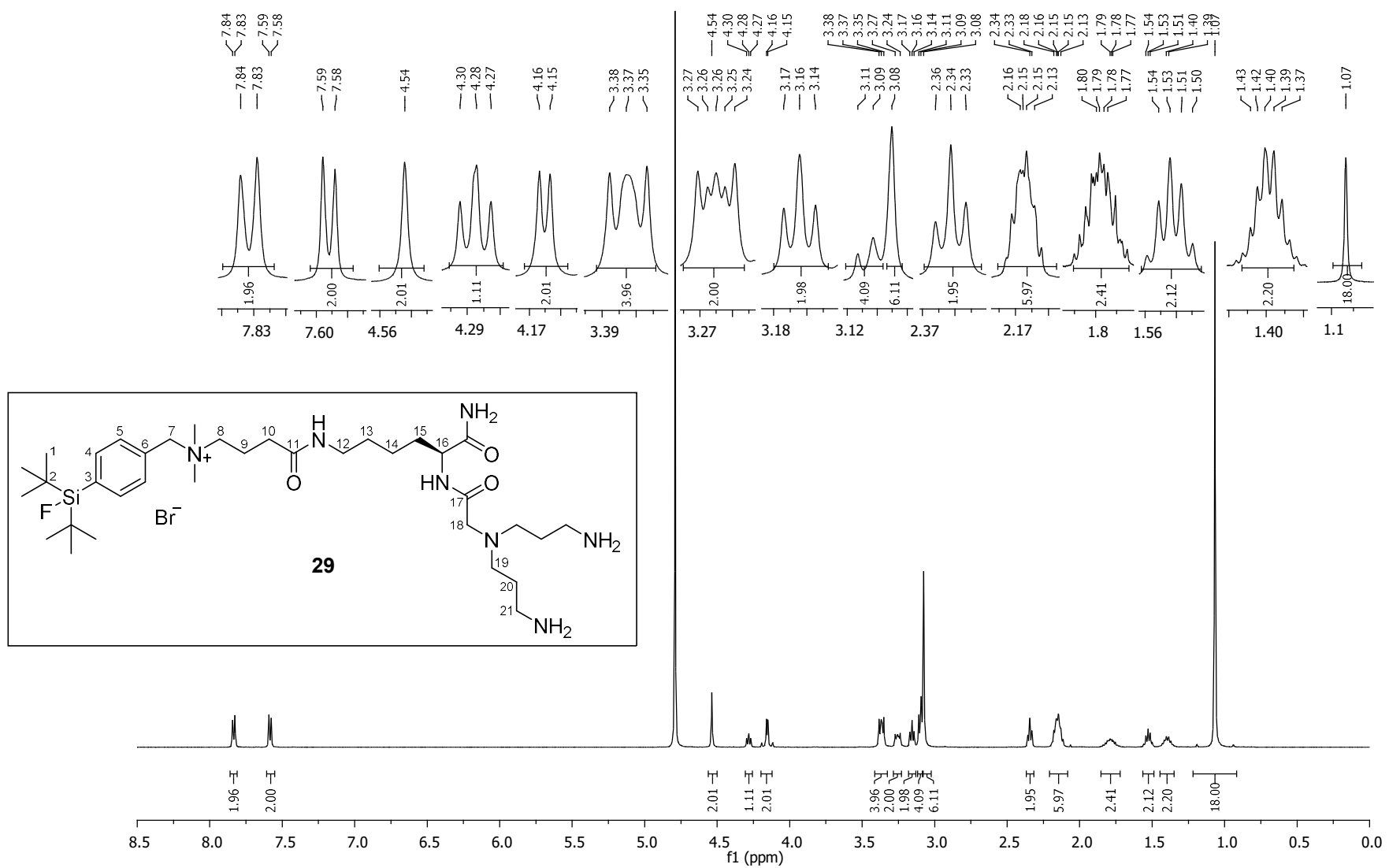


Figure S43. ¹H NMR spectrum of (S)-4-((6-Amino-5-(2-(bis(3-aminopropyl)amino)acetamido)-6-oxohexyl)amino)-N-(4-(di-*tert*-butylfluorosilyl)benzyl)-N,N-dimethyl-4-oxobutan-1-aminium bromide (**29**).

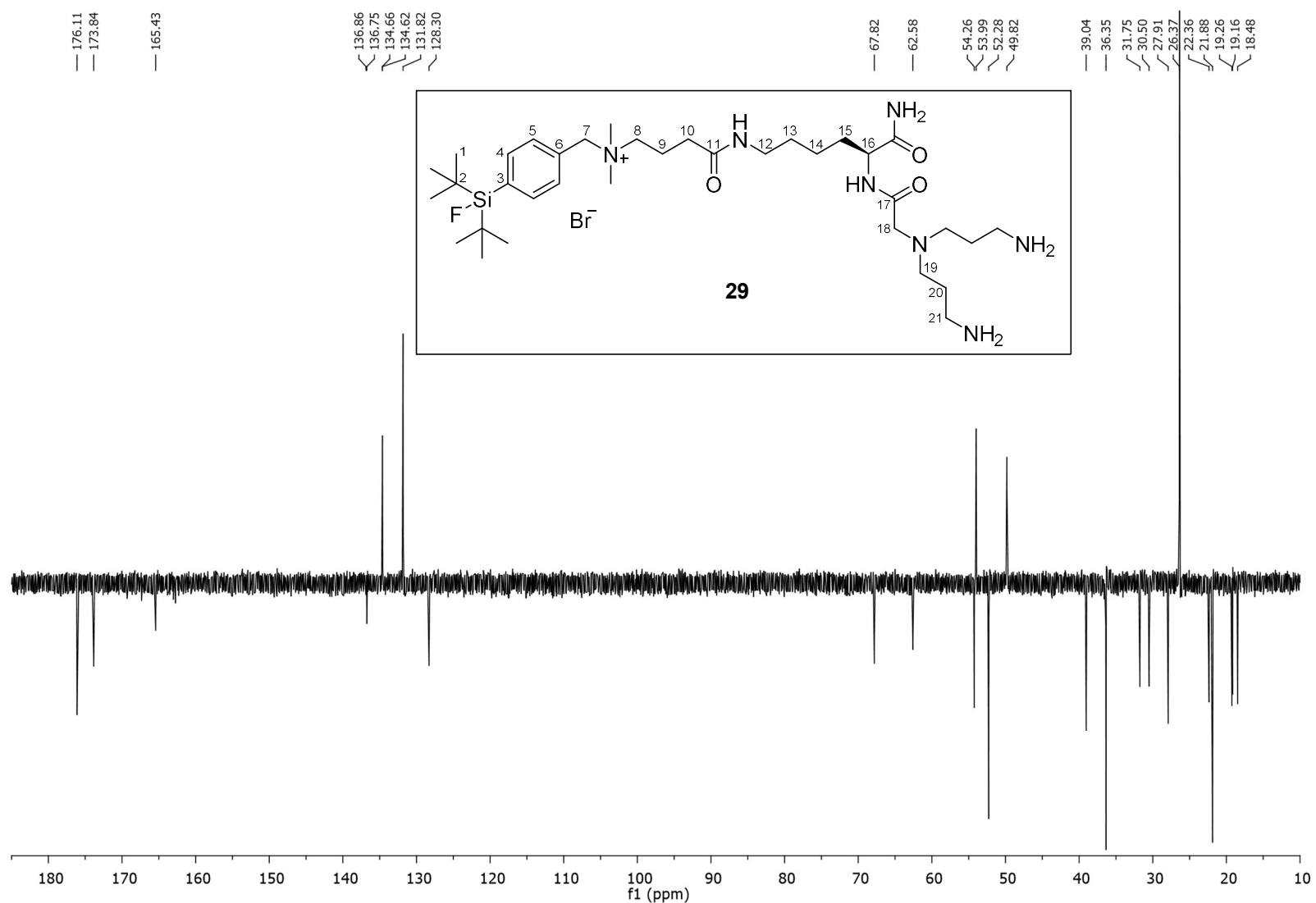


Figure S44. ^{13}C NMR spectrum of (S)-4-((6-Amino-5-(2-(bis(3-aminopropyl)amino)acetamido)-6-oxohexylamino)-N-(4-(di-*tert*-butylfluorosilyl)benzyl)- N,N -dimethyl-4-oxobutan-1-aminium bromide (**29**).

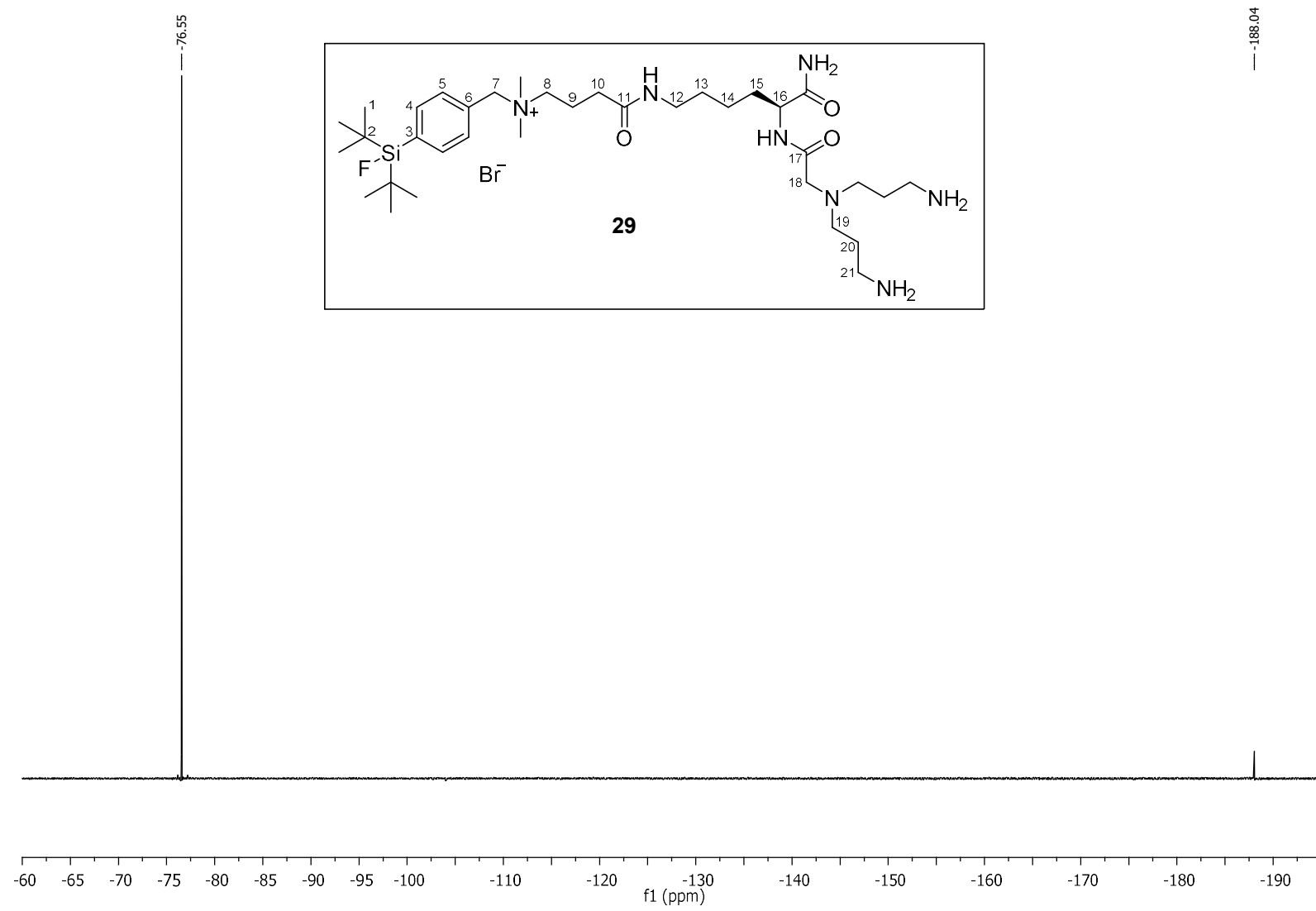


Figure S45. ^{19}F NMR spectrum of (*S*)-4-((6-Amino-5-(2-(bis(3-aminopropyl)amino)acetamido)-6-oxohexyl)amino)-*N*-(4-(di-*tert*-butylfluorosilyl)benzyl)-*N,N*-dimethyl-4-oxobutan-1-aminium bromide (**29**).

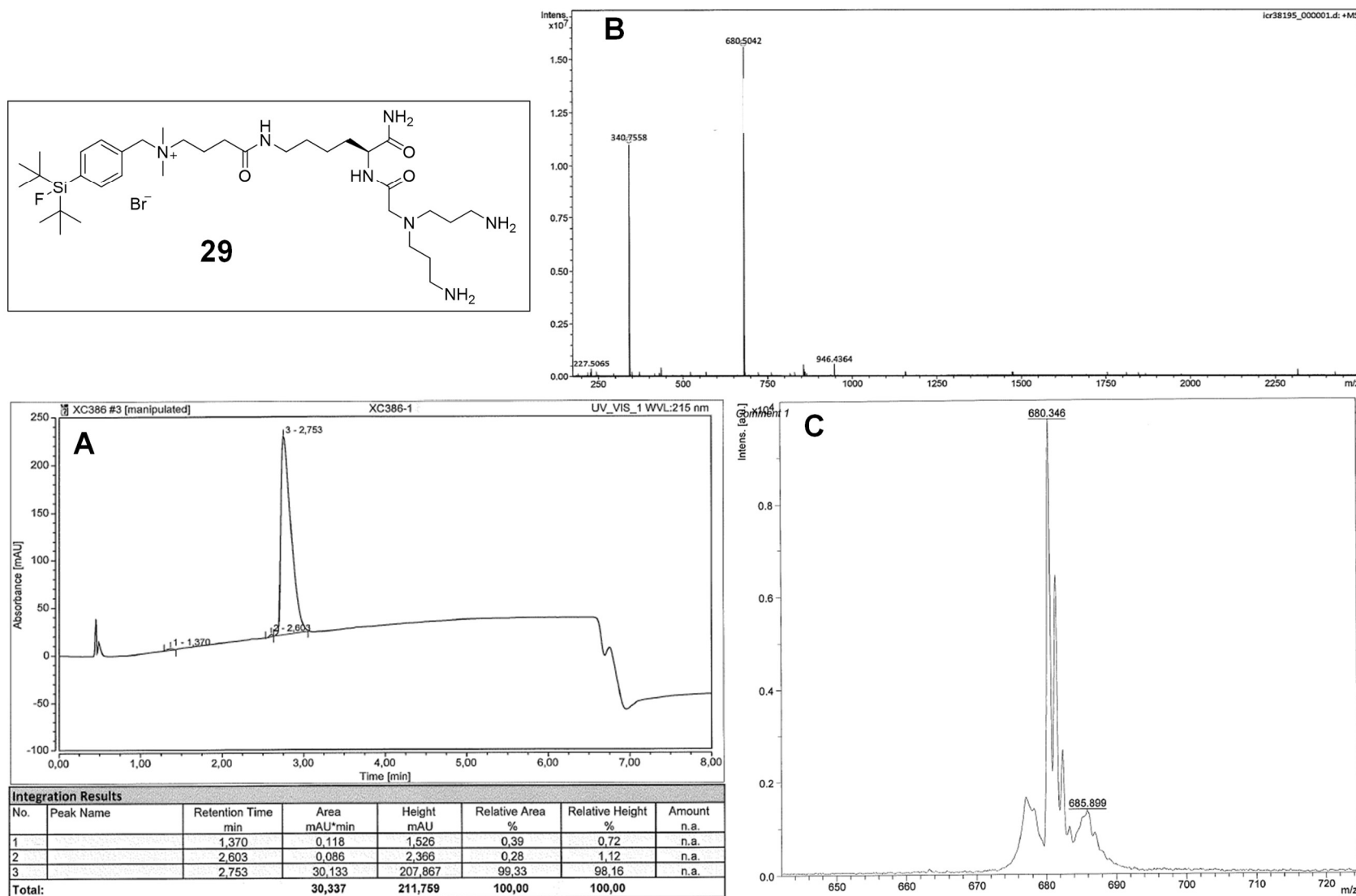


Figure S46. HPLC chromatogram (**A**) and mass spectra (**B**: ESI, **C** MALDI) of (*S*)-4-((6-Amino-5-(2-(bis(3-aminopropyl)amino)acetamido)-6-oxohexyl)amino)-*N*-(4-(di-*tert*-butylfluorosilyl)benzyl)-*N,N*-dimethyl-4-oxobutan-1-aminium bromide (**29**).

3. Mass and ^{19}F -NMR spectra of HBPLs 1–6 and mass spectra of their intermediates 30–35

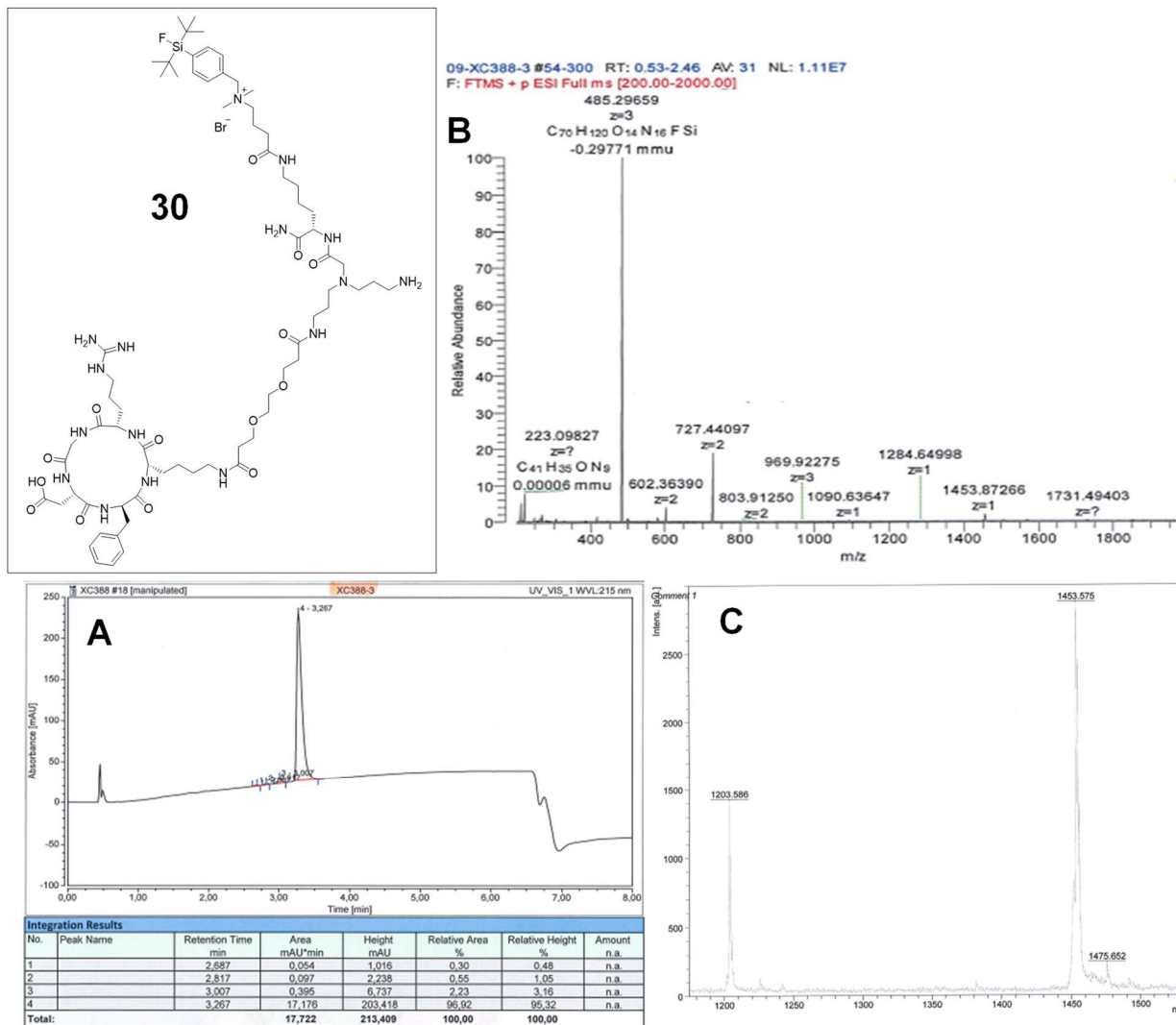


Figure S47. HPLC chromatogram (**A**) and mass spectra (**B**: ESI, **C**: MALDI) of SiFA/in-APG-PEG1-c(RGDfK) (**30**).

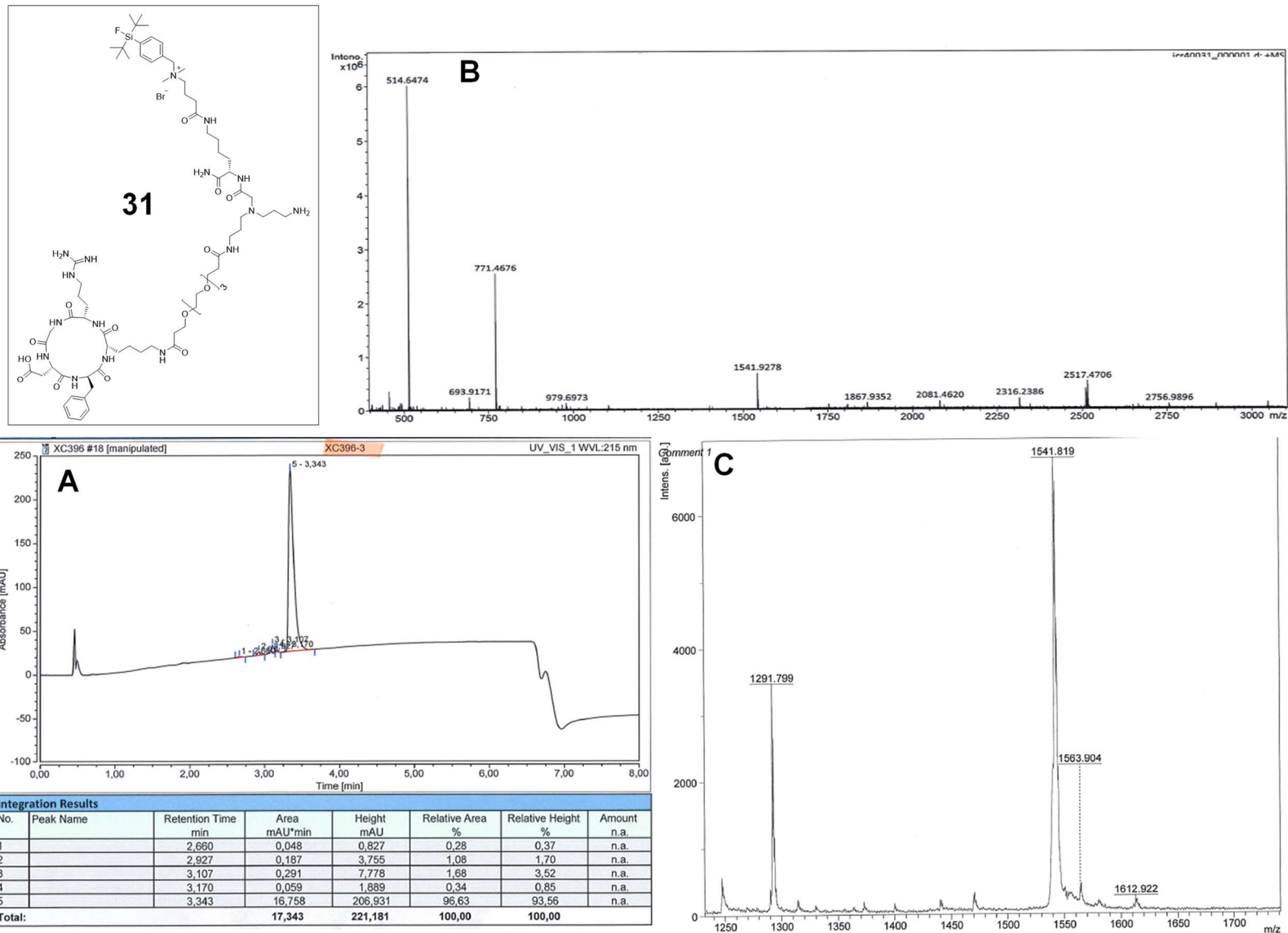


Figure S48. HPLC chromatogram (**A**) and mass spectra (**B**: ESI, **C**: MALDI) of SiFA/*in*-APG-PEG₃-c(RGDfK) (**31**).

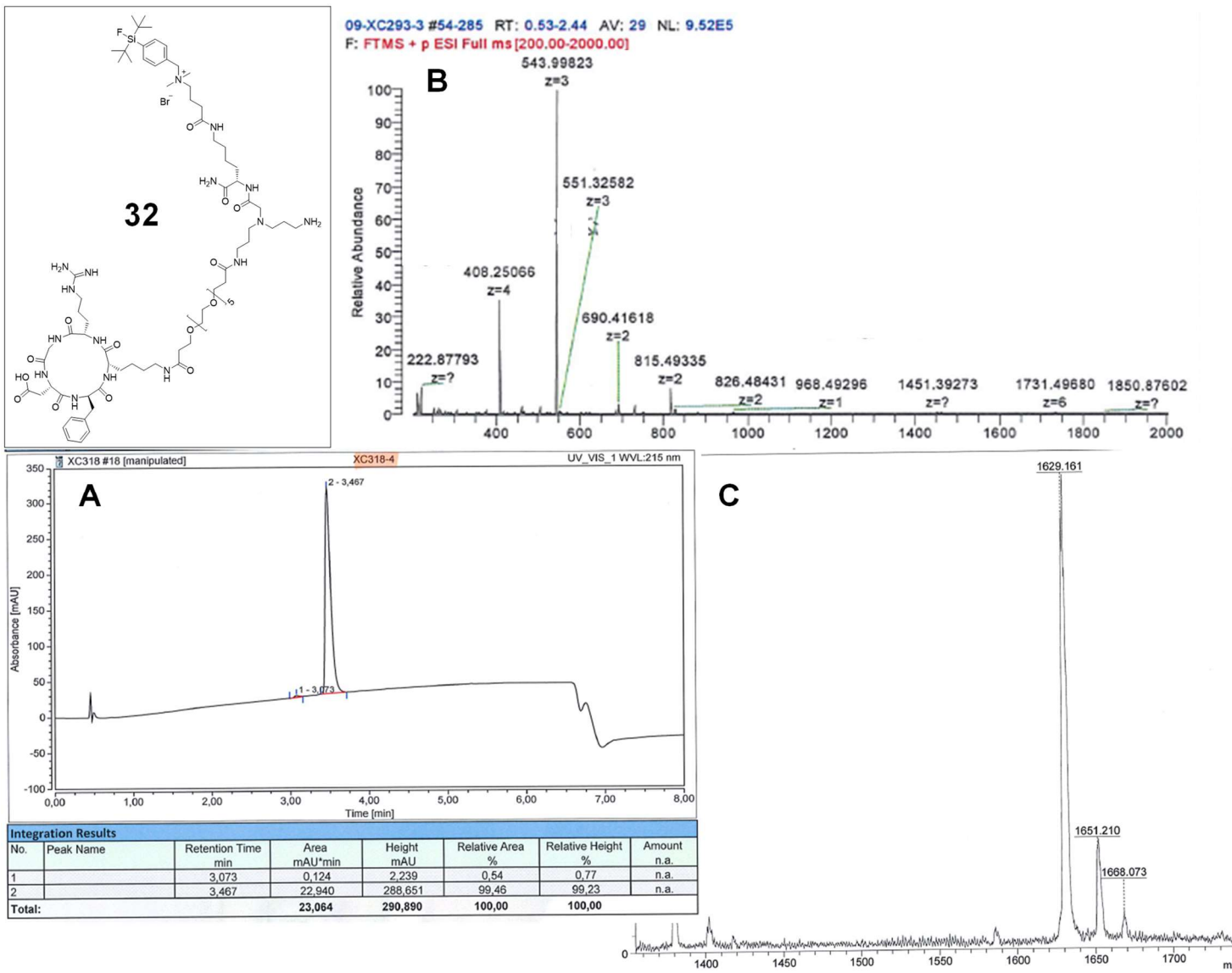


Figure S49. HPLC chromatogram (**A**) and mass spectra (**B**: ESI, **C**: MALDI) of SiFA/*in*-APG-PEG₅-c(RGDfK) (**32**).

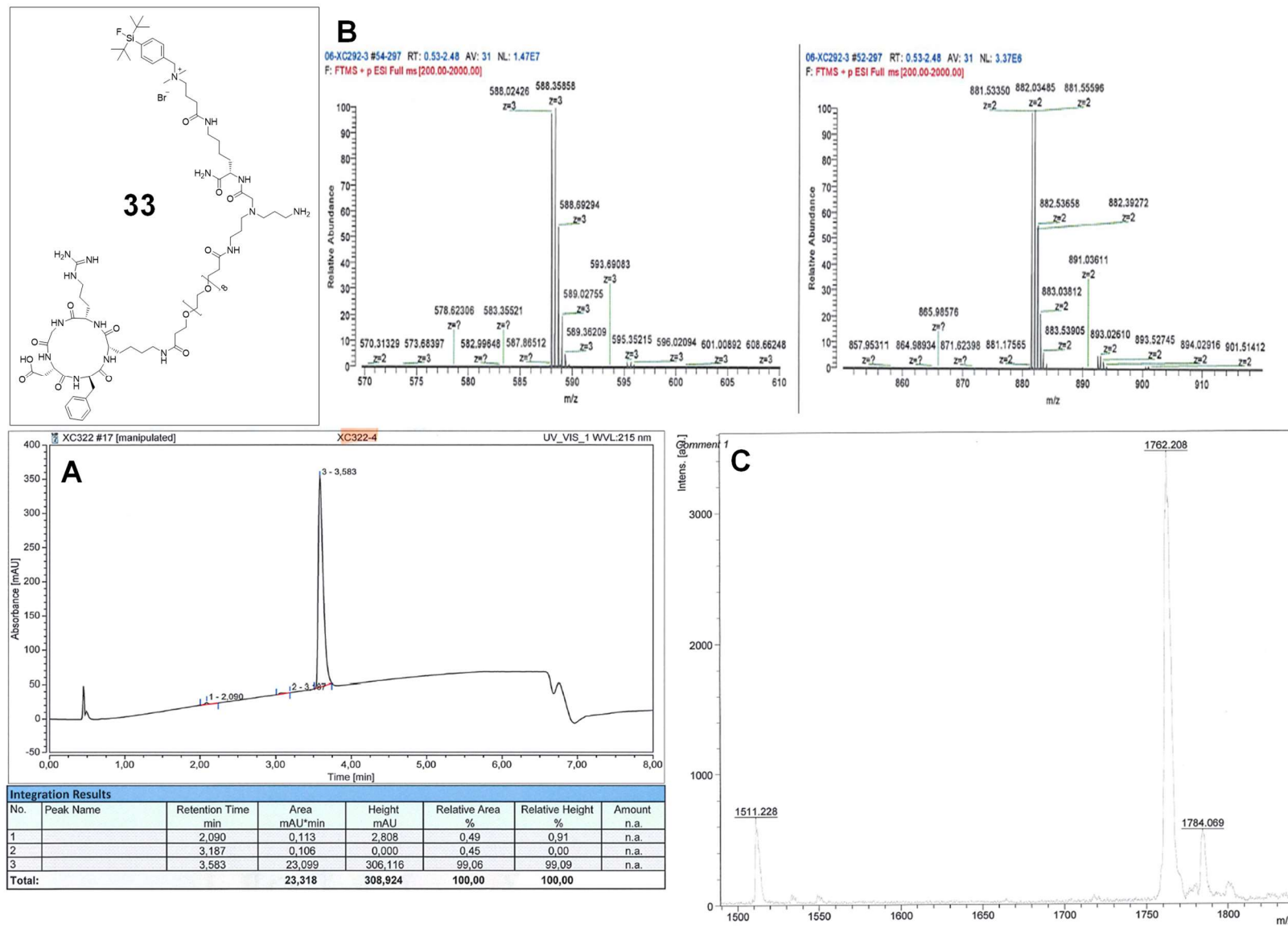


Figure S50. HPLC chromatogram (**A**) and mass spectra (**B**: ESI, **C**: MALDI) of SiFA/*in*-APG-PEG₈-c(RGDfK) (**33**).

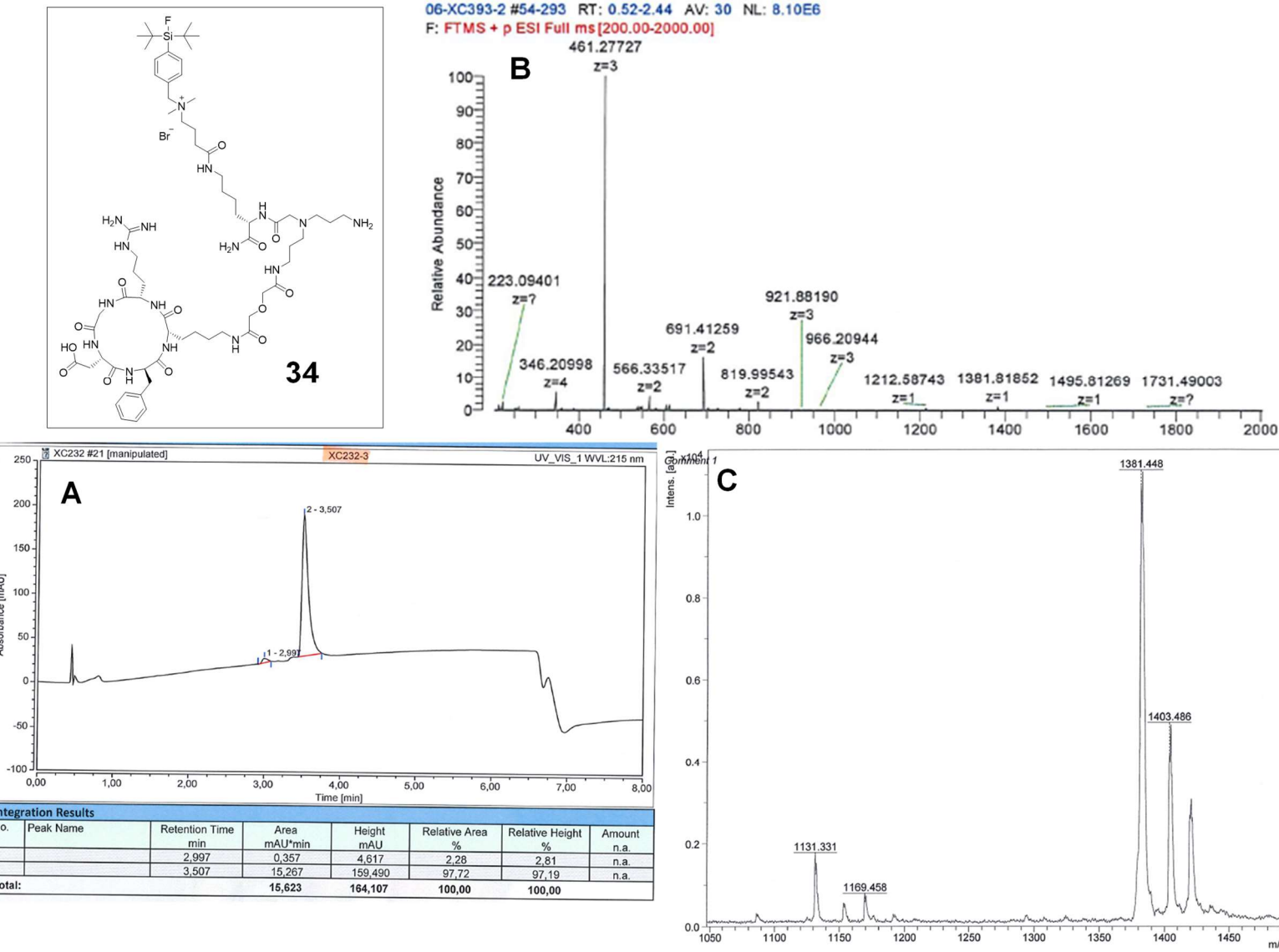


Figure S51. HPLC chromatogram (**A**) and mass spectra (**B**: ESI, **C**: MALDI) of SiFA/in-APG-DIG-c(RGDFK) (**34**).

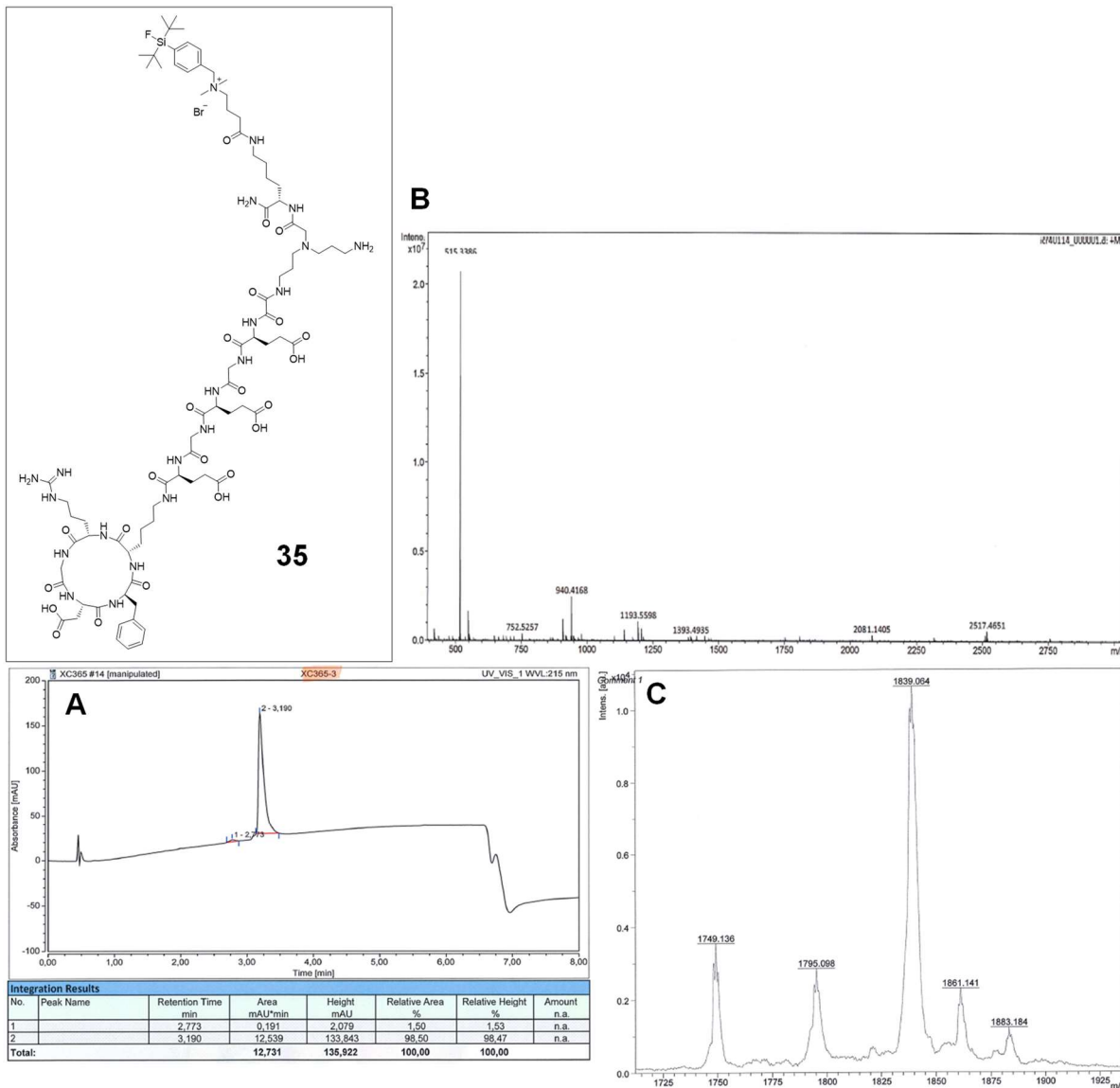


Figure S52. HPLC chromatogram (**A**) and mass spectra (**B**: ESI, **C**: MALDI) of SiFA/*in*-APG-Ox-EGEGE-c(RGDfK) (**35**).

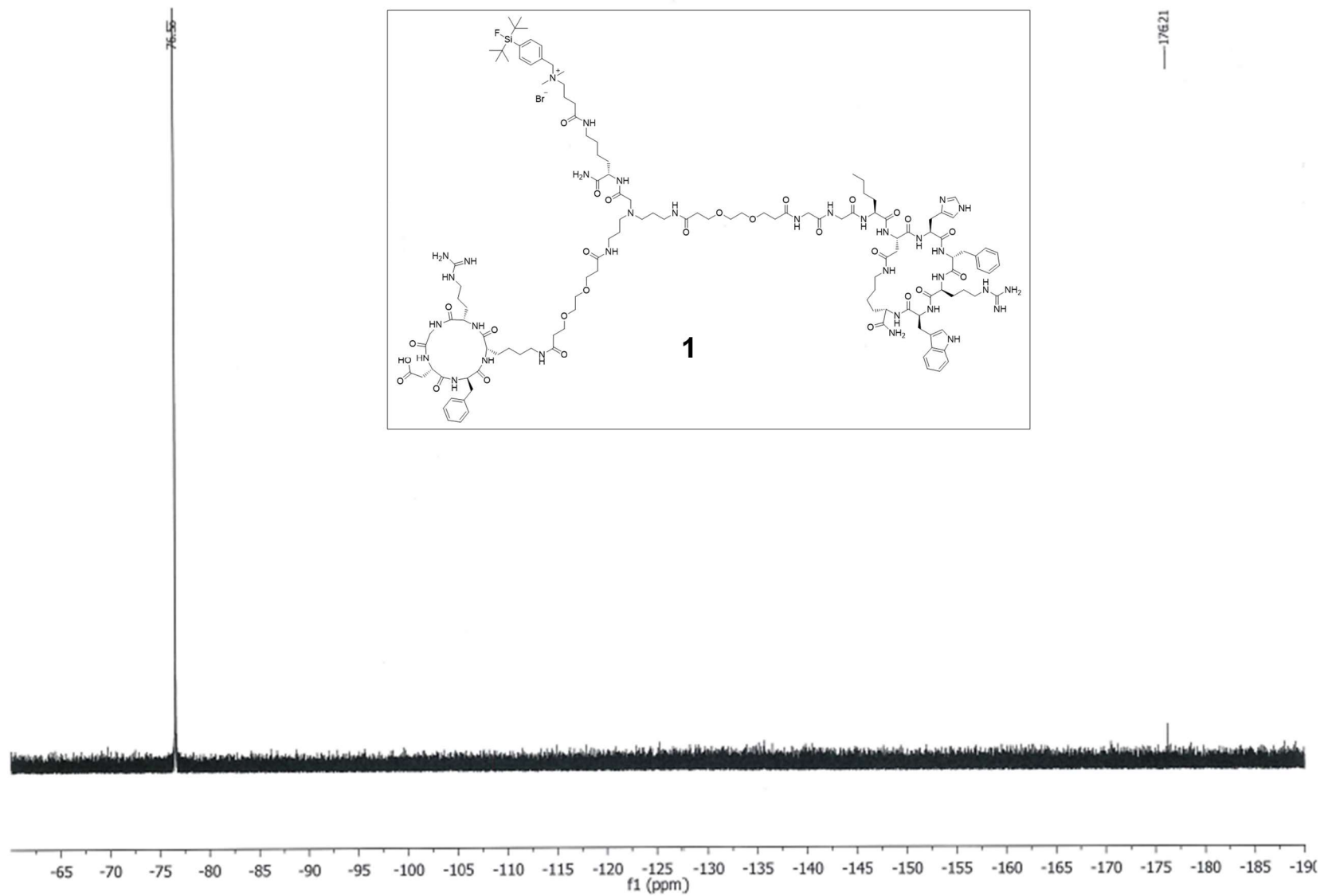


Figure S53. ¹⁹F NMR spectrum of SiFA/in-APG-PEG₁-c(RGDfK)/GG-Nle-c(DHfRWK) (**1**).

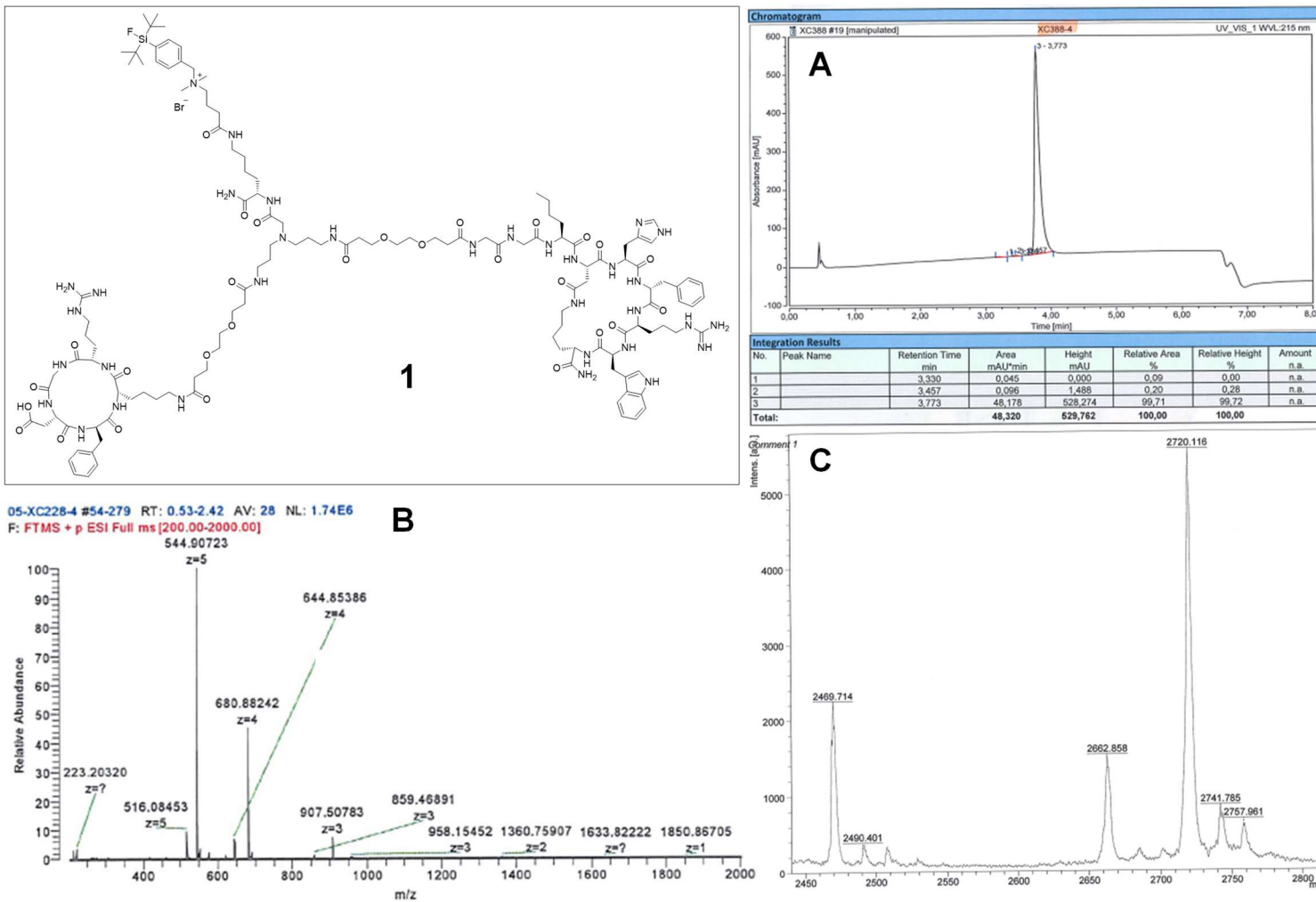


Figure S54. HPLC chromatogram (**A**) and mass spectra (**B**: ESI, **C**: MALDI) of SiFA/in-APG-PEG₁-c(RGDfK)/GG-Nle-c(DHfRWK) (**1**).

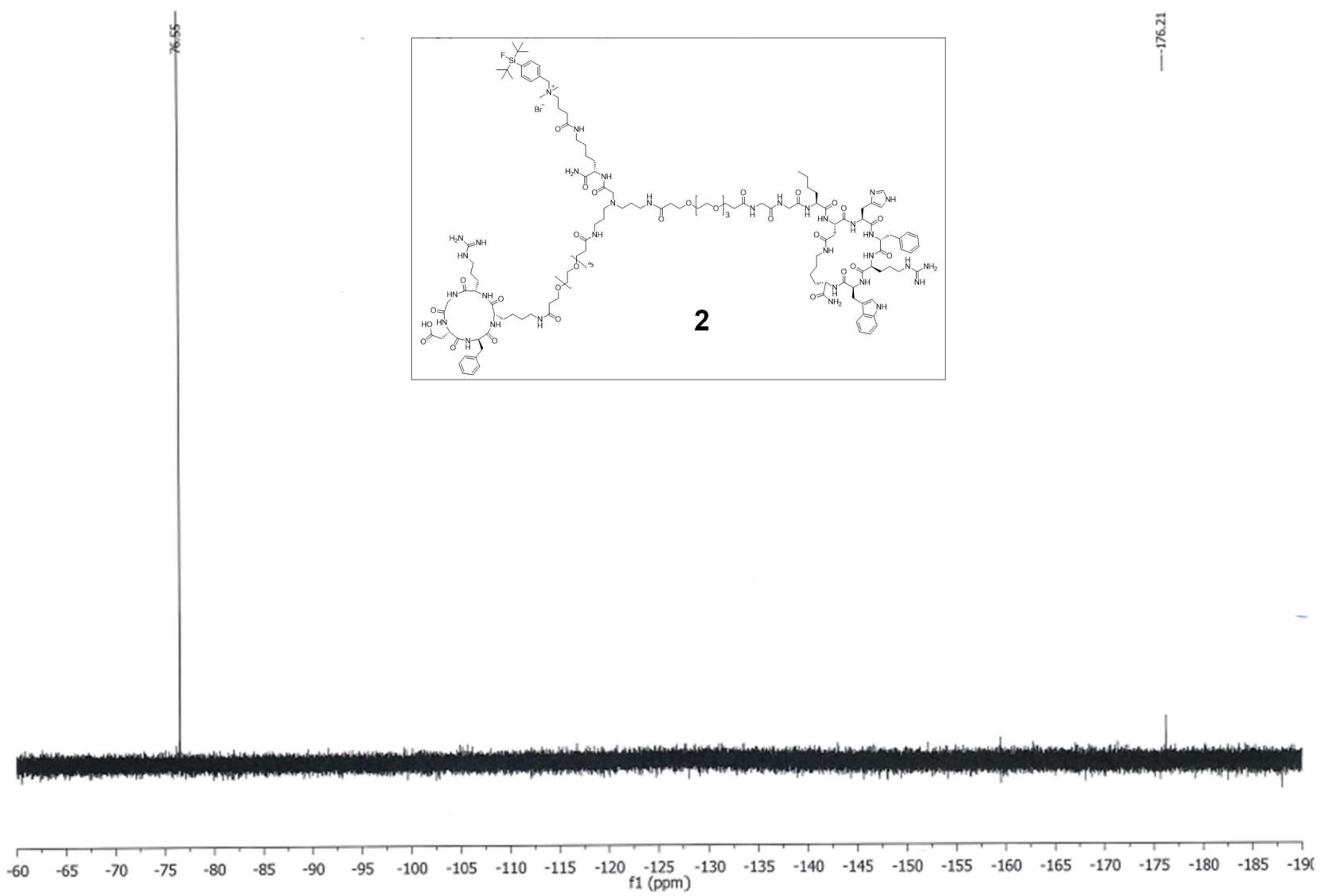


Figure S55. ¹⁹F NMR spectrum of SiFA/in-APG-PEG₃-c(RGDfK)/GG-Nle-c(DHfRWK) (**2**).

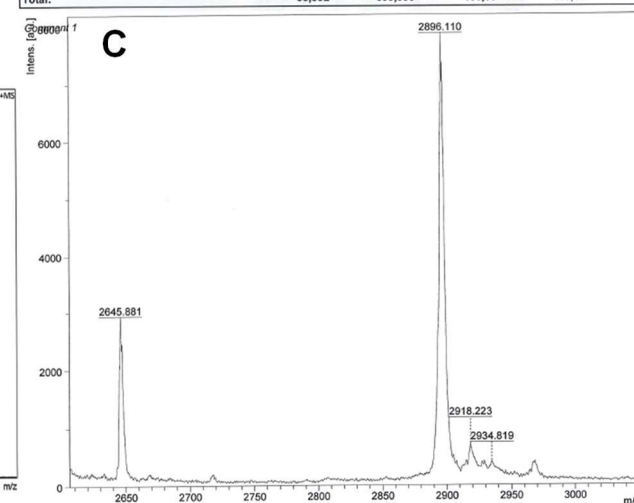
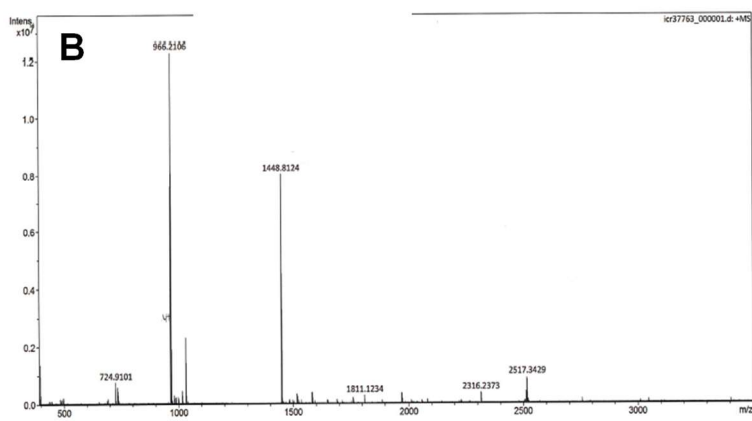
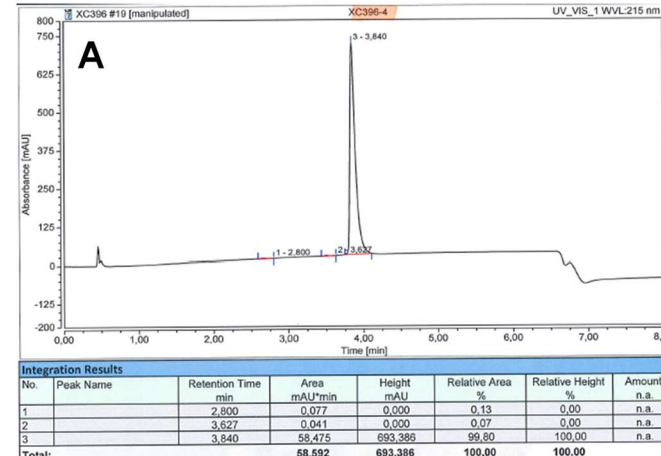
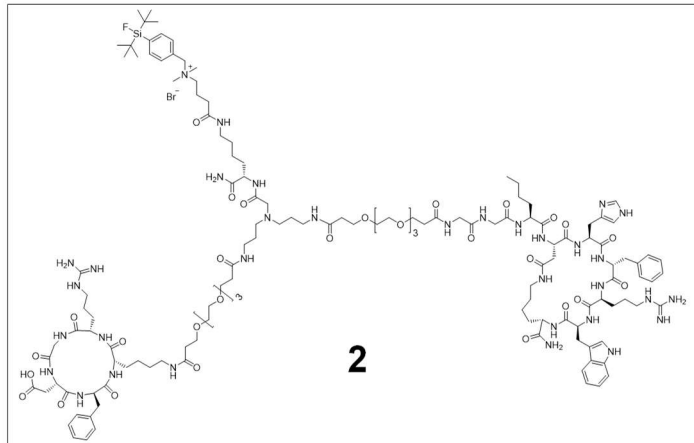


Figure S56. HPLC chromatogram (**A**) and mass spectra (**B**: ESI, **C**: MALDI) of SiFA/*in*-APG-PEG₃-c(RGDfK)/GG-Nle-c(DHfRWK) (**2**).

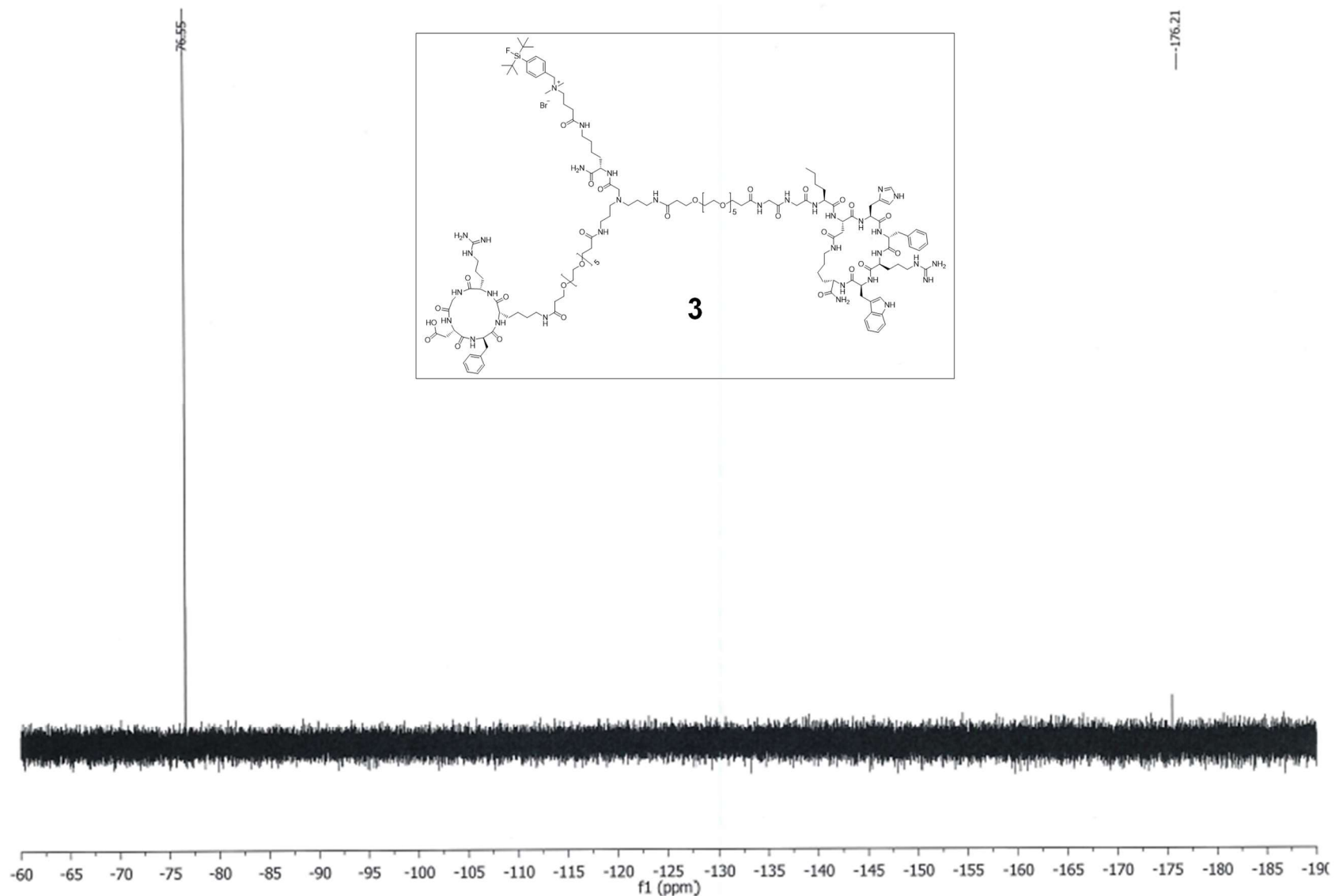


Figure S57. ^{19}F NMR spectrum of SiFA/*in*-APG-PEG₅-c(RGDfK)/GG-Nle-c(DHfRWK) (**3**).

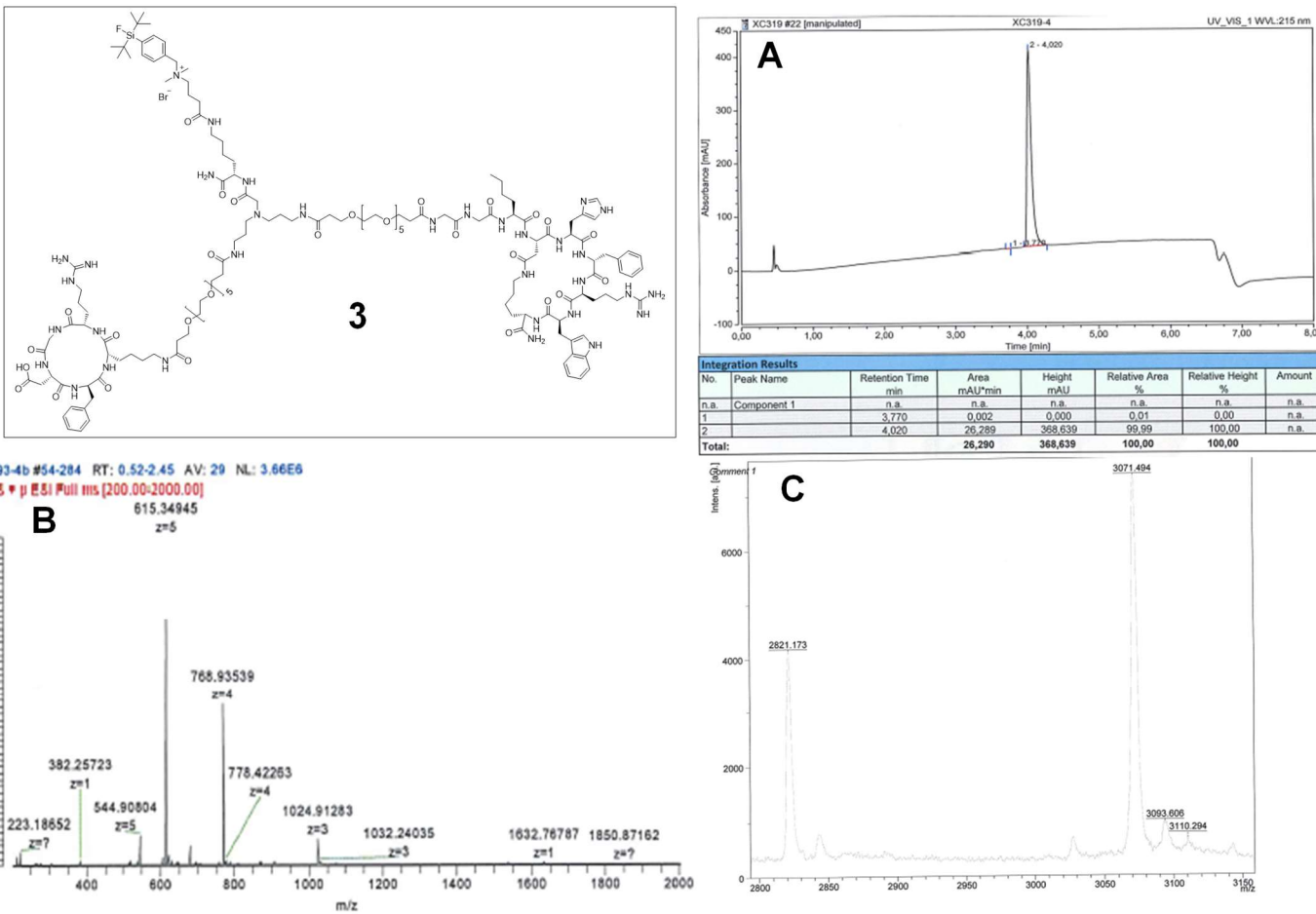


Figure S58. HPLC chromatogram (**A**) and mass spectra (**B**: ESI, **C**: MALDI) of SiFA/*in*-APG-PEG₅-c(RGDfK)/GG-Nle-c(DHfRWK) (**3**).

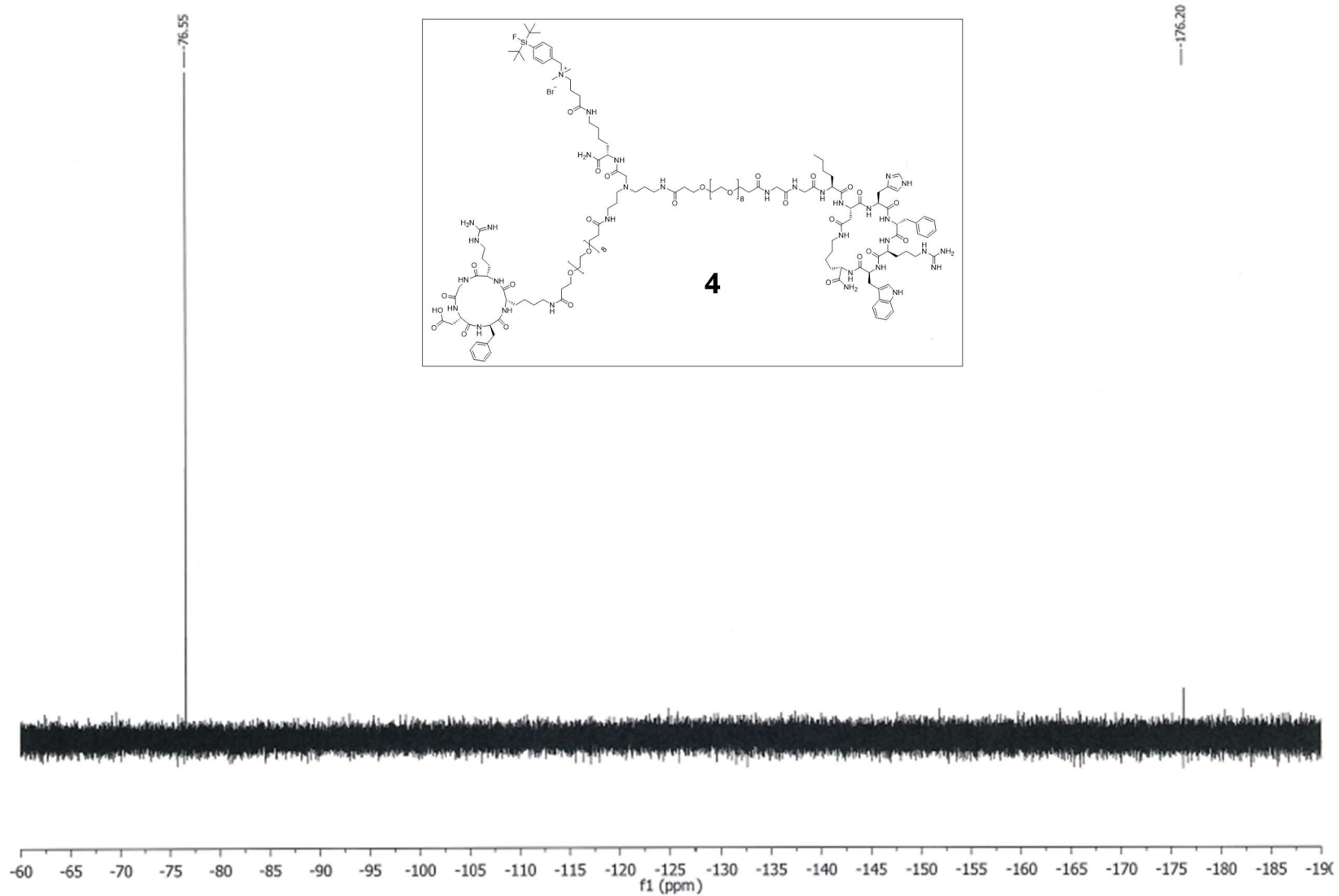


Figure S59. ^{19}F NMR spectrum of SiFA/*in*-APG-PEG₈-c(RGdfK)/GG-Nle-c(DHfRWK) (**4**).

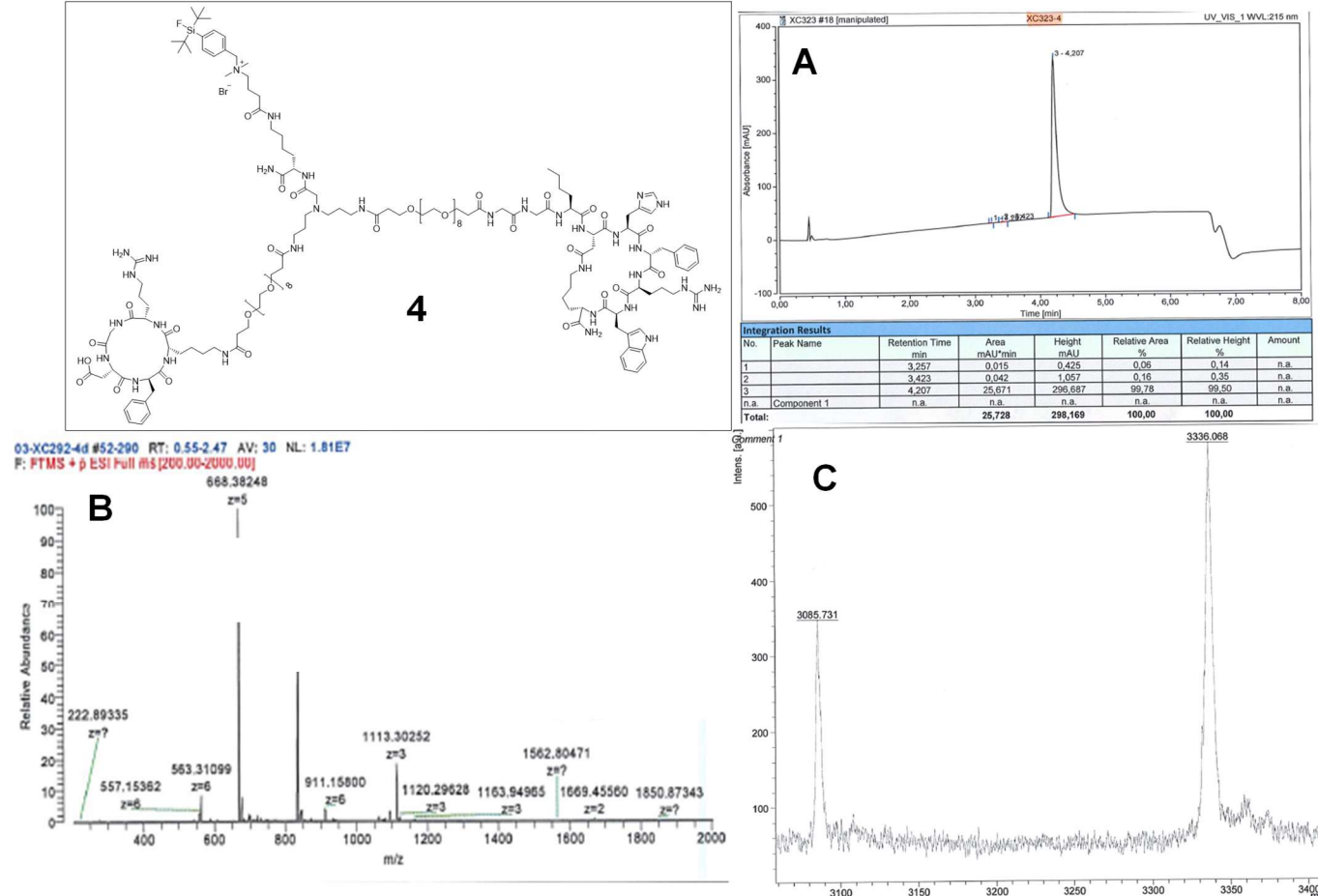


Figure S60. HPLC chromatogram (**A**) and mass spectra (**B**: ESI, **C**: MALDI) of SiFA/*in*-APG-PEG₈-c(RGDfK)/GG-Nle-c(DHfRWK) (**4**).

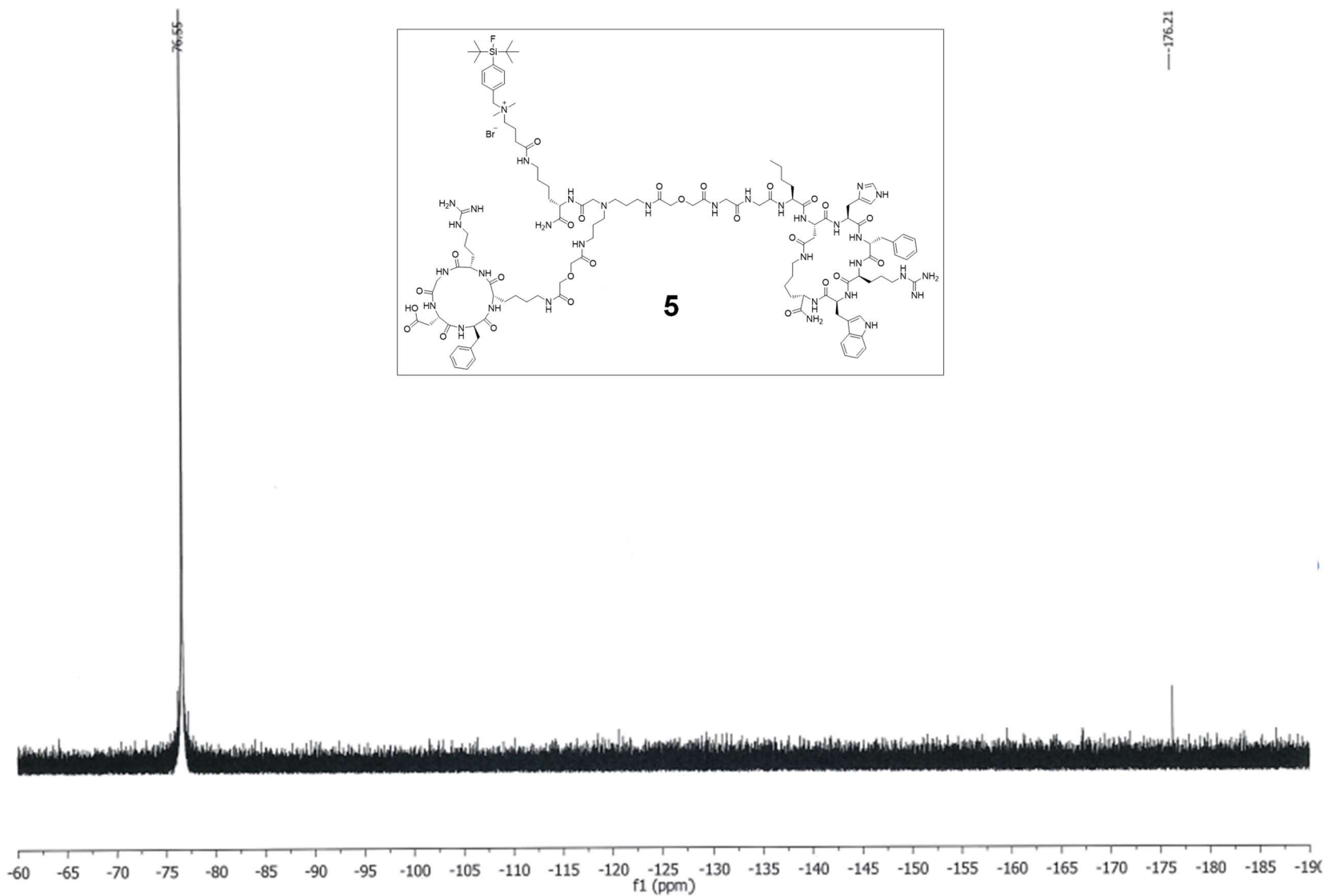


Figure S61. ¹⁹F NMR spectrum of SiFA/in-APG-DIG-c(RGDfK)/GG-Nle-c(DHfRWK) (**5**).

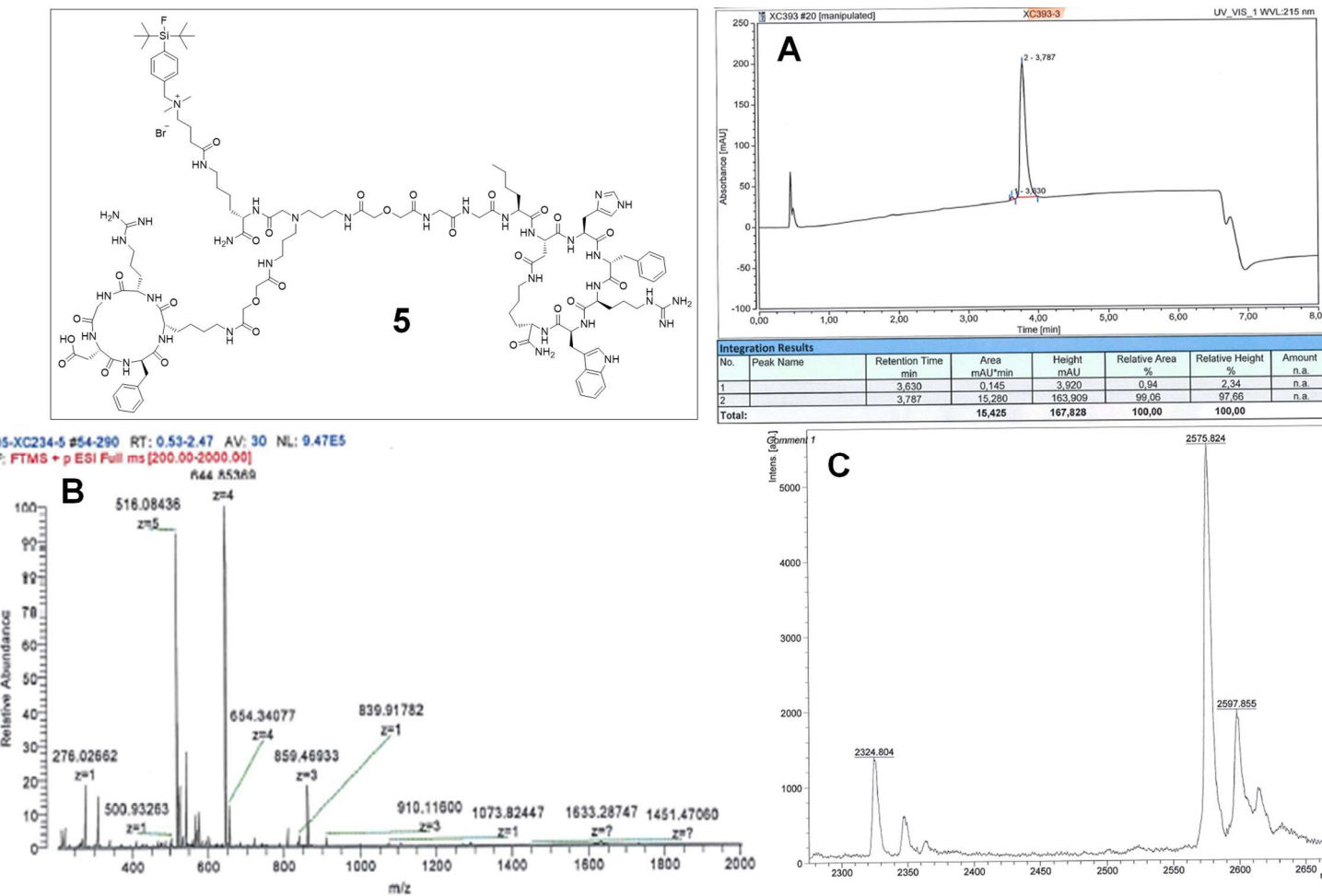


Figure S62. HPLC chromatogram (**A**) and mass spectra (**B**: ESI, **C**: MALDI) of SiFA/*in*-APG-DIG-c(RGDfK)/GG-Nle-c(DHfRWK) (**5**).

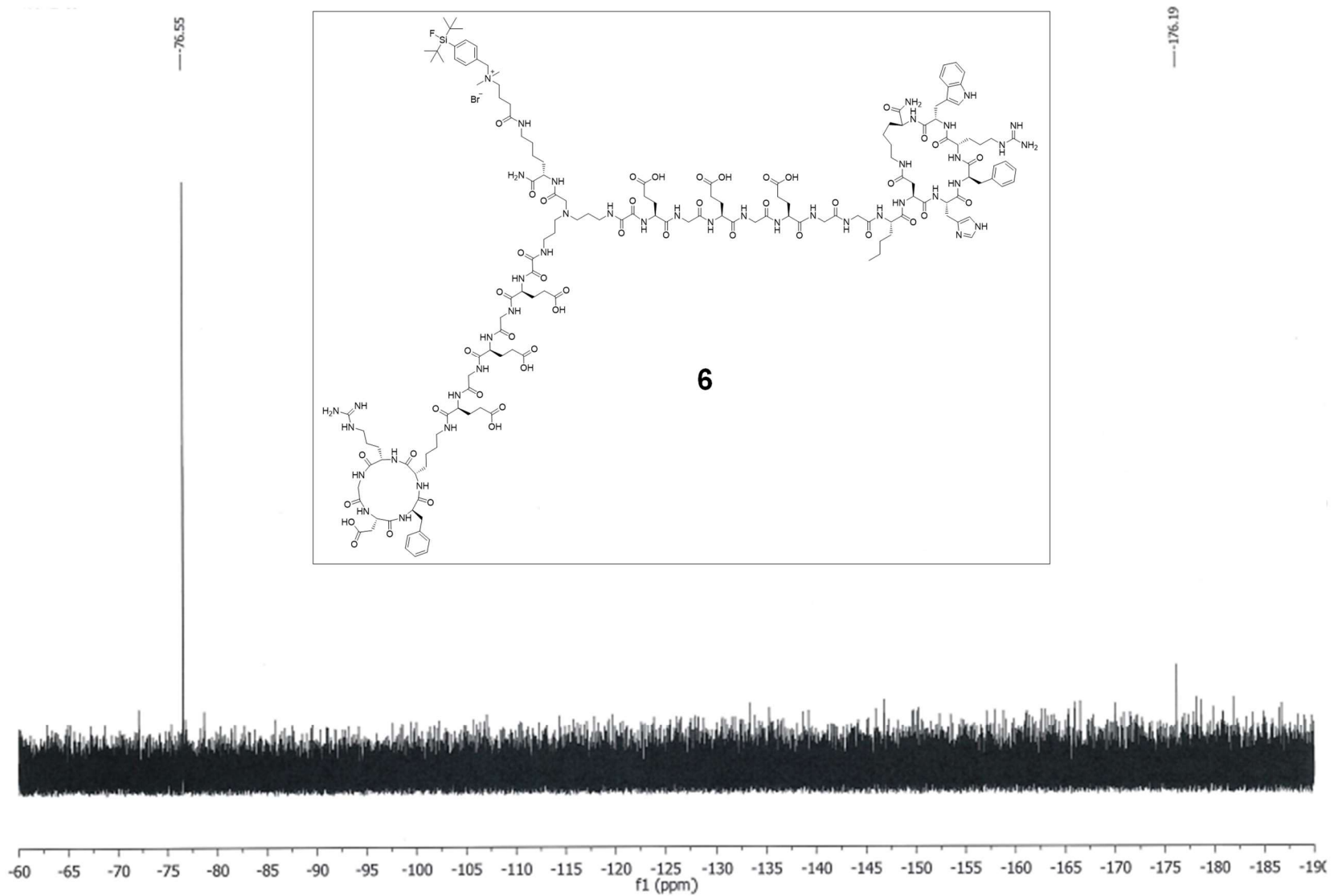


Figure S63. ${}^{19}\text{F}$ NMR spectrum of SiFAlin-APG-Ox-EGEGE-c(RGDfK)/GG-Nle-c(DHfRWK) (**6**).

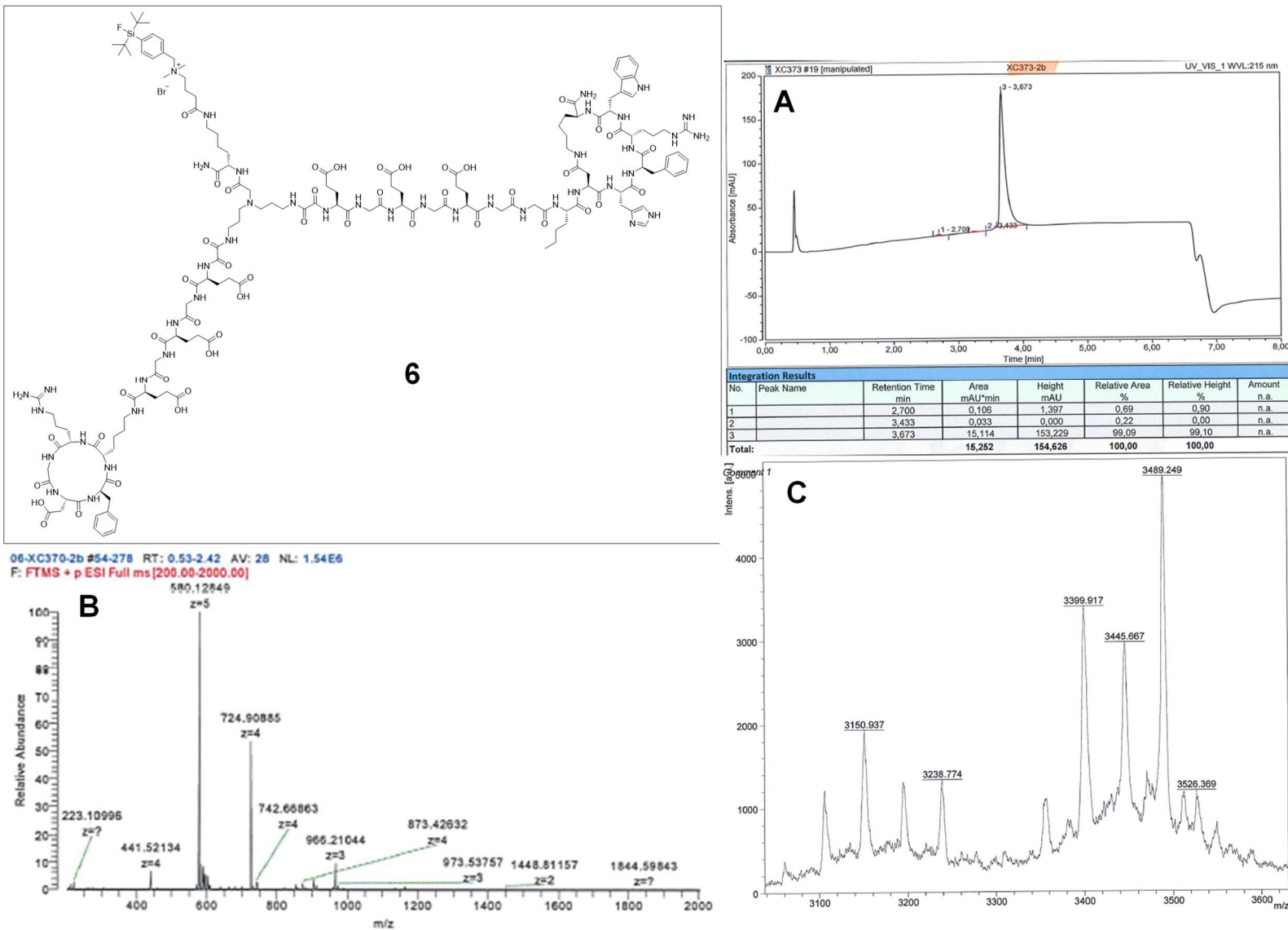


Figure S64. HPLC chromatogram (**A**) and mass spectra (**B**: ESI, **C**: MALDI) of SiFA/in-APG-Ox-EGEGE-c(RGDfK)/GG-Nle-c(DHfRWK) (**6**).

4. Mass data, HPLC chromatograms and mass spectra of peptidic side products a–z

HO-PEG₁-c(RGDfK) (a): MS (MALDI) *m/z* calcd for C₃₅H₅₄N₉O₁₂ [M+H]⁺ 792.39, found: 792.16; HRMS (ESI) *m/z* calcd for C₃₅H₅₄N₉O₁₂ [M+H]⁺ 792.3886, found 792.3890.

c(RGDfK)-PEG₁-c(RGDfK) (b): MS (MALDI) *m/z* calcd for C₆₂H₉₂N₁₈O₁₈ [M]⁺ 1376.68, found: 1376.51; HRMS (ESI) *m/z* calcd for C₆₂H₉₄N₁₈O₁₈ [M+2H]²⁺ 689.3491, found 689.3506; calcd for C₆₂H₉₃N₁₈O₁₈ [M+H]⁺ 1377.6910, found 1377.6972.

HO-PEG₃-c(RGDfK) (c): MS (MALDI) *m/z* calcd for C₃₉H₆₁N₉O₁₄ [M]⁺ 879.43, found: 879.54; HRMS (ESI) *m/z* calcd for C₃₉H₆₂N₉O₁₄ [M+H]⁺ 880.4411, found 880.4407.

c(RGDfK)-PEG₃-c(RGDfK) (d): MS (MALDI) *m/z* calcd for C₆₆H₁₀₀N₁₈O₂₀ [M]⁺ 1464.74, found: 1464.78; HRMS (ESI) *m/z* calcd for C₆₆H₁₀₁N₁₈O₂₀ [M+H]⁺ 1465.7434, found 1465.7475.

HO-PEG₅-c(RGDfK) (e): MS (MALDI) *m/z* calcd for C₄₃H₇₀N₉O₁₆ [M+H]⁺ 968.49, found: 968.19; HRMS (ESI) *m/z* calcd for C₄₃H₇₀N₉O₁₆ [M+H]⁺ 968.4935, found 968.4941.

c(RGDfK)-PEG₅-c(RGDfK) (f): MS (MALDI) *m/z* calcd for C₇₀H₁₀₉N₁₈O₂₂ [M]⁺ 1553.80, found: 1553.12; HRMS (ESI) *m/z* calcd for C₇₀H₁₁₀N₁₈O₂₂ [M+2H]²⁺ 777.4016, found 777.4054; calcd for C₇₀H₁₀₉N₁₈O₂₂ [M+H]⁺ 1553.7958, found 1553.8101.

HO-PEG₈-c(RGDfK) (g): MS (MALDI) *m/z* calcd for C₄₉H₈₂N₉O₁₉ [M+H]⁺ 1100.57, found: 1100.24; HRMS (ESI) *m/z* calcd for C₄₉H₈₂N₉O₁₉ [M+H]⁺ 1100.5721, found 1100.5722.

c(RGDfK)-PEG₈-c(RGDfK) (h): MS (MALDI) *m/z* calcd for C₇₆H₁₂₁N₁₈O₂₅ [M+H]⁺ 1685.87, found: 1685.15; HRMS (ESI) *m/z* calcd for C₇₆H₁₂₁N₁₈NaO₂₅ [M+H+Na]²⁺ 854.4318, found 854.4318; calcd for C₇₆H₁₂₁N₁₈O₂₅ [M+H]⁺ 1685.8745, found 1685.8771.

HO-PEG₁-GG-Nle-c(DHfRWK) (i): MS (MALDI) *m/z* calcd for C₆₀H₈₆N₁₇O₁₅ [M+H]⁺ 1284.65, found: 1284.15; HRMS (ESI) *m/z* calcd for C₆₀H₈₇N₁₇O₁₅ [M+H]²⁺ 642.8278, found 642.8286; calcd for C₆₀H₈₆N₁₇O₁₅ [M+H]⁺: 1284.6517, found 1284.6534.

c(DHfRWK)-Nle-GG-PEG₁-GG-Nle-c(DHfRWK) (j): MS (MALDI) *m/z* calcd for C₁₁₂H₁₅₇N₃₄O₂₄ [M+H]⁺ 2362.21, found: 2362.06; HRMS (ESI) *m/z* calcd for C₁₁₂H₁₅₉N₃₄O₂₄ [M+3H]³⁺ 788.4095, found 788.4087; calcd for C₁₁₂H₁₅₈N₃₄O₂₄ [M+2H]²⁺ 1182.1105, found 1182.1107.

HO-PEG₃-GG-Nle-c(DHfRWK) (k): MS (MALDI) *m/z* calcd for C₆₄H₉₄N₁₇O₁₇ [M+H]⁺ 1372.70, found: 1372.49; HRMS (ESI) *m/z* calcd for C₆₄H₉₄N₁₇O₁₇ [M+H]²⁺ 686.3501, found 686.3624; calcd for C₆₄H₉₄N₁₇O₁₇ [M+H]⁺ 1372.7008, found 1372.7041.

c(DHfRWK)-Nle-GG-PEG₃-GG-Nle-c(DHfRWK) (l): MS (MALDI) *m/z* calcd for C₁₁₆H₁₆₅N₃₄O₂₆ [M+H]⁺ 2450.26, found: 2450.78; HRMS (ESI) *m/z* calcd for C₁₁₆H₁₆₆N₃₄O₂₆ [M+2H]²⁺ 1226.1368, found 1226.1374.

HO-PEG₅-GG-Nle-c(DHfRWK) (m): MS (MALDI) *m/z* calcd for C₆₈H₁₀₁N₁₇O₁₉ [M]⁺ 1459.75, found: 1459.03; HRMS (ESI) *m/z* calcd for C₆₈H₁₀₂N₁₇O₁₉ [M+H]⁺ 1460.7532, found 1460.7528.

c(DHfRWK)-Nle-GG-PEG₅-GG-Nle-c(DHfRWK) (n): MS (MALDI) *m/z* calcd for C₁₂₀H₁₇₃N₃₄O₂₈ [M+H]⁺ 2538.32, found: 2538.09; HRMS (ESI) *m/z* calcd for C₁₂₀H₁₇₅N₃₄O₂₈ [M+3H]³⁺ 847.1111, found 847.1110; calcd for C₁₂₀H₁₇₄N₃₄O₂₈ [M+2H]²⁺ 1270.1630, found 1270.1641.

HO-PEG₈-GG-Nle-c(DHfRWK) (o): MS (MALDI) *m/z* calcd for C₇₄H₁₁₄N₁₇O₂₂ [M+H]⁺ 1592.83, found: 1592.11; HRMS (ESI) *m/z* calcd for C₇₄H₁₁₄N₁₇O₂₂ [M+H]⁺ 1592.8319, found 1592.8321.

c(DHfRWK)-Nle-GG-PEG₈-GG-Nle-c(DHfRWK) (p): MS (MALDI) *m/z* calcd for C₁₂₆H₁₈₅N₃₄O₃₁ [M+H]⁺ 2670.39, found: 2670.33; HRMS (ESI) *m/z* calcd for C₁₂₆H₁₈₈N₃₄O₃₁ [M+4H]⁴⁺ 668.6048, found 668.6048; calcd for C₁₂₆H₁₈₇N₃₄O₃₁ [M+3H]³⁺ 891.1373, found 891.1372; calcd for C₁₂₆H₁₈₆N₃₄O₃₁ [M+2H]²⁺ 1336.2023, found 1336.2039.

c(RGDfK)-DIG-c(RGDfK) (q): MS (MALDI) *m/z* calcd for C₅₈H₈₅N₁₈O₁₇ [M+H]⁺ 1305.63, found: 1305.49; HRMS (ESI) *m/z* calcd for C₅₈H₈₆N₁₈O₁₇ [M+2H]²⁺ 653.3204, found 653.3207; calcd for C₅₈H₈₅N₁₈O₁₇ [M+H]⁺ 1305.6335, found 1305.6356.

c(RGDfK)-EGEGE-Ox-EGEGE-c(RGDfK) (r): MS (MALDI) *m/z* calcd for C₅₈H₈₅N₁₈O₁₇ [M+H]⁺ 2263.95, found: 2263.82; HRMS (ESI) *m/z* calcd for C₉₄H₁₃₆N₂₈O₃₈ [M+2H]²⁺ 1132.9796, found 1132.9793.

c(DHfRWK)-Nle-GG-DIG-GG-Nle-c(DHfRWK) (s): MS (MALDI) *m/z* calcd for C₁₀₈H₁₄₈N₃₄O₂₃ [M]⁺ 2289.15, found: 2289.51; HRMS (ESI) *m/z* calcd for C₁₀₈H₁₅₁N₃₄O₂₃ [M+3H]³⁺ 764.3903, found 764.3896; calcd for C₁₀₈H₁₅₀N₃₄O₂₃ [M+2H]²⁺ 1146.0818, found 1146.0820.

c(DHfRWK)-Nle-GG-EGEGE-Ox-EGEGE-GG-Nle-c(DHfRWK) (t): MS (MALDI) *m/z* calcd for C₁₄₄H₁₉₉N₄₄O₄₄ [M+H]⁺ 3248.47, found: 3248.29; HRMS (ESI) *m/z* calcd for C₁₄₄H₂₀₁N₄₄O₄₄ [M+3H]³⁺ 1083.8287, found 1083.8283; calcd for C₁₄₄H₂₀₀N₄₄O₄₄ [M+2H]²⁺ 1625.2394, found 1625.2388.

SiFAlin-APG-[PEG₁-c(RGDfK)]₂ (u): MS (MALDI) *m/z* calcd for C₁₀₅H₁₆₉FN₂₅O₂₅Si [M]⁺ 2227.25, found: 2227.78; HRMS (ESI) *m/z* calcd for C₁₀₅H₁₇₁FN₂₅O₂₅Si [M+2H]³⁺ 743.4216, found 743.4216; calcd for C₁₀₅H₁₇₀FN₂₅O₂₅Si [M+H]²⁺ 1114.6288, found 1114.6282.

SiFAlin-APG-[PEG₃-c(RGDfK)]₂ (v): MS (MALDI) *m/z* calcd for C₁₁₃H₁₈₆FN₂₅O₂₉Si [M+H]⁺ 2404.36, found: 2404.59; HRMS (ESI) *m/z* calcd for C₁₁₃H₁₈₇FN₂₅O₂₉Si [M+2H]³⁺ 802.1232, found 802.1231; calcd for C₁₁₃H₁₈₆FN₂₅O₂₉Si [M+H]²⁺ 1202.6812, found 1202.6806.

SiFAlin-APG-[PEG₅-c(RGDfK)]₂ (w): MS (MALDI) *m/z* calcd for C₁₂₁H₂₀₂FN₂₅O₃₃Si [M+H]⁺ 2580.46, found: 2580.38; HRMS (ESI) *m/z* calcd for C₁₂₁H₂₀₄FN₂₅O₃₃Si [M+3H]⁴⁺ 645.8705, found 645.8709; calcd for C₁₂₁H₂₀₃FN₂₅O₃₃Si [M+2H]³⁺ 860.8249, found 860.8249; calcd for C₁₂₁H₂₀₂FN₂₅O₃₃Si [M+H]²⁺ 1290.7336, found 1290.7334.

SiFAlin-APG-[PEG₈-c(RGDfK)]₂ (x): MS (MALDI) *m/z* calcd for C₁₃₃H₂₂₅FN₂₅O₃₉Si [M+H]⁺ 2843.61, found: 2843.59; HRMS (ESI) *m/z* calcd for C₁₃₃H₂₂₈FN₂₅O₃₉Si [M+3H]⁴⁺ 711.9098, found 711.9095; calcd for C₁₃₃H₂₂₇FN₂₅O₃₉Si [M+2H]³⁺ 948.8773, found 948.8771; calcd for C₁₃₃H₂₂₆FN₂₅O₃₉Si [M+H]²⁺ 1422.8123, found 1422.8132.

SiFAlin-APG-[DIG-c(RGDfK)]₂ (y): MS (MALDI) *m/z* calcd for C₉₇H₁₅₃FN₂₅O₂₃Si [M]⁺ 2083.13, found: 2083.43; HRMS (ESI) *m/z* calcd for C₉₇H₁₅₀FN₂₅O₂₃Si [M-3H]⁺ 2081.1118, found 2081.4647.

SiFAlin-APG-[Ox-EGEGE-c(RGDfK)]₂ (z): MS (MALDI) *m/z* calcd for C₁₃₁H₂₀₀FN₃₅O₄₃Si [M+H]⁺ 2998.43, found: 2998.28; HRMS (ESI) *m/z* calcd for C₁₂₃H₁₇₉N₃₅O₄₃ [M-C₇H₁₇FSi]⁺ 1417.6459, found 1417.6307.

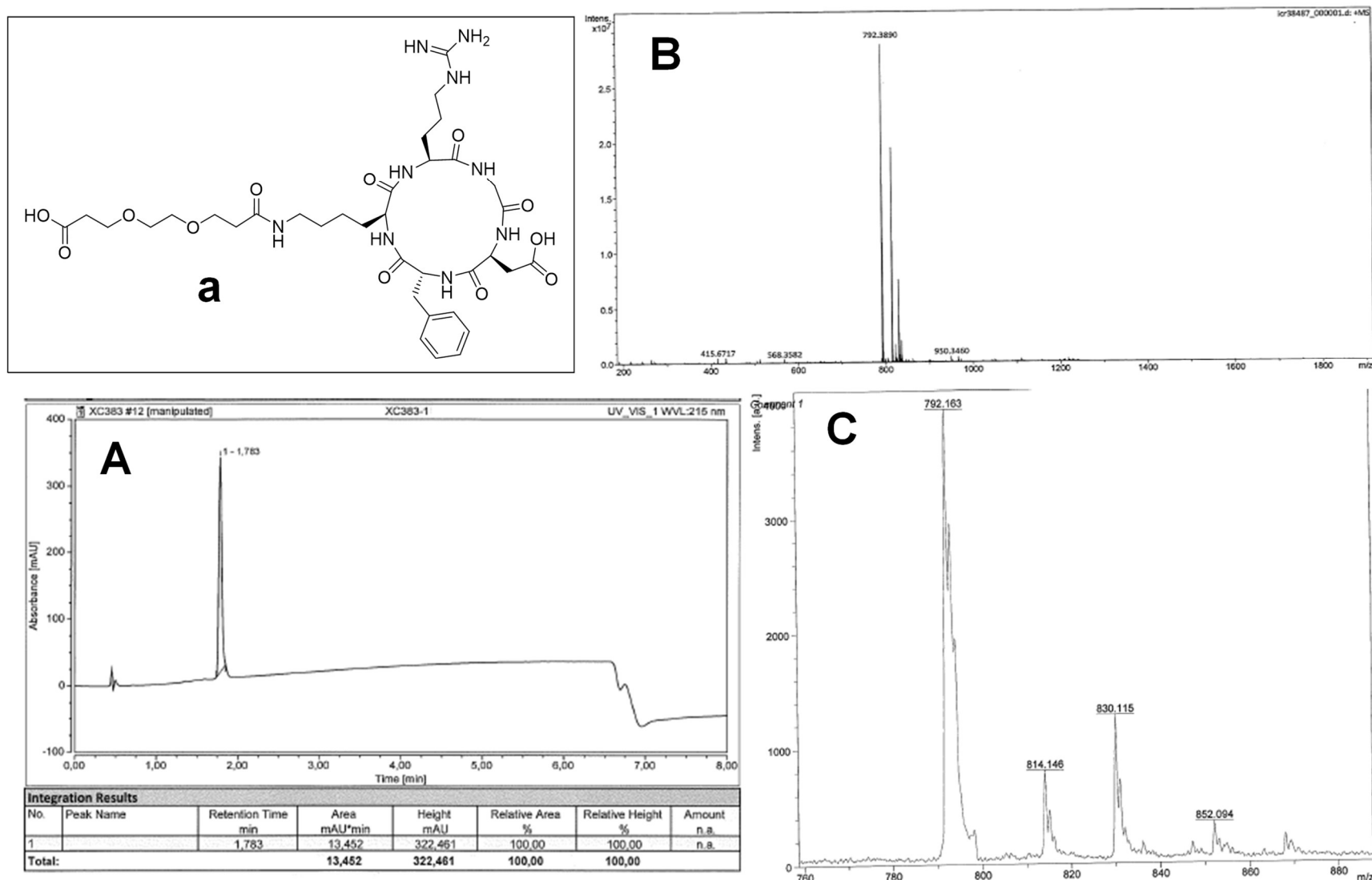


Figure S65. HPLC chromatogram (**A**) and mass spectra (**B**: ESI, **C**: MALDI) of HO-PEG₁-c(RGDfK) (**a**).

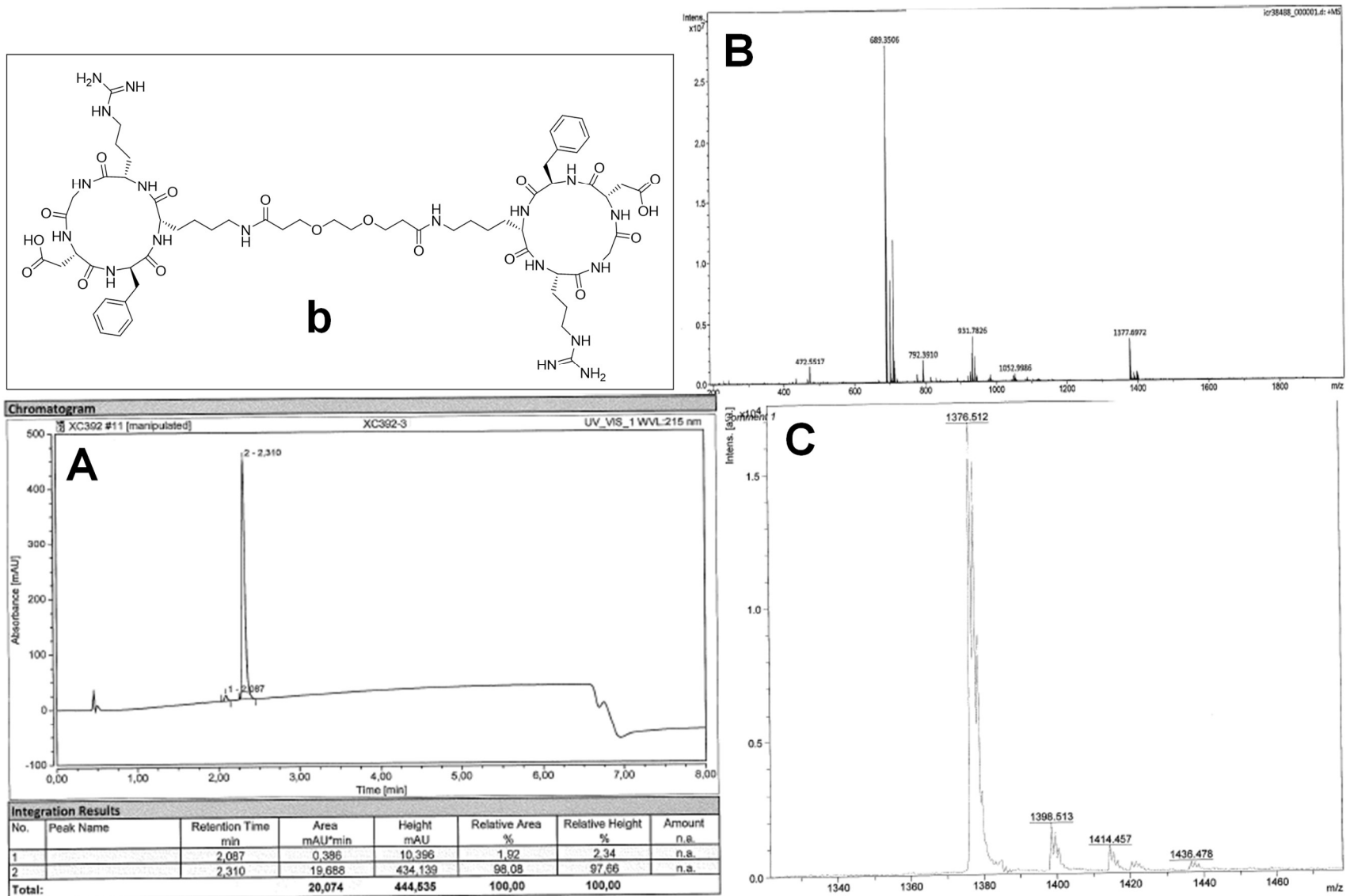


Figure S66. HPLC chromatogram (**A**) and mass spectra (**B**: ESI, **C**: MALDI) of c(RGDfK)-PEG₁-c(RGDfK) (**b**).

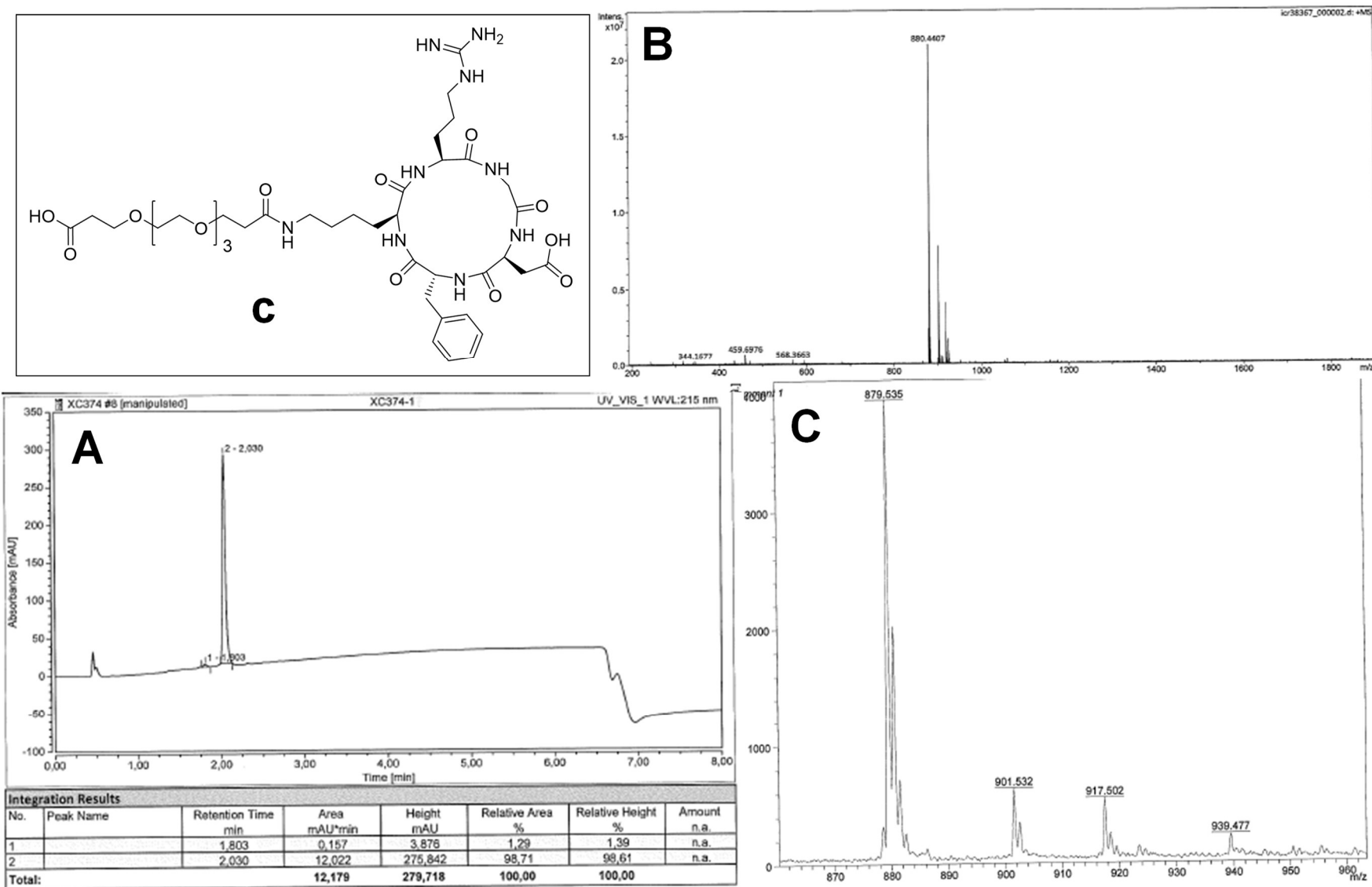


Figure S67. HPLC chromatogram (**A**) and mass spectra (**B**: ESI, **C**: MALDI) of HO-PEG₃-c(RGDfK) (**c**).

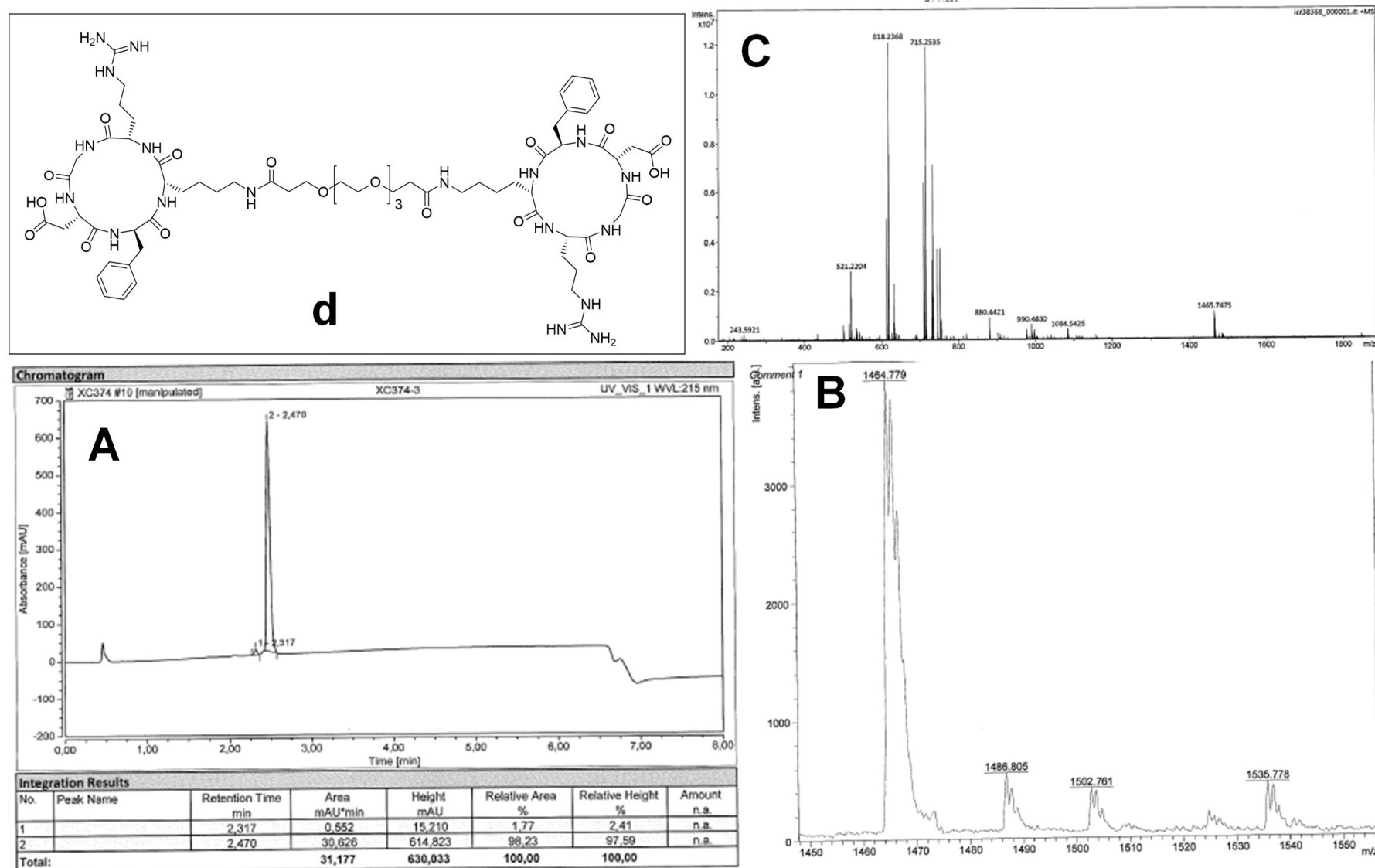


Figure S68. HPLC chromatogram (**A**) and mass spectra (**B**: ESI, **C**: MALDI) of c(RGDfK)-PEG₃-c(RGDfK) (**d**).

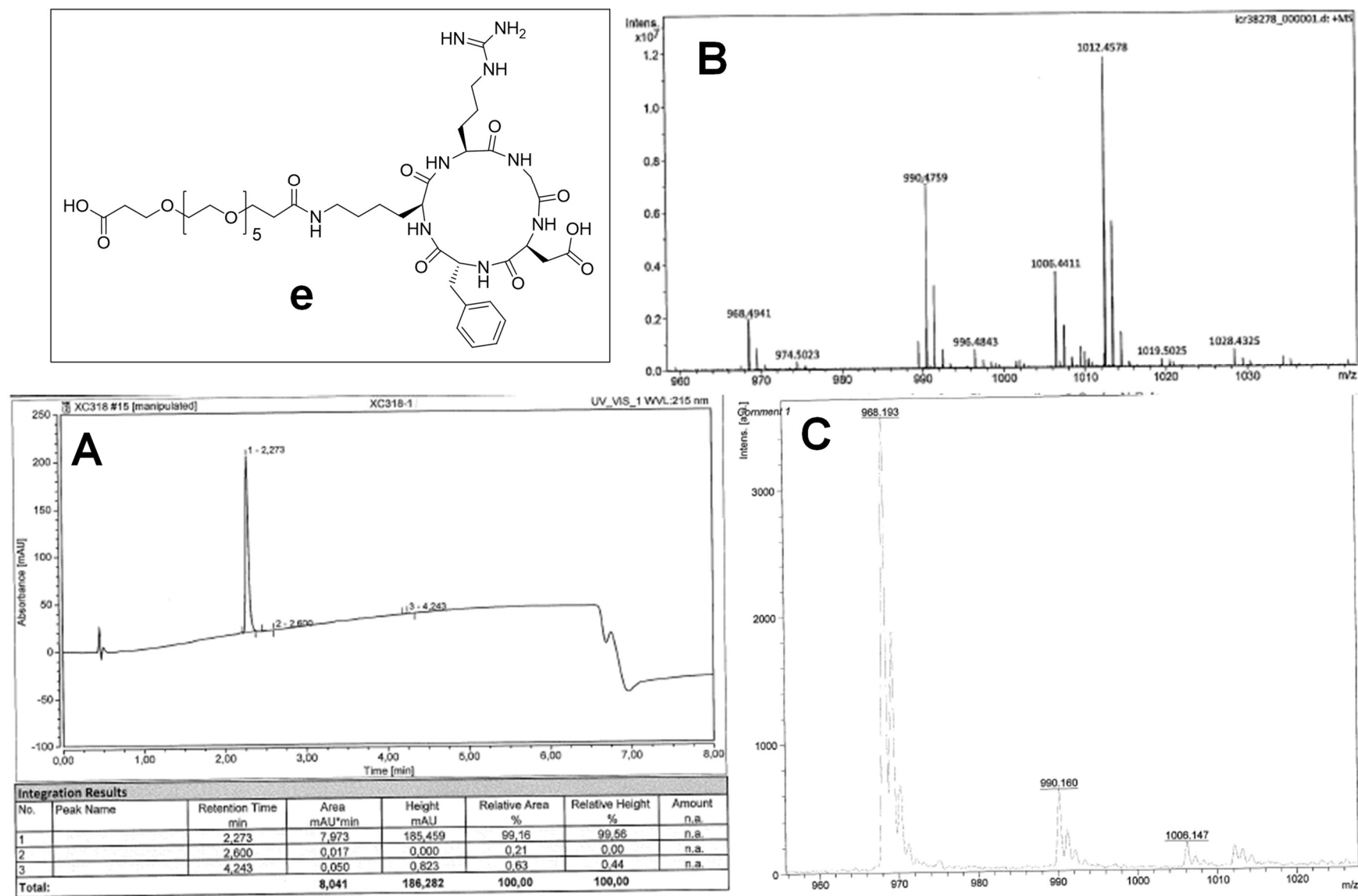


Figure S69. HPLC chromatogram (A) and mass spectra (B: ESI, C: MALDI) of HO-PEG₅-c(RGDfK) (e).

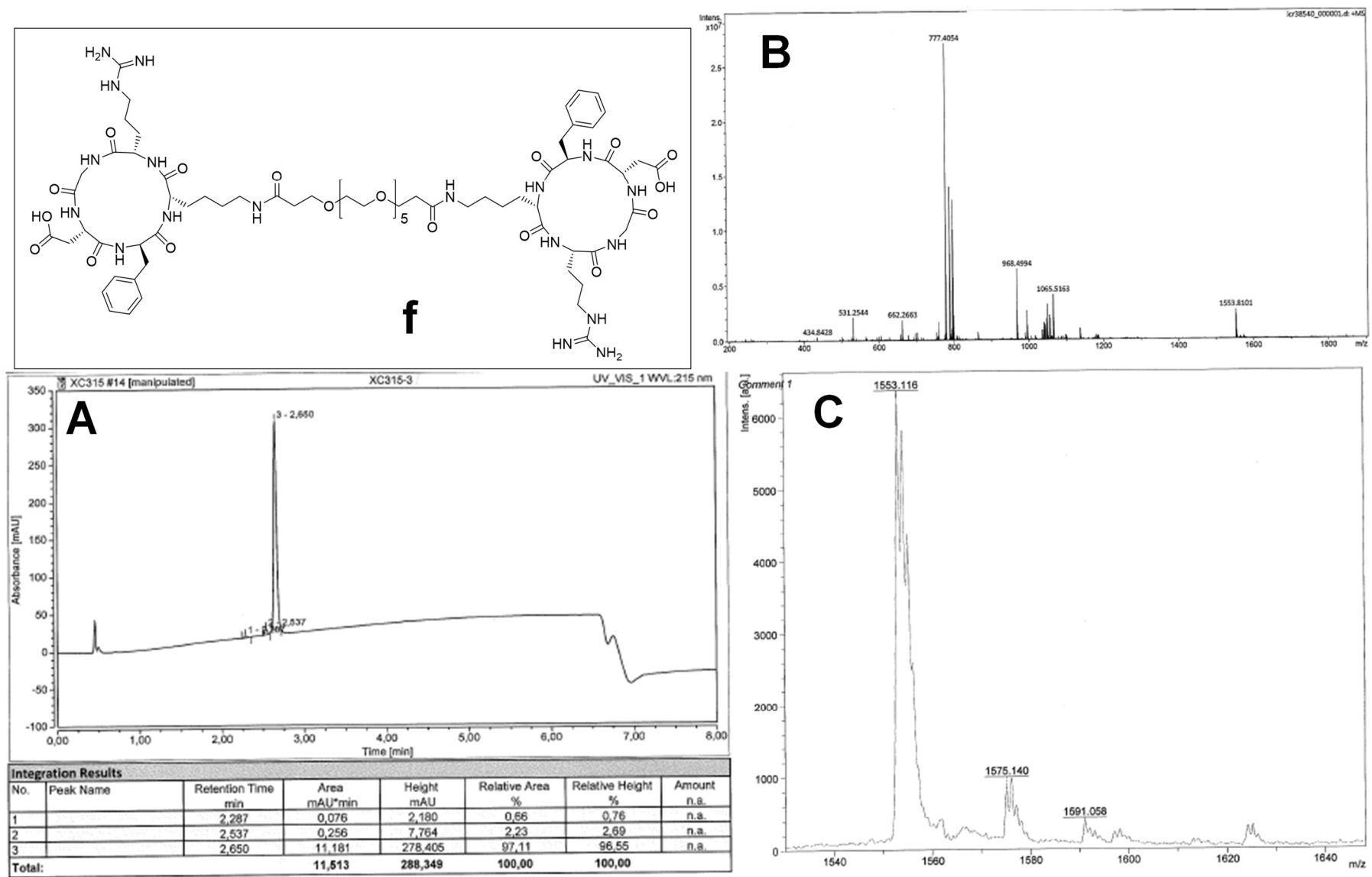


Figure S70. HPLC chromatogram (**A**) and mass spectra (**B**: ESI, **C**: MALDI) of c(RGDfK)-PEG₅-c(RGDfK) (**f**).

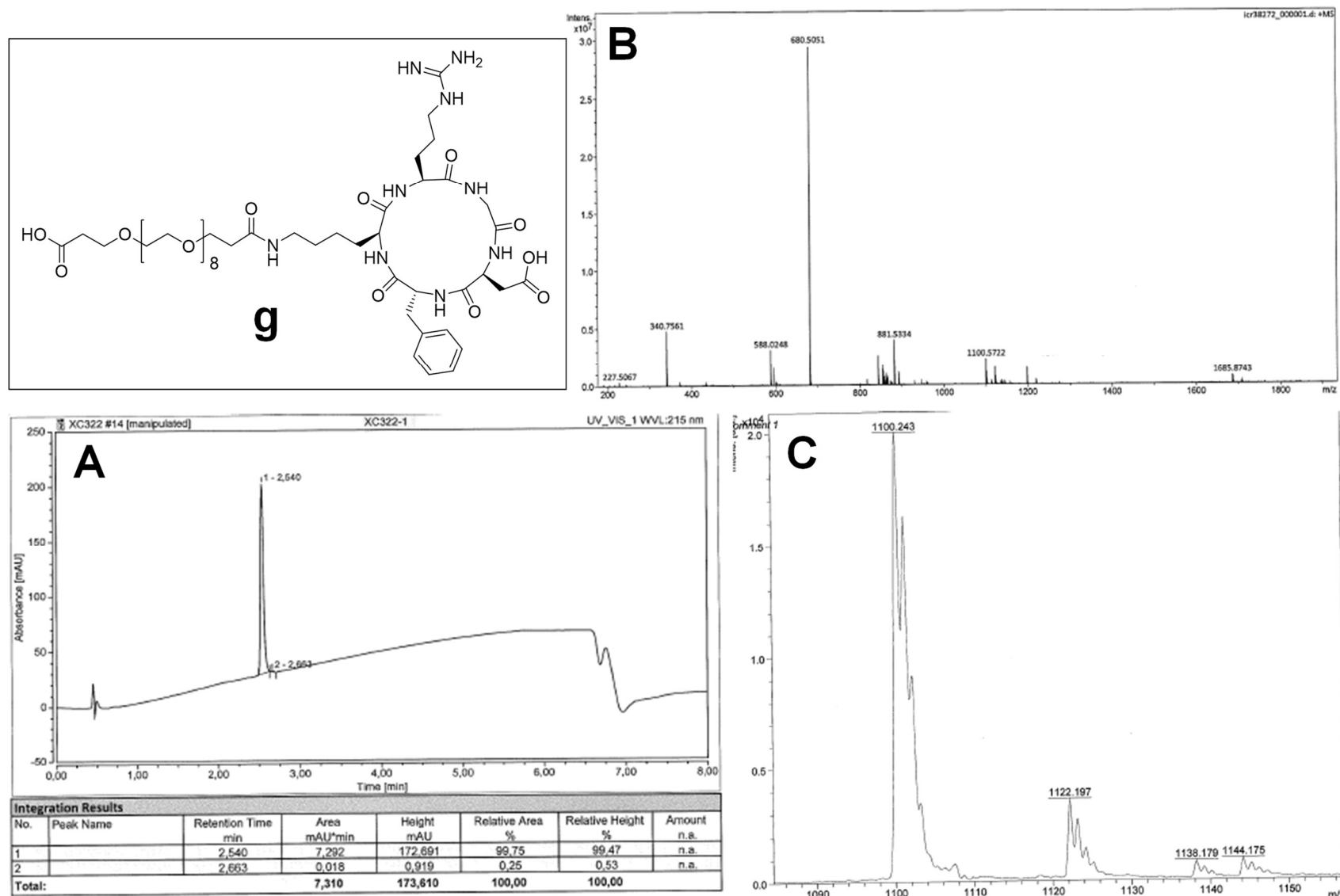


Figure S71. HPLC chromatogram (**A**) and mass spectra (**B**: ESI, **C**: MALDI) of HO-PEG₈-c(RGDfK) (**g**).

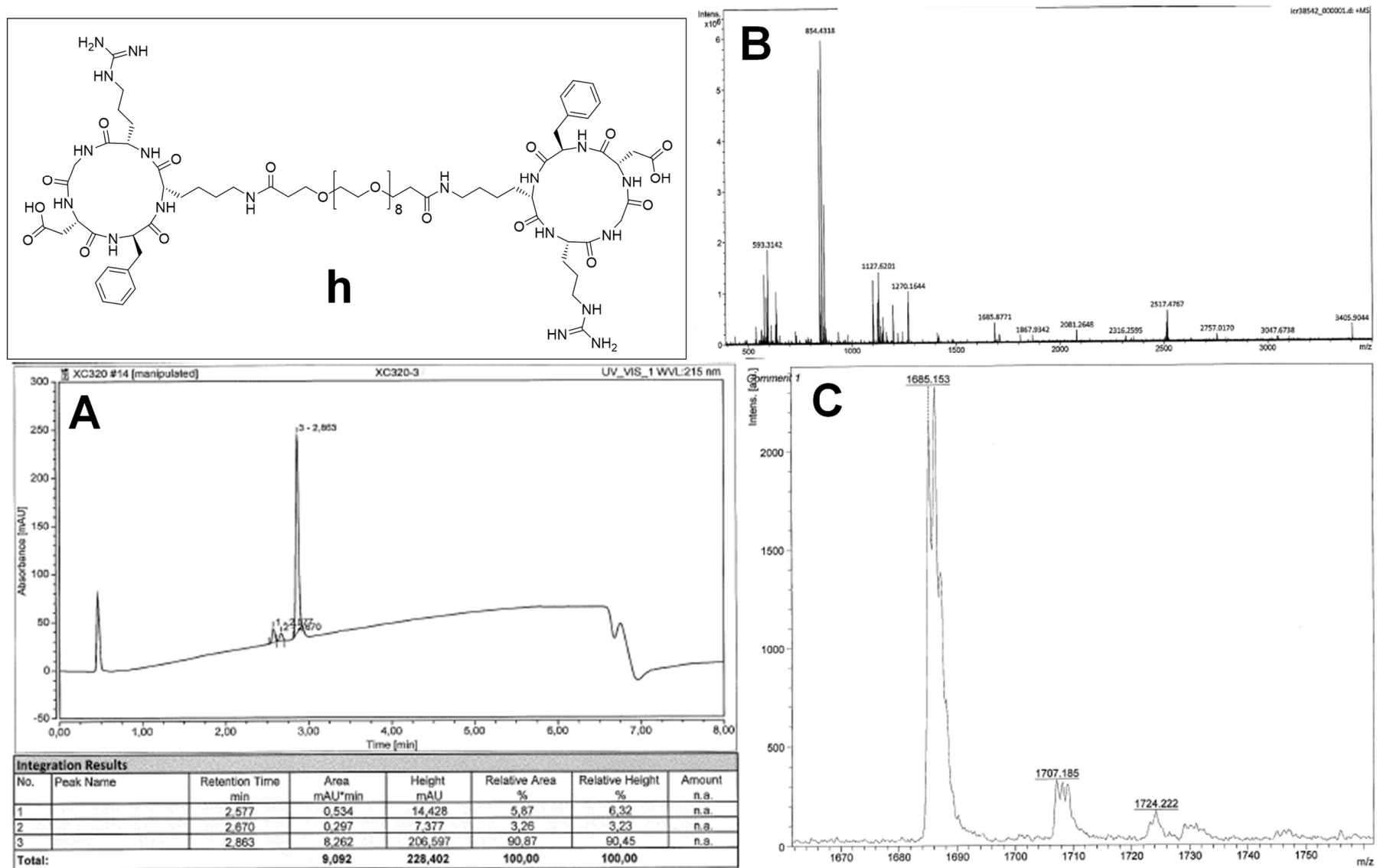


Figure S72. HPLC chromatogram (**A**) and mass spectra (**B**: ESI, **C**: MALDI) of c(RGDfK)-PEG₈-c(RGDfK) (**h**).

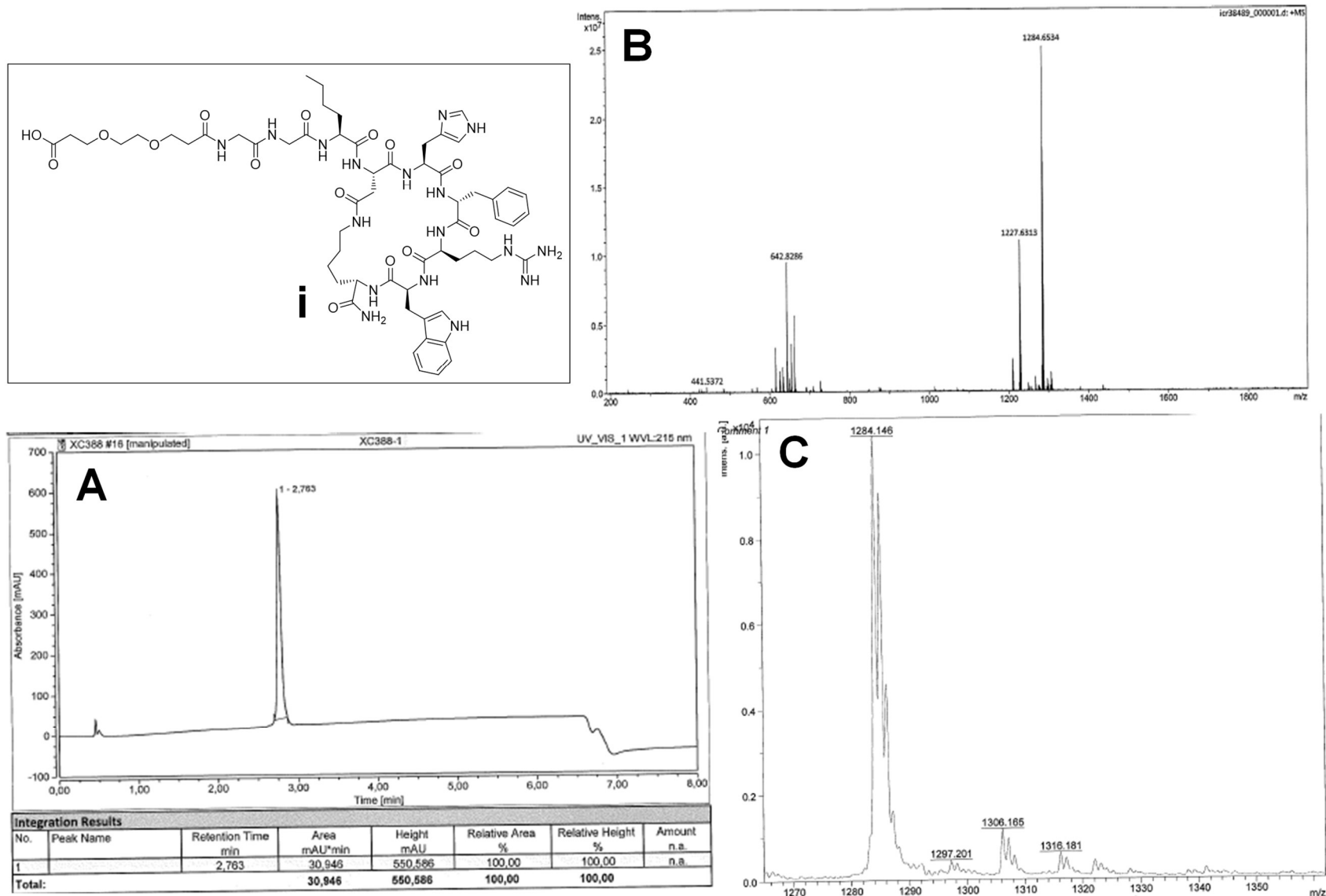


Figure S73. HPLC chromatogram (A) and mass spectra (B: ESI, C: MALDI) of HO-PEG₁-GG-Nle-c(DHfRWK) (i).

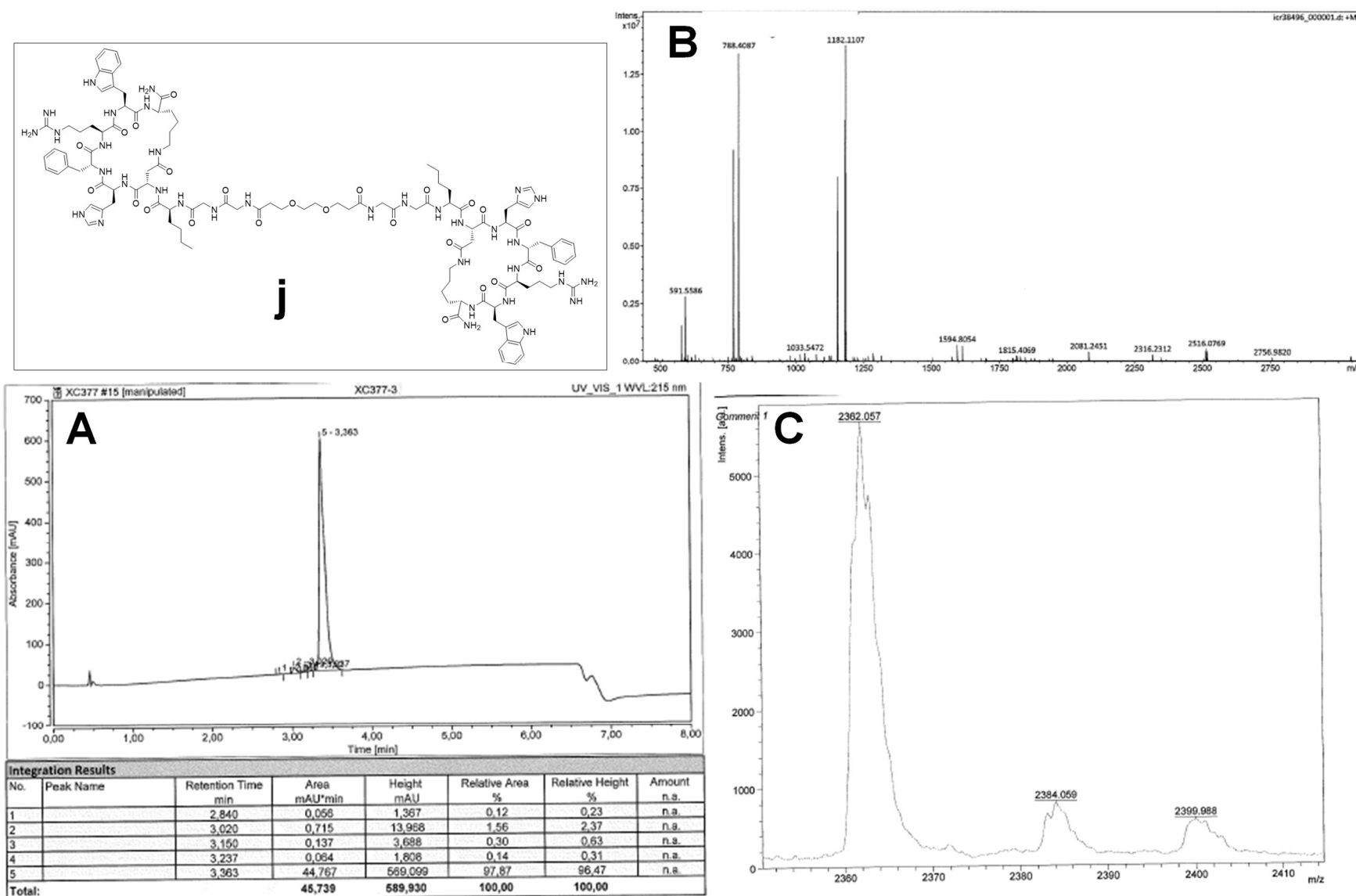


Figure S74. HPLC chromatogram (**A**) and mass spectra (**B**: ESI, **C**: MALDI) of c(DHfRWK)-Nle-GG-PEG₁-GG-Nle-c(DHfRWK) (**j**).

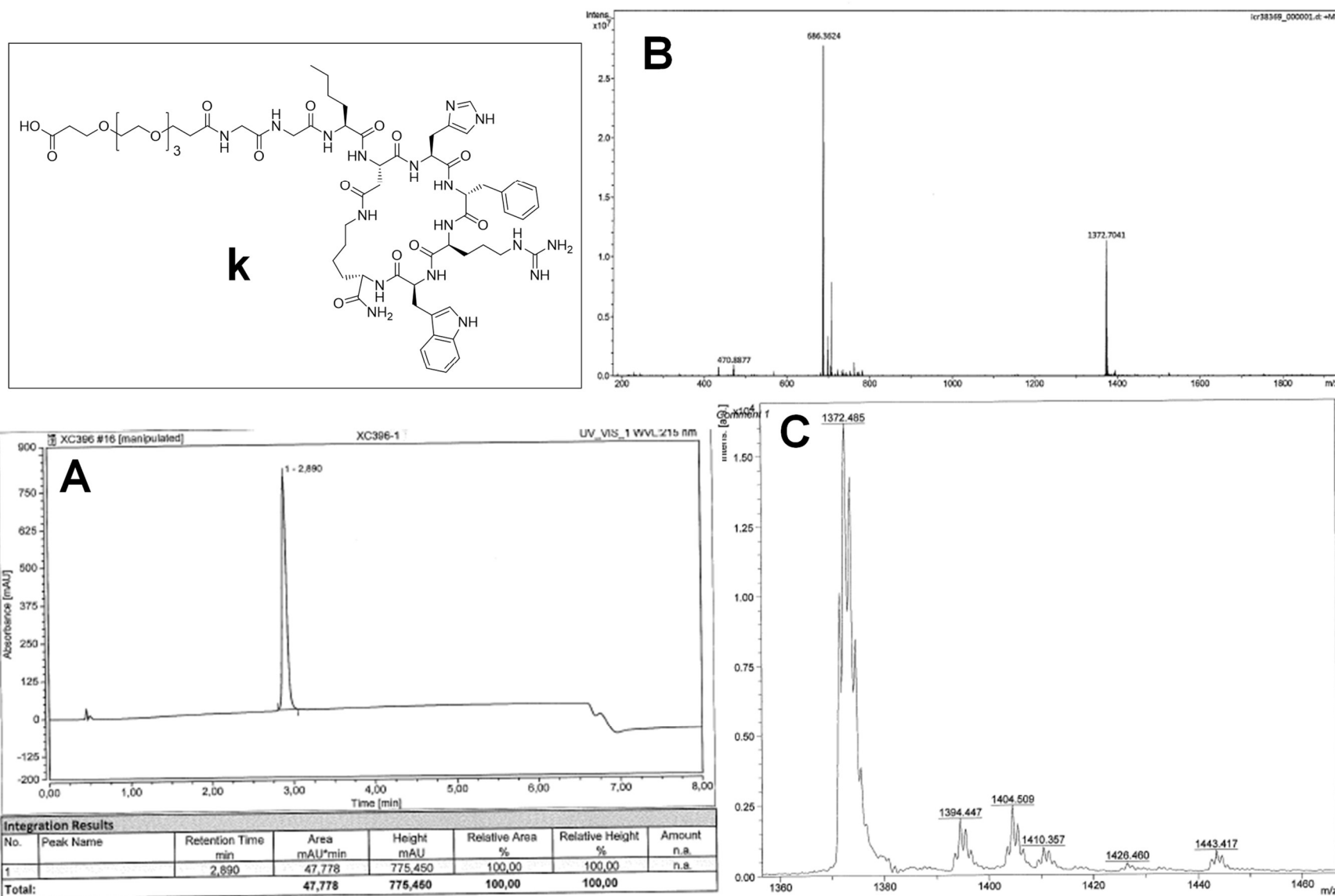


Figure S75. HPLC chromatogram (**A**) and mass spectra (**B**: ESI, **C**: MALDI) of HO-PEG₃-GG-Nle-c(DHfRWK) (**k**).

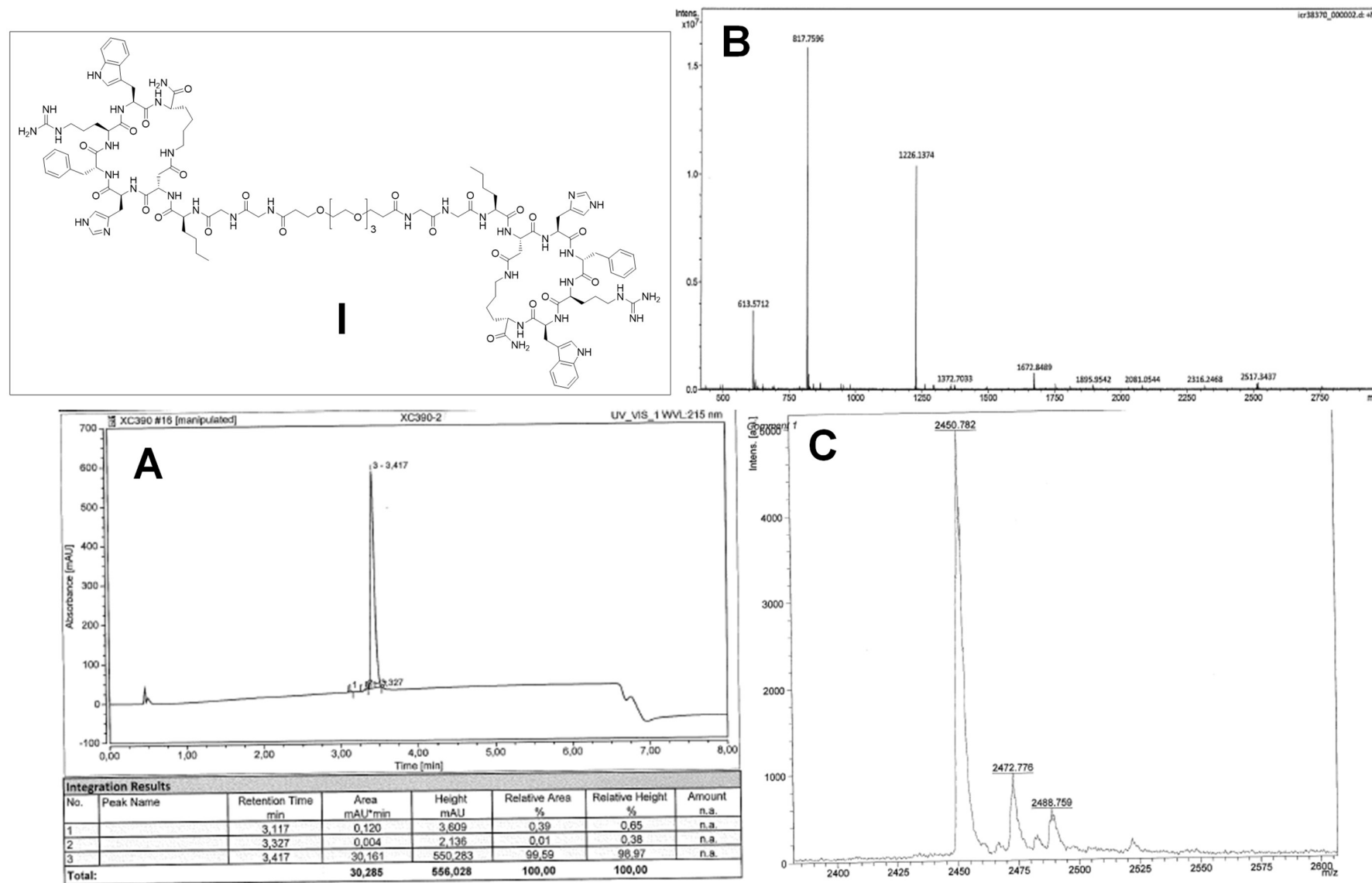


Figure S76. HPLC chromatogram (**A**) and mass spectra (**B**: ESI, **C**: MALDI) of c(DHfRWK)-Nle-GG-PEG₃-GG-Nle-c(DHfRWK) (**I**).

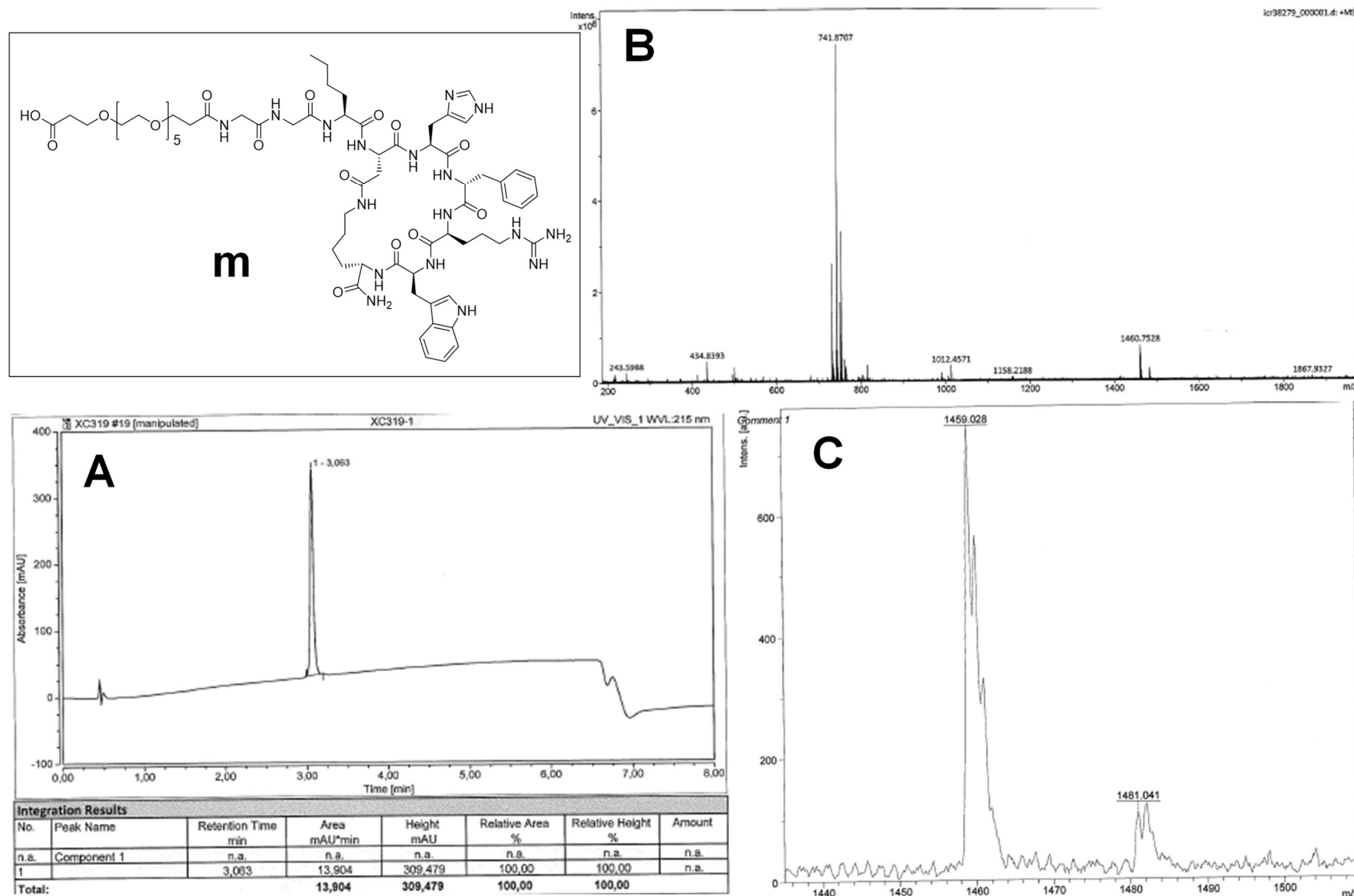
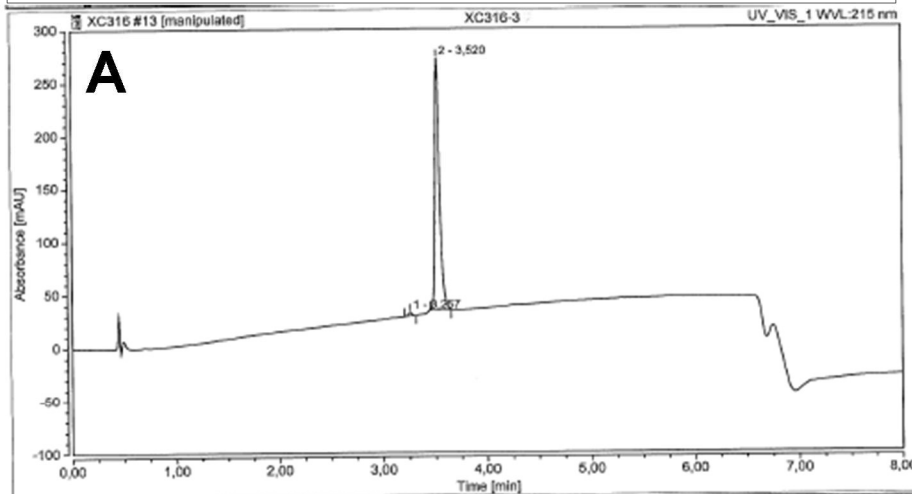
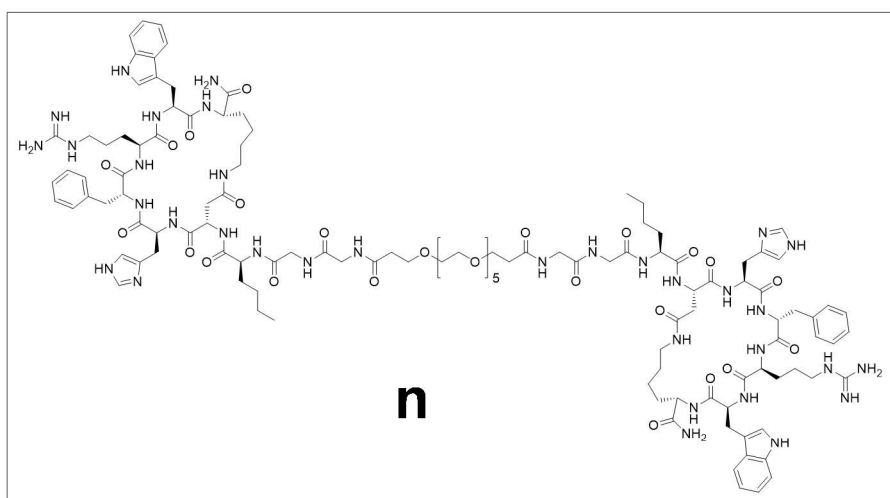


Figure S77. HPLC chromatogram (**A**) and mass spectra (**B**: ESI, **C**: MALDI) of HO-PEG₅-GG-Nle-c(DHfRWK) (**m**).



Integration Results

No.	Peak Name	Retention Time [min]	Area mAU'min	Height mAU	Relative Area %	Relative Height %	Amount n.a.
1		3,257	0,127	3,383	1,02	1,41	n.a.
2		3,520	12,316	237,193	96,98	98,59	n.a.
Total:			12,443	240,576	100,00	100,00	

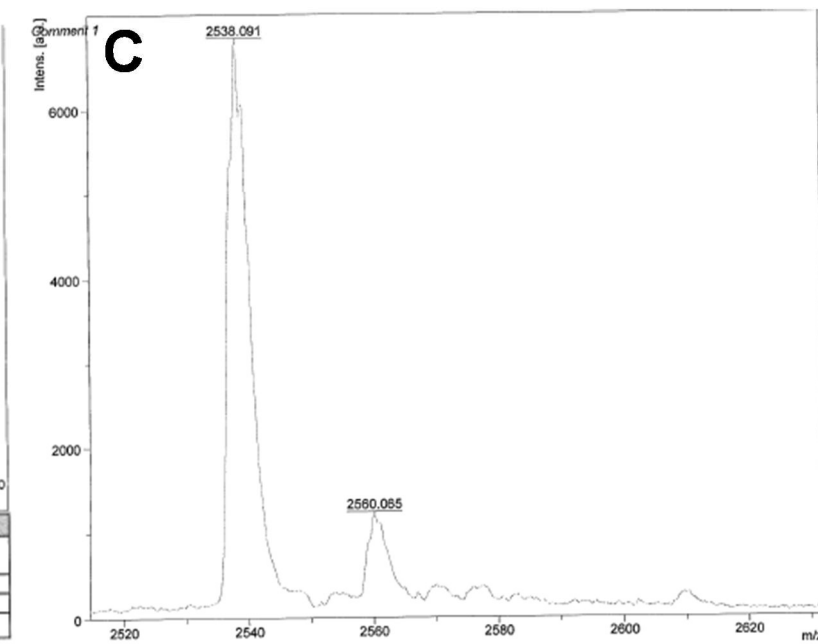
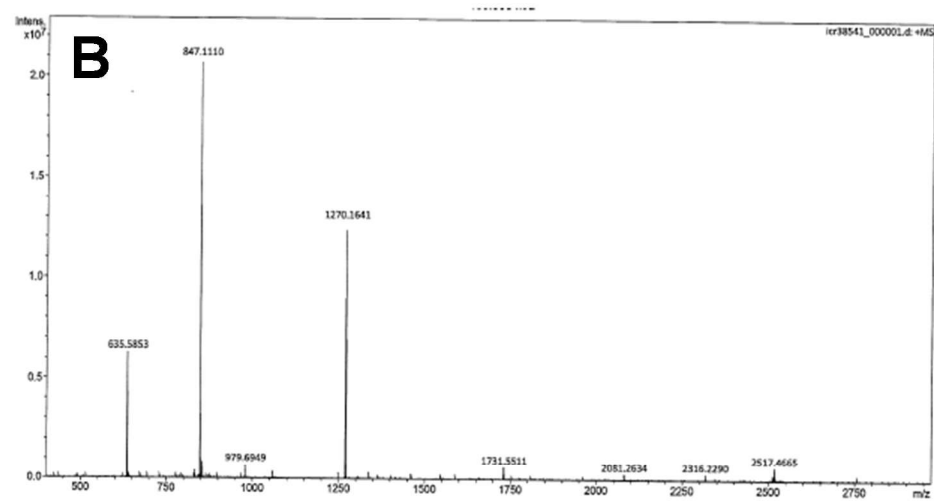


Figure S78. HPLC chromatogram (**A**) and mass spectra (**B**: ESI, **C**: MALDI) of c(DHfRWK)-Nle-GG-PEG₅-GG-Nle-c(DHfRWK) (**n**).

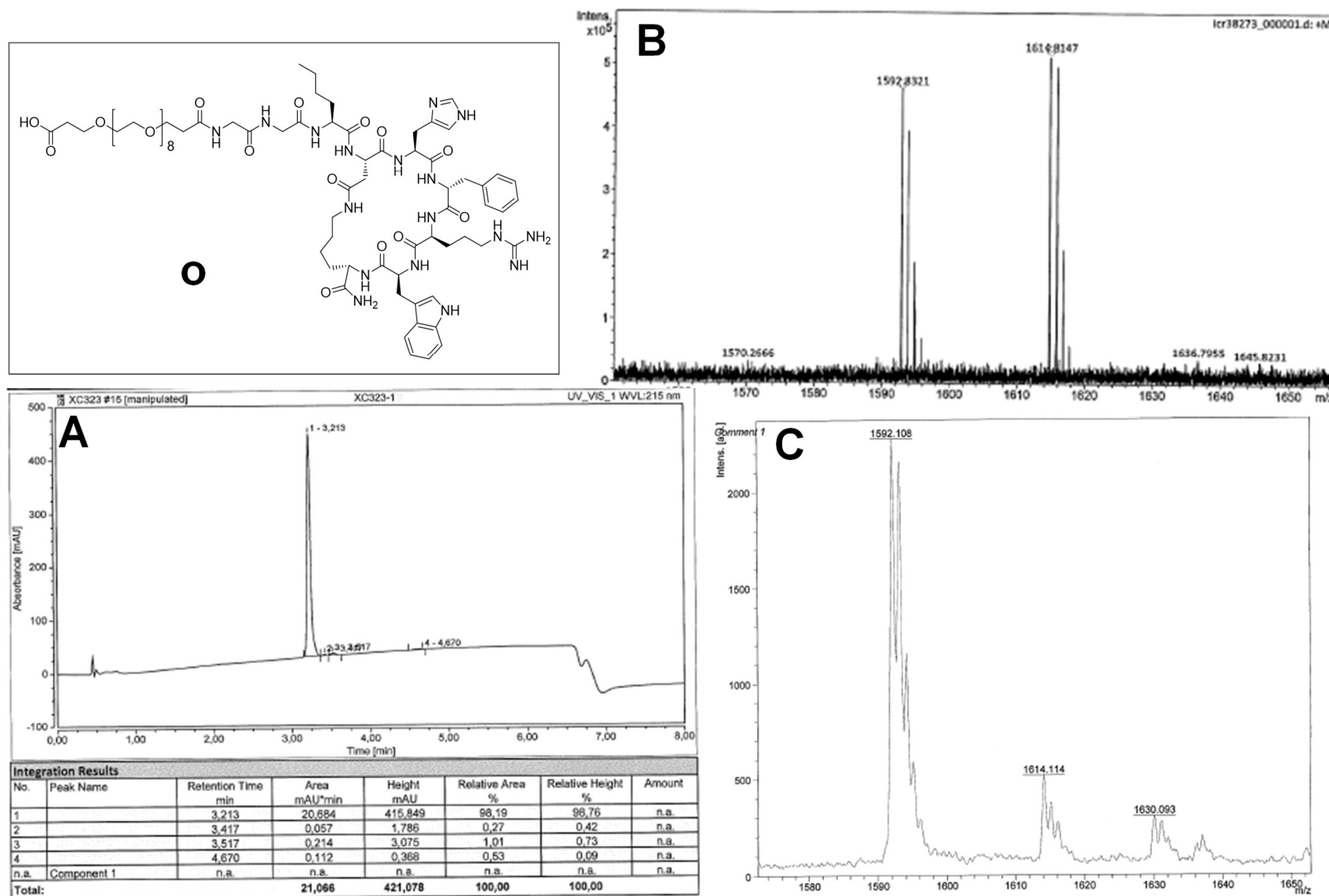


Figure S79. HPLC chromatogram (**A**) and mass spectra (**B**: ESI, **C**: MALDI) of HO-PEG₈-GG-Nle-c(DHfRWK) (**o**).

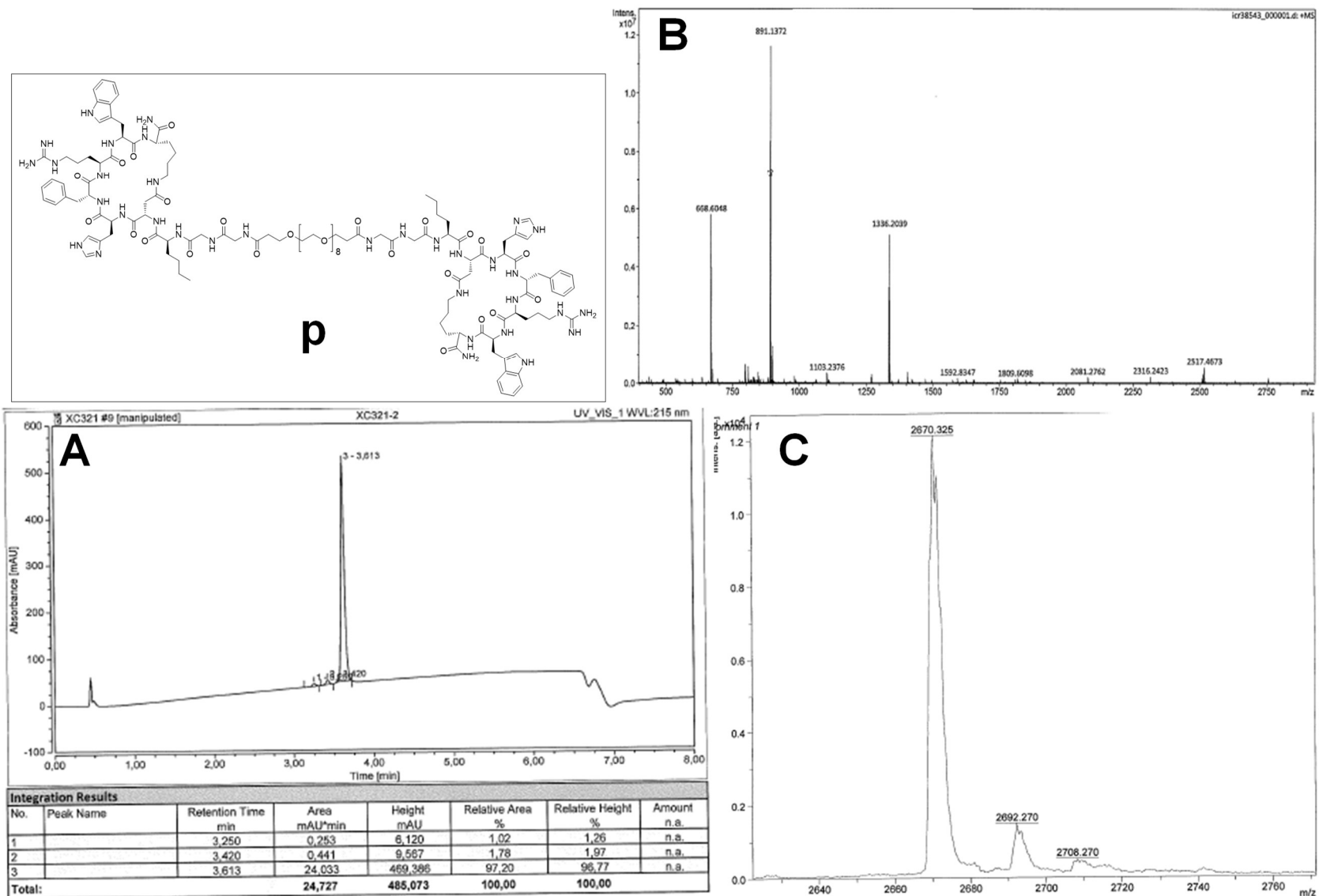
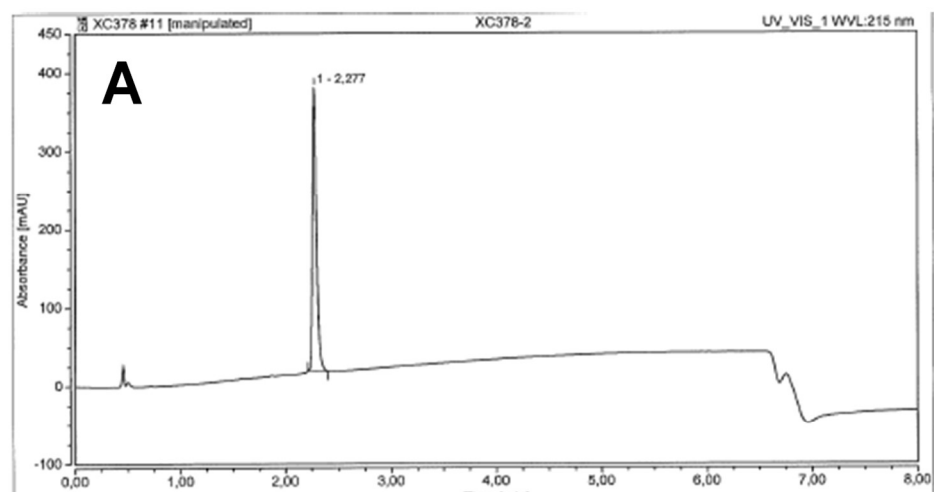
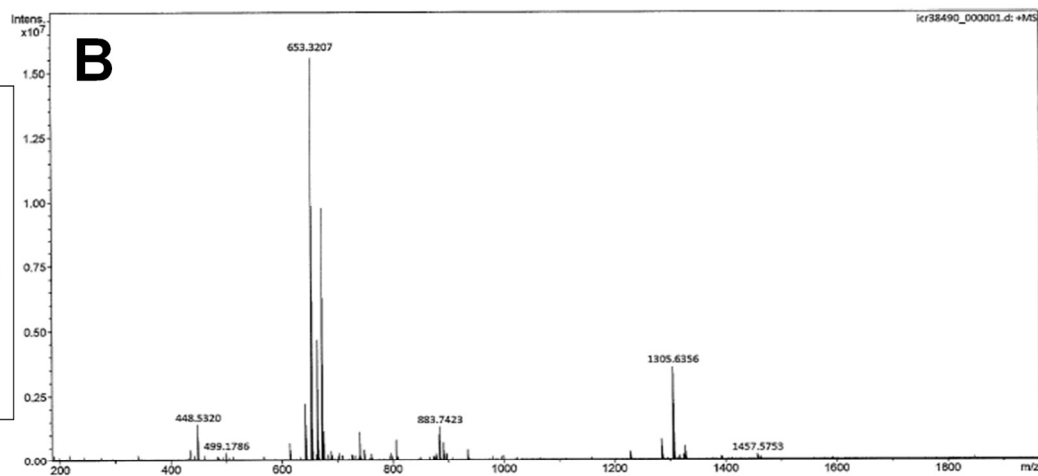
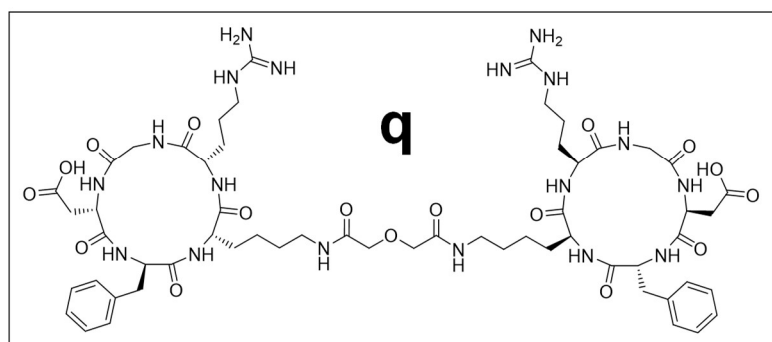


Figure S80. HPLC chromatogram (**A**) and mass spectra (**B**: ESI, **C**: MALDI) of c(DHfRWK)-Nle-GG-PEG₈-GG-Nle-c(DHfRWK) (**p**).



Integration Results							
No.	Peak Name	Retention Time min	Area mAU*min	Height mAU	Relative Area %	Relative Height %	Amount n.a.
1		2.277	16,181	362.287	100,00	100,00	n.a.
Total:			16,181	362.287	100,00	100,00	

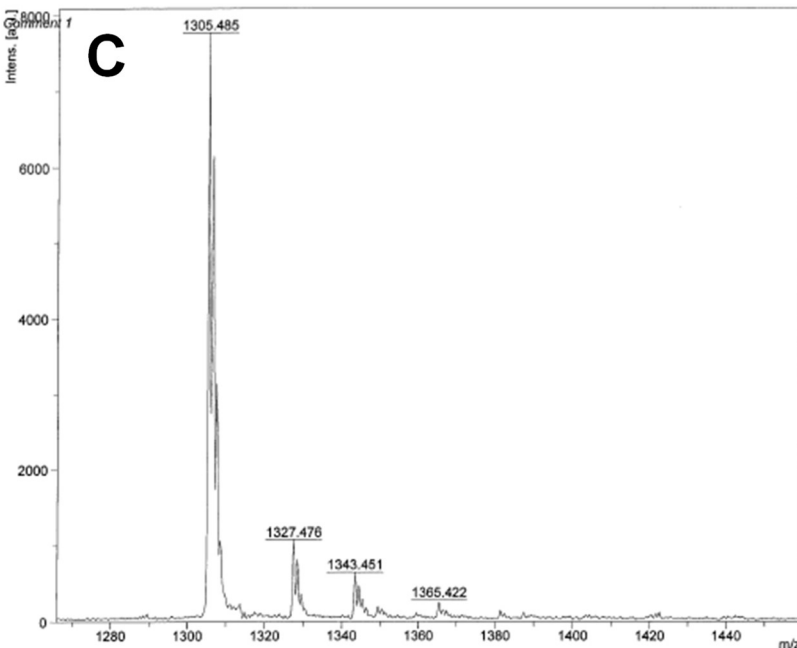


Figure S81. HPLC chromatogram (A) and mass spectra (B: ESI, C: MALDI) of c(RGDfK)-DIG-c(RGDfK) (q).

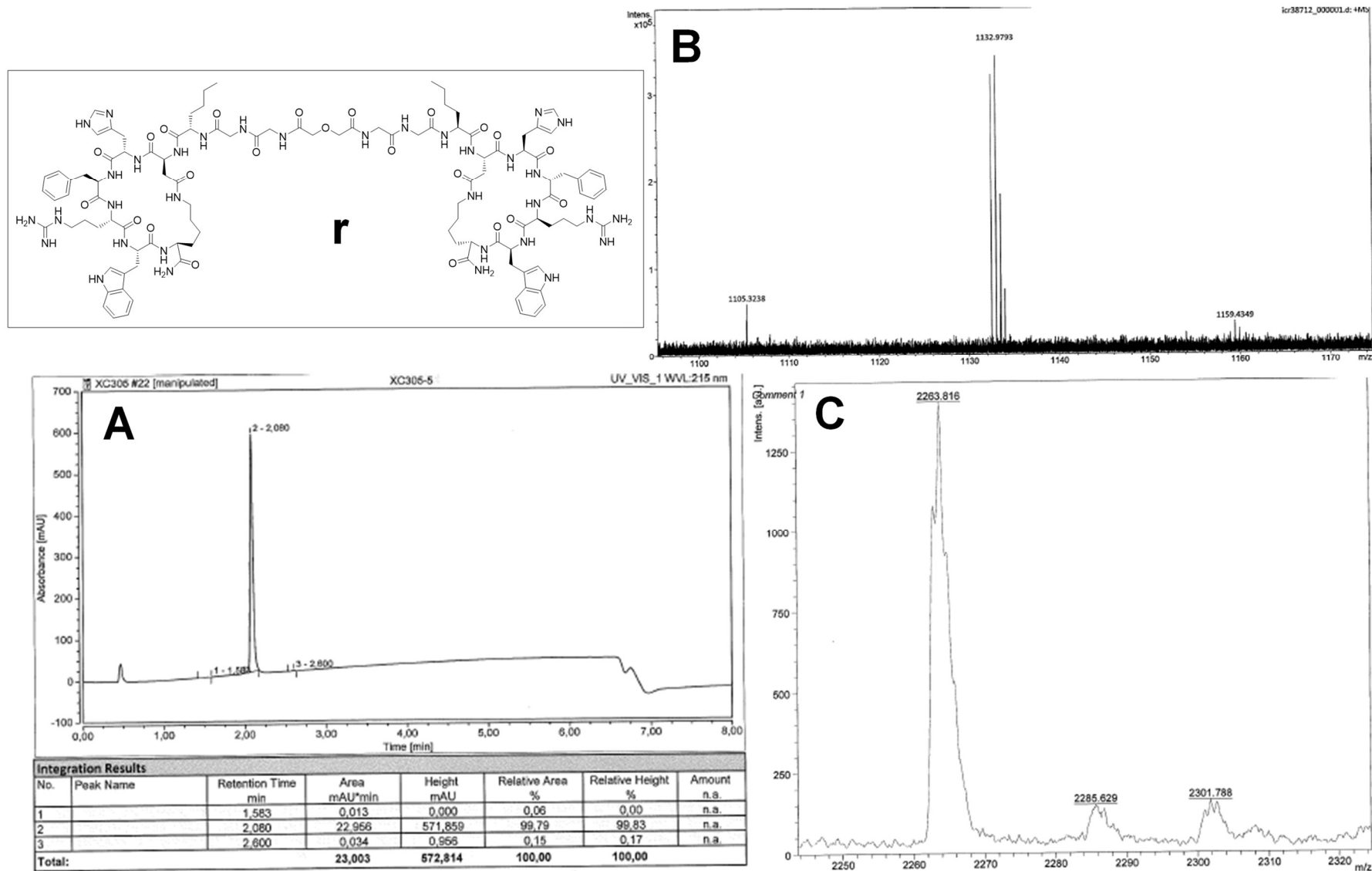


Figure S82. HPLC chromatogram (**A**) and mass spectra (**B**: ESI, **C**: MALDI) of c(RGDfK)-EGEGE-Ox-EGEGE-c(RGDfK) (**r**).

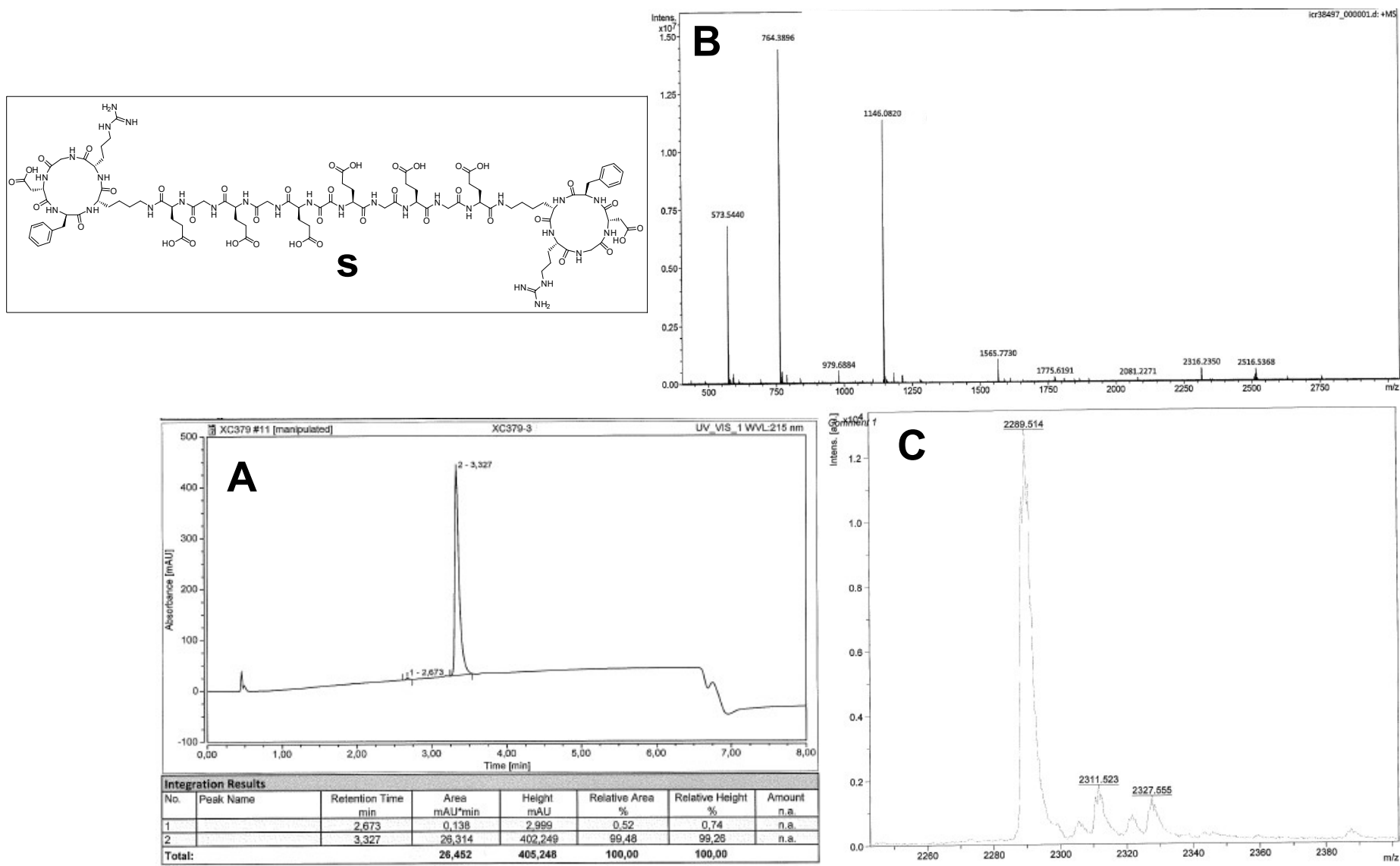
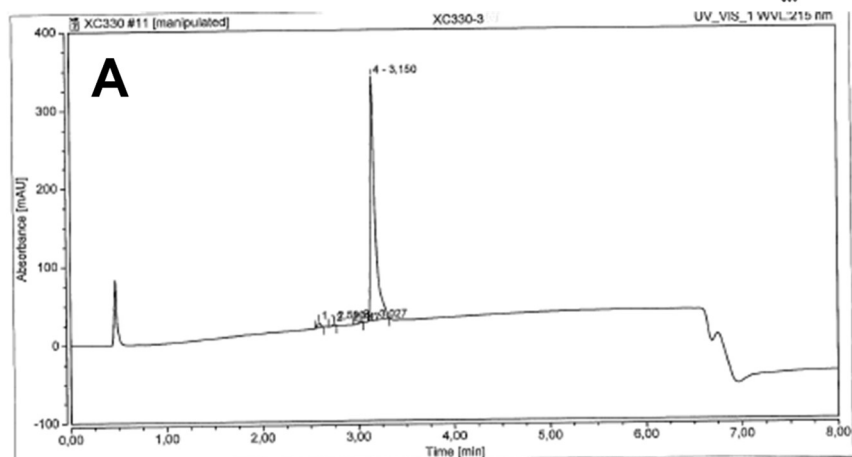
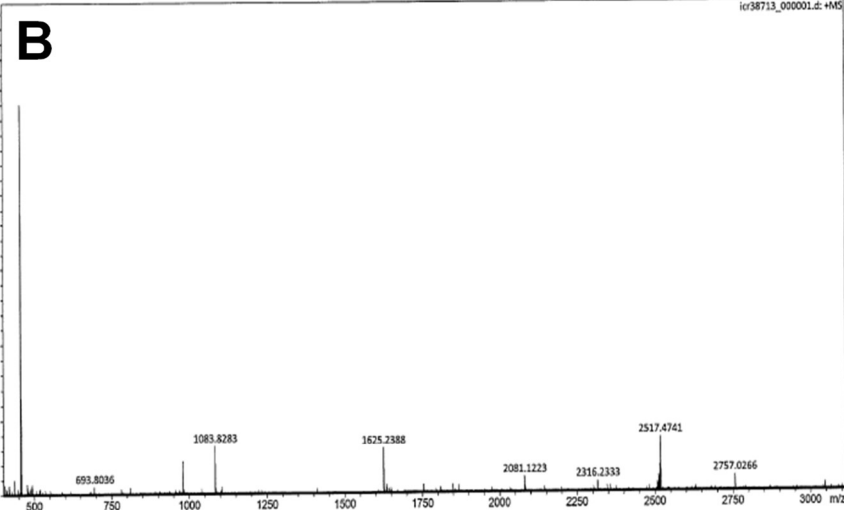
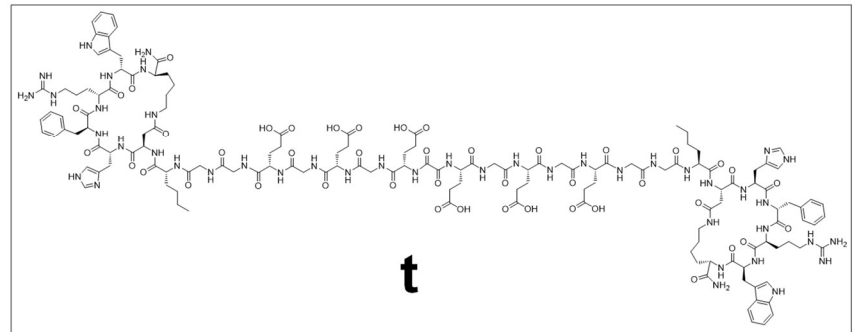


Figure S83. HPLC chromatogram (**A**) and mass spectra (**B**: ESI, **C**: MALDI) of c(DHfRWK)-Nle-GG-DIG-GG-Nle-c(DHfRWK) (**S**).



Integration Results							
No.	Peak Name	Retention Time min	Area mAU ² /min	Height mAU	Relative Area %	Relative Height %	Amount n.a.
1		2.590	0.228	6.158	1.25	1.92	n.a.
2		2.747	0.062	1.779	0.34	0.55	n.a.
3		3.027	0.070	1.997	0.38	0.62	n.a.
4		3.150	18.067	311.128	98.04	96.91	n.a.
Total:			18,429	321,063	100,00	100,00	

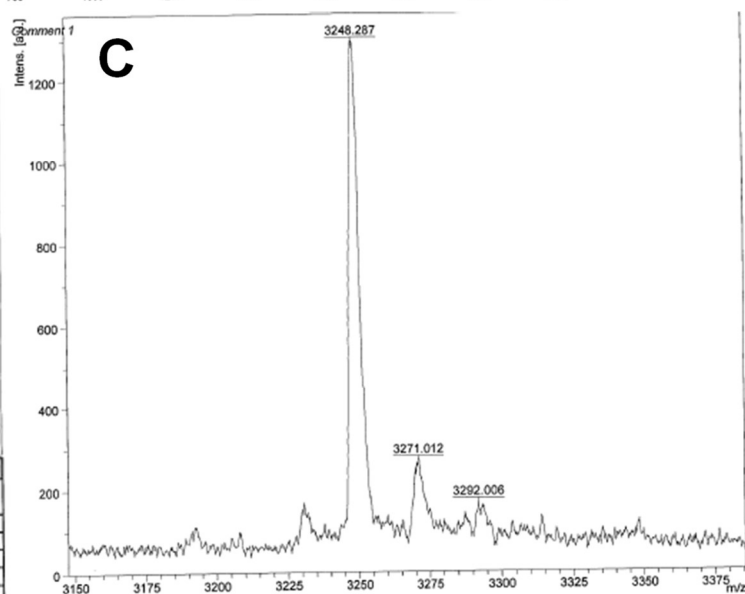


Figure S84. HPLC chromatogram (**A**) and mass spectra (**B**: ESI, **C**: MALDI) of c(DHfRWK)-Nle-GG-EGEGER-Ox-EGEGER-GG-Nle-c(DHfRWK) (**t**).

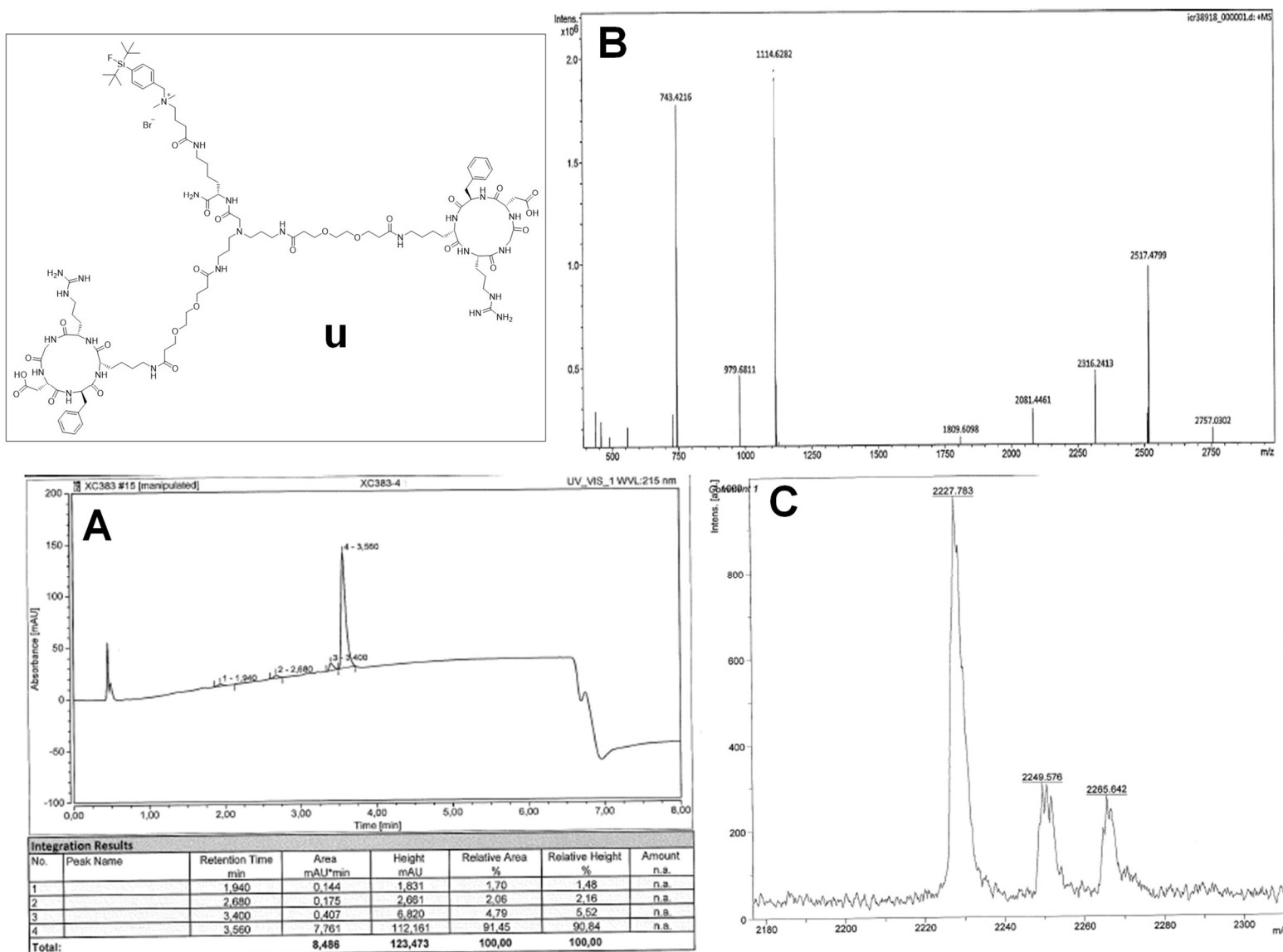


Figure S85. HPLC chromatogram (**A**) and mass spectra (**B**: ESI, **C**: MALDI) of SiFA/in-APG-[PEG1-c(RGDfK)]₂ (**U**).

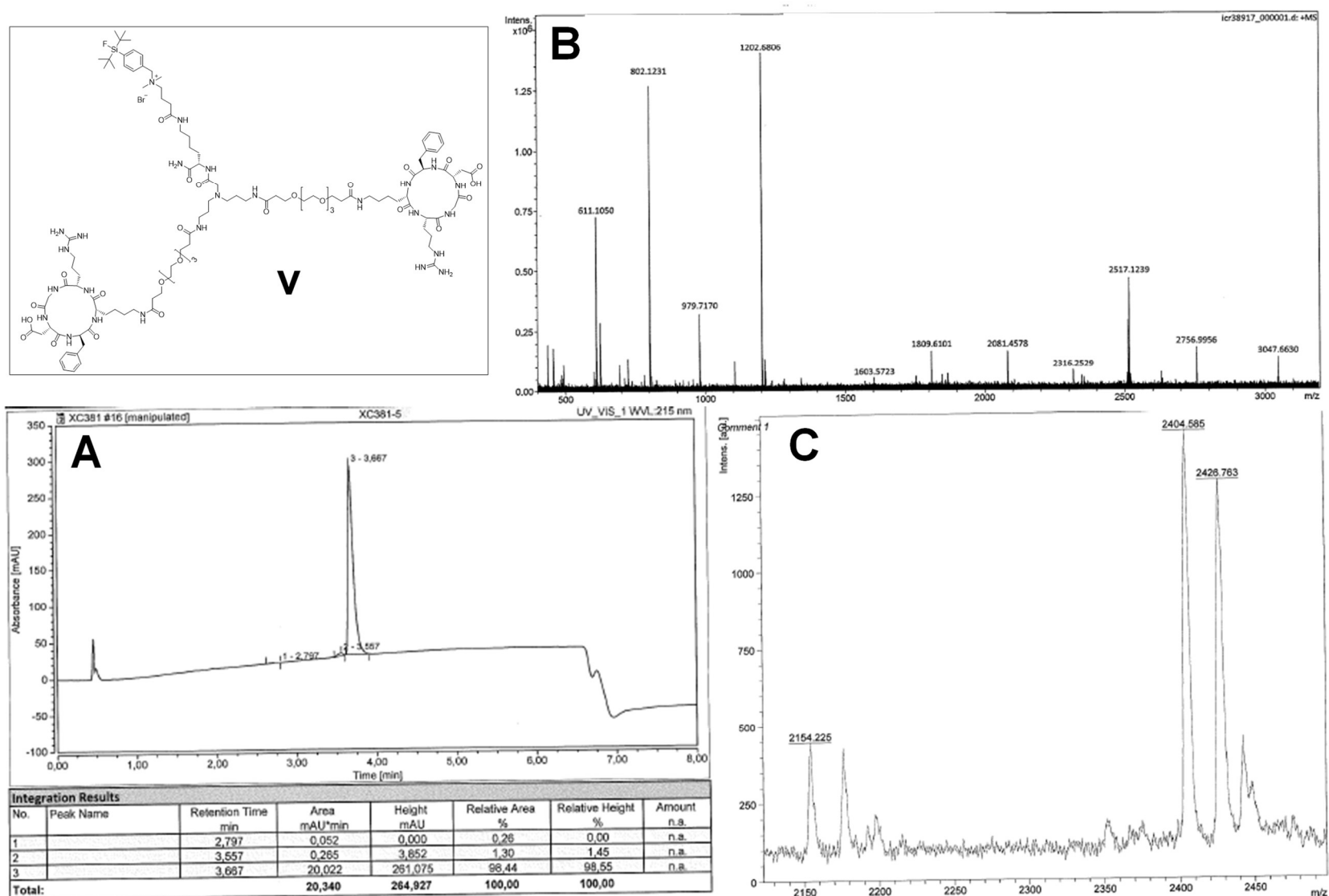


Figure S86. HPLC chromatogram (**A**) and mass spectra (**B**: ESI, **C**: MALDI) of SiFA/in-APG-[PEG₃-c(RGDFK)]₂ (**V**).

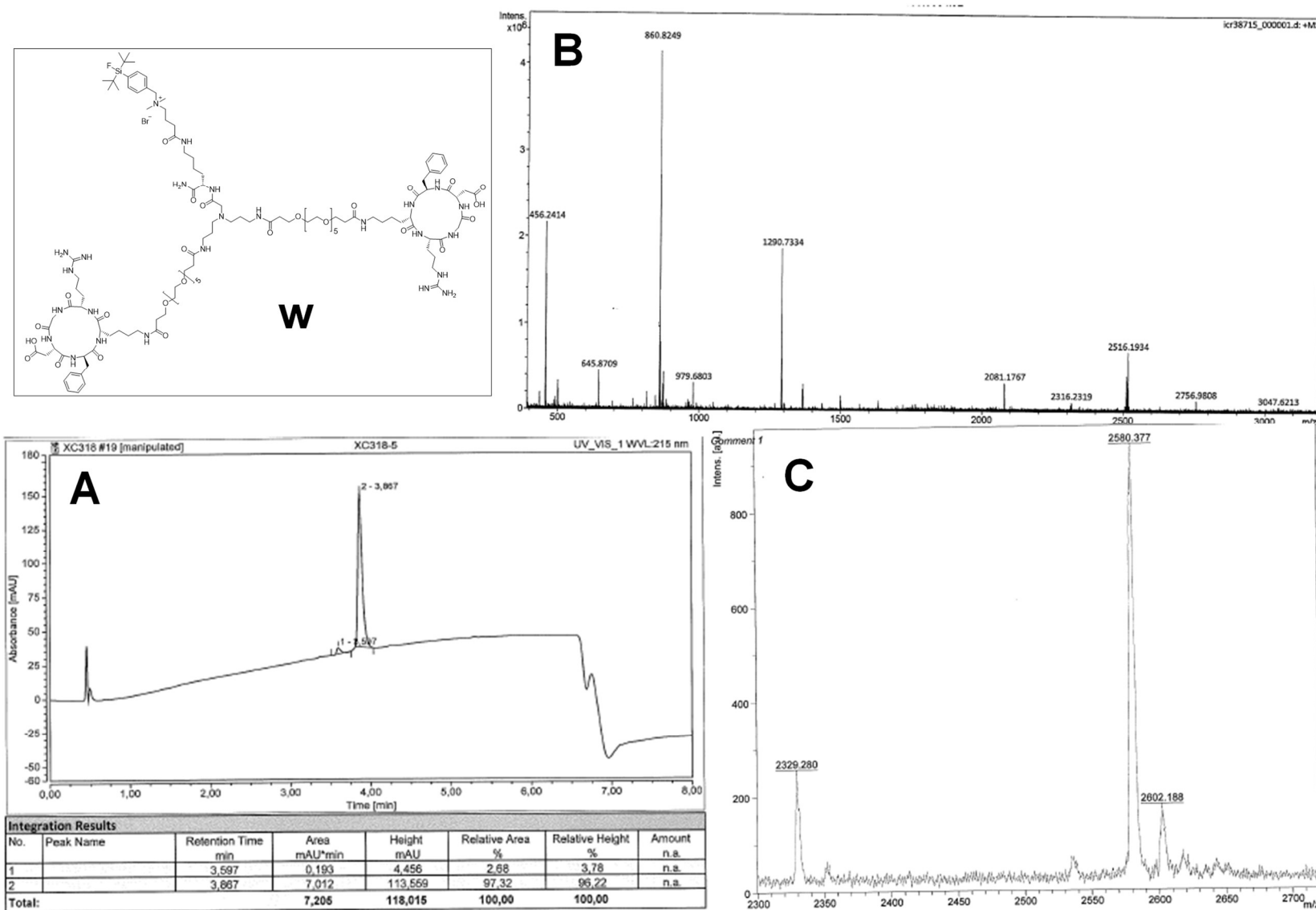


Figure S87. HPLC chromatogram (**A**) and mass spectra (**B**: ESI, **C**: MALDI) of SiFA/in-APG-[PEG₅-c(RGDfK)]₂ (**W**).

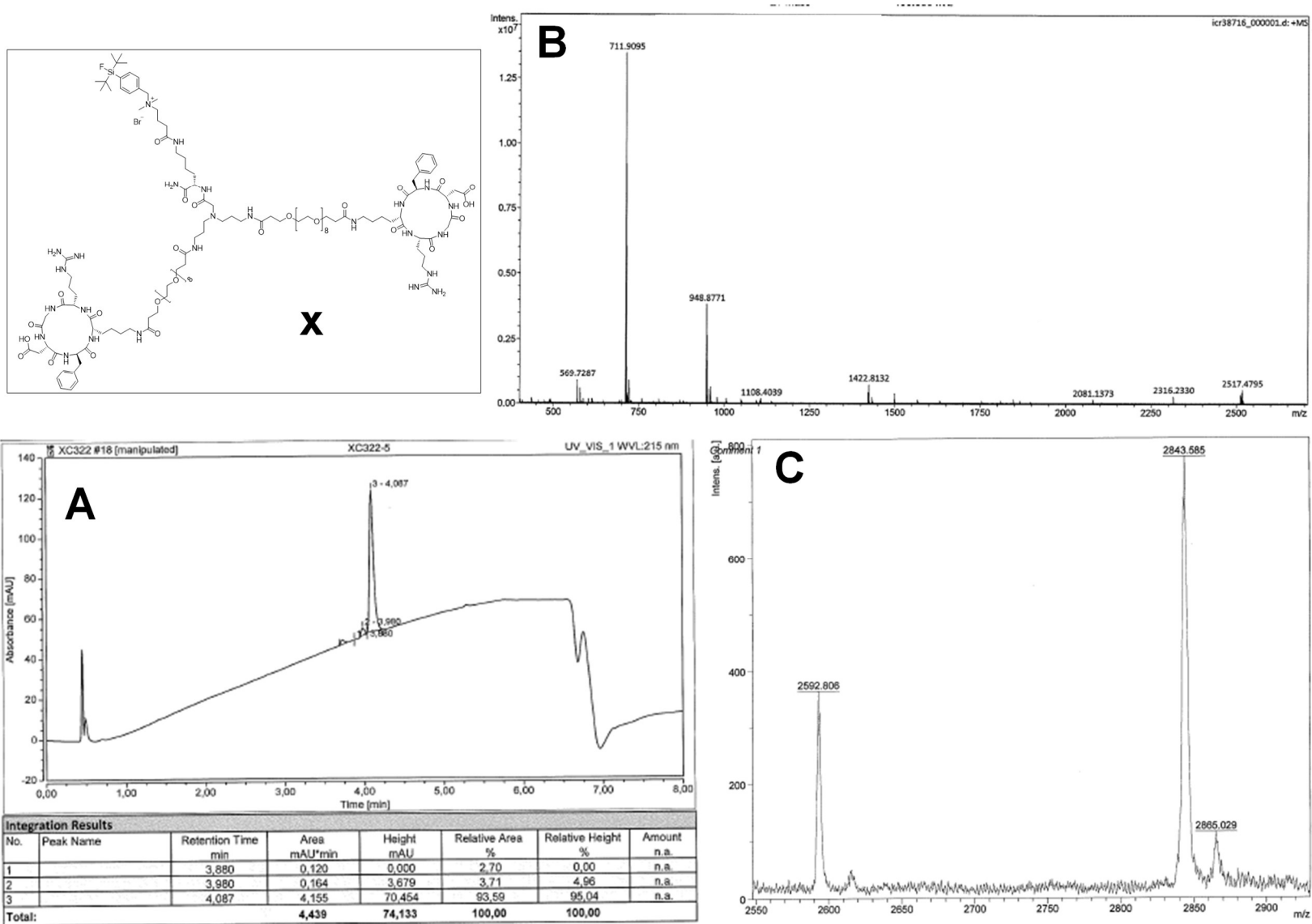


Figure S88. HPLC chromatogram (**A**) and mass spectra (**B**: ESI, **C**: MALDI) of SiFA/in-APG-[PEG₈-c(RGDfK)]₂ (**X**).

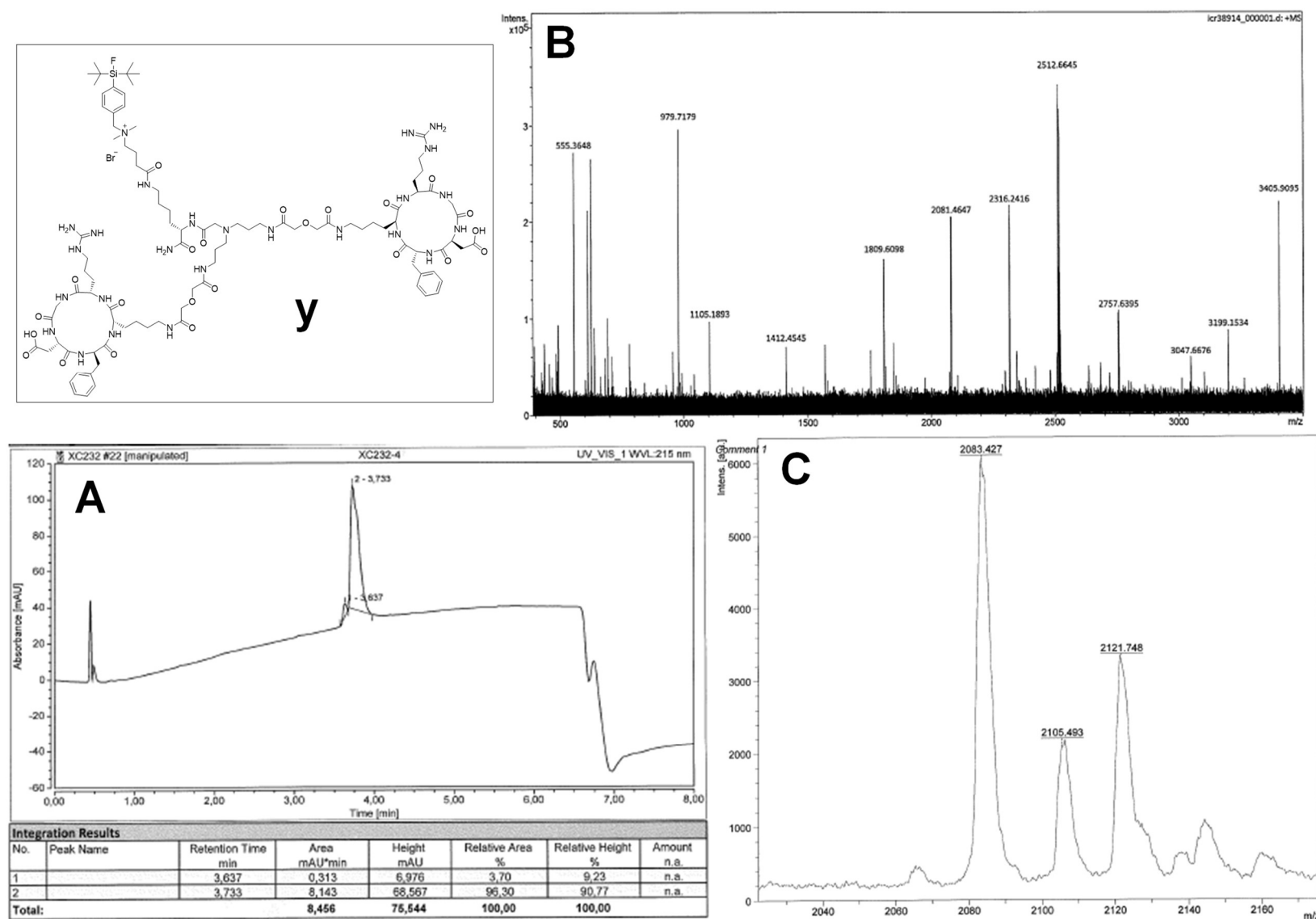


Figure S89. HPLC chromatogram (**A**) and mass spectra (**B**: ESI, **C**: MALDI) of SiFA/*in*-APG-[DIG-c(RGDfK)]₂ (**y**).

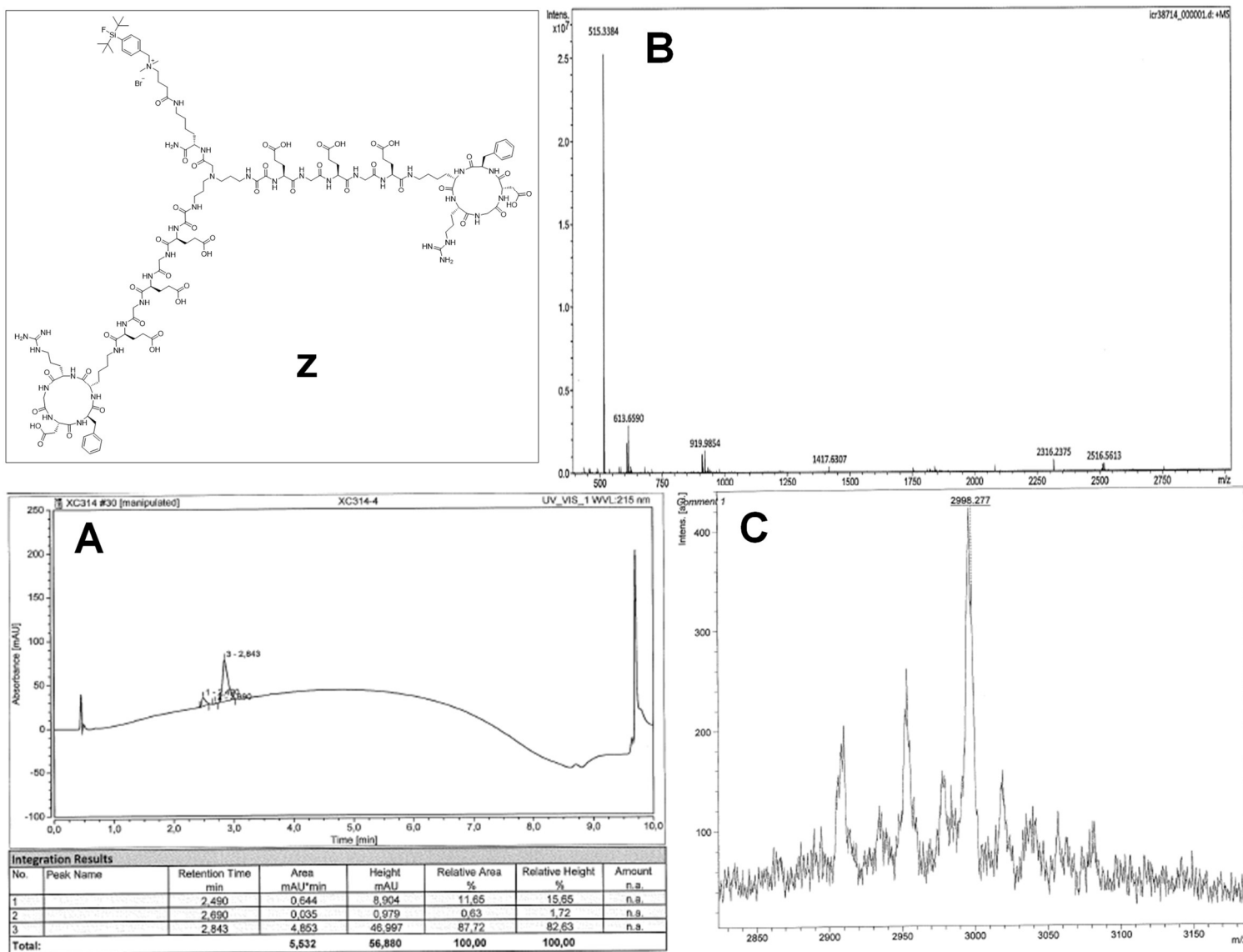


Figure S90. HPLC chromatogram (**A**) and mass spectra (**B**: ESI, **C**: MALDI) of SiFA/in-APG-[Ox-EGEGE-c(RGDfK)]₂ (**Z**).

5. Radio-HPLC chromatograms of [¹⁸F]1-[¹⁸F]6 from the investigation regarding serum stability

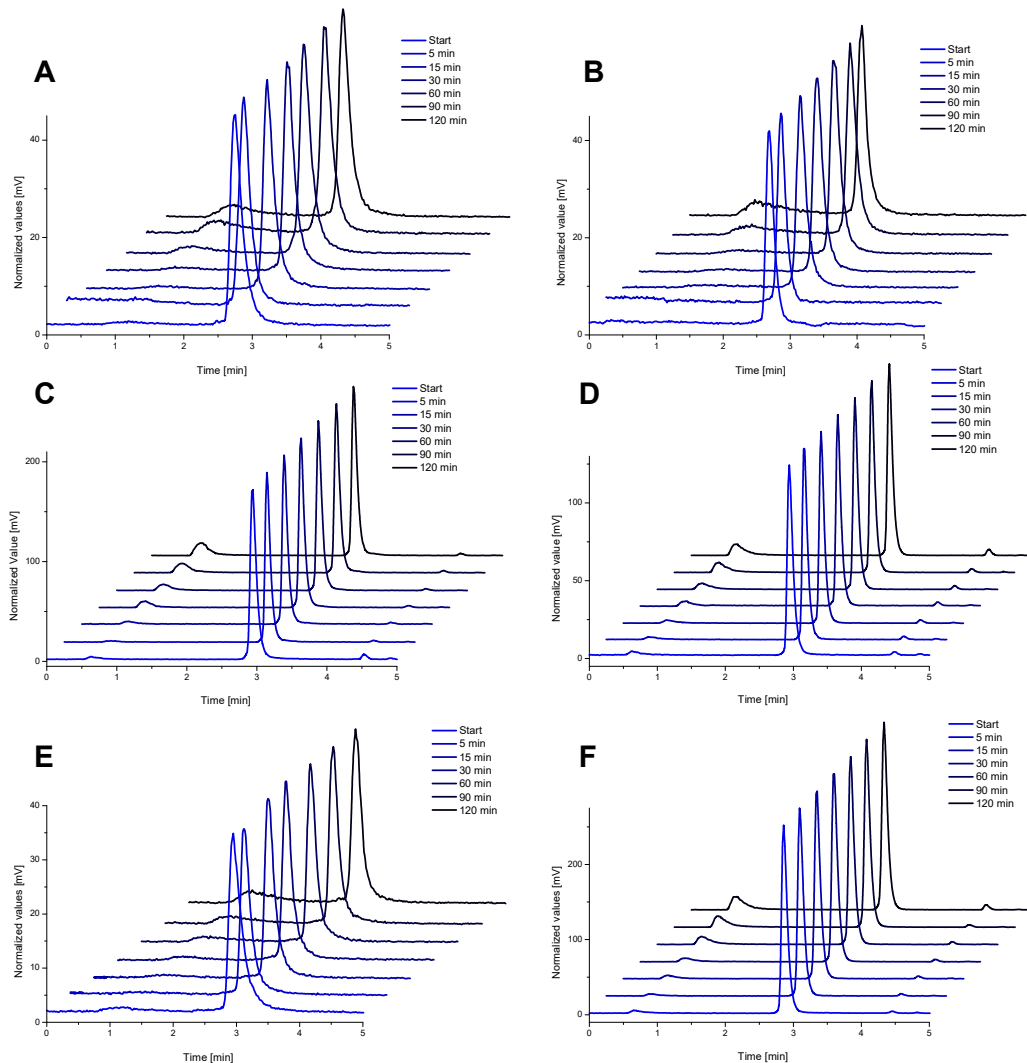


Figure S91. Depiction of the radio-HPLC chromatograms for [¹⁸F]1 – [¹⁸F]6 at certain time points. **A** [¹⁸F]1; **B** [¹⁸F]2; **C** [¹⁸F]3; **D** [¹⁸F]4; **E** [¹⁸F]5; **F** [¹⁸F]6.

6. Binding curves of the monomeric peptides c(RGDfK) and GG-Nle-c(DHfRWK)

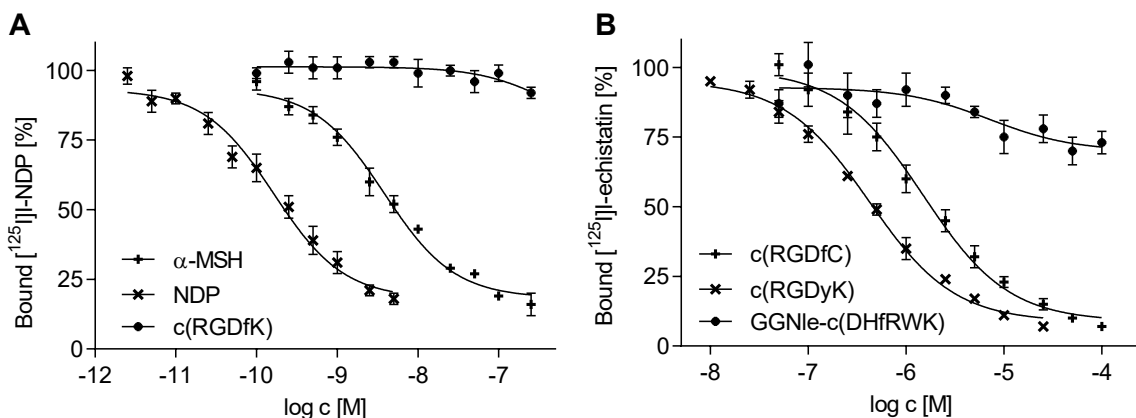


Figure S92. Depiction of the determined binding curves of c(RGDfK) on MC1R-positive B16F10-cells (**A**) and GG-Nle-c(DHfRWK) on $\alpha\beta_3$ -positive U87MG-cells (**B**). Values are depicted as mean ($n = 9$), error bars represent SD.

7. Ex vivo biodistribution data of [¹⁸F]2 and [¹⁸F]4

Table S1. Determined ID/g-values of ex vivo biodistribution data of [¹⁸F]2 and [¹⁸F]4. Values are given as mean (n = 3) ± SD.

Tissue	ID/g ([¹⁸ F]2) [%]				ID/g ([¹⁸ F]4) [%]			
	[¹⁸ F]2	NDP blocking	c(RGDyK) blocking	double blocking	[¹⁸ F]4	NDP blocking	c(RGDyK) blocking	double blocking
blood	0.99 ± 0.23	0.84 ± 0.12	1.14 ± 0.15	1.13 ± 0.10	0.59 ± 0.08	2.07 ± 0.94	0.83 ± 0.06	1.00 ± 0.15
spleen	2.73 ± 0.85	2.75 ± 0.55	0.94 ± 0.19	1.07 ± 0.32	1.79 ± 0.31	1.51 ± 0.15	1.71 ± 0.62	0.69 ± 0.10
liver	17.20 ± 6.58	14.88 ± 5.07	4.94 ± 1.39	8.50 ± 2.71	8.30 ± 2.77	5.16 ± 0.56	10.37 ± 3.65	4.04 ± 1.06
kidneys	13.24 ± 3.57	17.27 ± 2.08	12.09 ± 2.30	24.02 ± 6.34	7.72 ± 2.57	23.11 ± 4.97	21.35 ± 4.04	26.54 ± 6.59
pancreas	0.91 ± 0.29	0.80 ± 0.15	0.36 ± 0.04	0.55 ± 0.15	0.25 ± 0.08	0.52 ± 0.12	0.66 ± 0.19	0.32 ± 0.04
lung	2.89 ± 1.04	2.98 ± 0.87	1.07 ± 0.15	1.30 ± 0.36	3.45 ± 1.15	1.25 ± 0.06	2.75 ± 1.04	0.88 ± 0.14
heart	1.24 ± 0.36	1.06 ± 0.31	0.62 ± 0.09	0.93 ± 0.18	0.56 ± 0.19	0.73 ± 0.06	1.51 ± 0.57	0.52 ± 0.06
brain	0.18 ± 0.02	0.13 ± 0.03	0.13 ± 0.05	0.07 ± 0.01	0.10 ± 0.03	0.19 ± 0.07	0.07 ± 0.02	0.07 ± 0.01
bone	8.01 ± 3.48	9.74 ± 2.85	4.12 ± 0.73	4.47 ± 1.57	18.07 ± 6.02	4.61 ± 0.71	4.99 ± 0.71	2.99 ± 0.78
muscle	4.37 ± 2.58	1.37 ± 0.26	0.38 ± 0.04	0.34 ± 0.07	0.07 ± 0.02	0.63 ± 0.07	1.62 ± 0.42	2.58 ± 1.28
tail	37.99 ± 14.37	37.64 ± 8.67	68.98 ± 3.84	53.33 ± 12.82	25.29 ± 8.43	52.78 ± 5.59	44.27 ± 12.11	55.60 ± 7.12
B16F10 tumor	2.32 ± 0.49	1.83 ± 0.24	1.98 ± 0.18	1.14 ± 0.42	2.58 ± 0.86	1.33 ± 0.27	2.29 ± 0.24	2.49 ± 0.09
U87MG tumor	2.33 ± 0.46	3.19 ± 0.33	1.48 ± 0.12	1.00 ± 0.11	3.92 ± 1.31	2.53 ± 0.15	2.67 ± 0.66	0.90 ± 0.05
stomach	1.56 ± 0.29	1.52 ± 0.31	0.54 ± 0.04	0.54 ± 0.12	0.38 ± 0.13	1.03 ± 0.11	0.99 ± 0.16	0.42 ± 0.03
small intestine	2.46 ± 1.77	2.75 ± 0.36	0.75 ± 0.11	0.90 ± 0.23	0.07 ± 0.02	1.60 ± 0.26	1.46 ± 0.53	0.54 ± 0.08
colon	1.58 ± 0.44	1.44 ± 0.34	0.50 ± 0.07	0.63 ± 0.20	0.77 ± 0.26	0.96 ± 0.13	0.80 ± 0.32	0.42 ± 0.05

Table S2. Determined tumor-to-blood, tumor-to-muscle, tumor-to-liver, and tumor-to-kidney ratios of [¹⁸F]2 and [¹⁸F]4. Values are given as mean ($n = 3$) \pm SD. Asterisks indicate statistically significant values (*: $p < 0.05$, **: $p < 0.01$ and ***: $p < 0.001$).

Ratio	[¹⁸ F]2		[¹⁸ F]4	
	B16F10	U87MG	B16F10	U87MG
tumor/blood	2.42 ± 0.73	2.40 ± 0.67	4.36 ± 1.37	$5.08 \pm 0.75^{**}$
tumor/muscle	0.68 ± 0.41	0.79 ± 0.66	$38.56 \pm 9.24^{**}$	$45.72 \pm 8.62^{***}$
tumor/liver	0.16 ± 0.11	0.14 ± 0.03	0.36 ± 0.23	0.39 ± 0.14
tumor/kidneys	0.19 ± 0.10	0.18 ± 0.02	0.38 ± 0.24	$0.40 \pm 0.07^{**}$

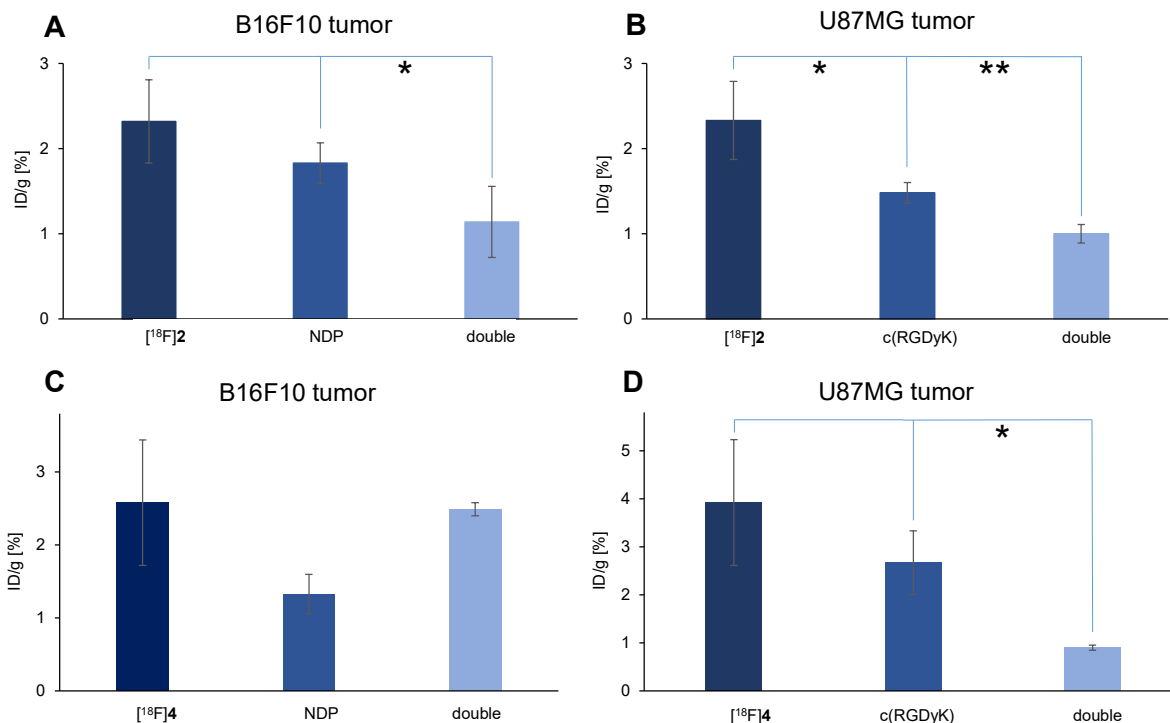


Figure S93. Depiction of tumor uptake of [¹⁸F]2 and [¹⁸F]4 with the respective blocking substances. **A** [¹⁸F]2 in B16F10 tumor; **B** [¹⁸F]2 in U87MG tumor; **C** [¹⁸F]4 in B16F10 tumor; **D** [¹⁸F]4 in U87MG tumor. Values are depicted as mean ($n = 3$), error bars represent SD.